

## INFORMATION TO USERS

This manuscript has been reproduced from the microfilm master. UMI films the text directly from the original or copy submitted. Thus, some thesis and dissertation copies are in typewriter face, while others may be from any type of computer printer.

**The quality of this reproduction is dependent upon the quality of the copy submitted.** Broken or indistinct print, colored or poor quality illustrations and photographs, print bleedthrough, substandard margins, and improper alignment can adversely affect reproduction.

In the unlikely event that the author did not send UMI a complete manuscript and there are missing pages, these will be noted. Also, if unauthorized copyright material had to be removed, a note will indicate the deletion.

Oversize materials (e.g., maps, drawings, charts) are reproduced by sectioning the original, beginning at the upper left-hand corner and continuing from left to right in equal sections with small overlaps.

ProQuest Information and Learning  
300 North Zeeb Road, Ann Arbor, MI 48106-1346 USA  
800-521-0600

UMI<sup>®</sup>



**AN INVESTIGATION OF THE PERFORMANCE OF TRICKLE  
VENTILATORS**

**Panagiota Karava**

**A Thesis**

**in**

**The Department**

**of**

**Building Engineering**

**Presented in Partial Fulfillment of the Requirements  
for the Degree of Master of Applied Science at  
Concordia University  
Montreal, Quebec, Canada**

**July 2002**

**© Panagiota Karava, 2002**



**National Library  
of Canada**

**Acquisitions and  
Bibliographic Services**

**395 Wellington Street  
Ottawa ON K1A 0N4  
Canada**

**Bibliothèque nationale  
du Canada**

**Acquisitions et  
services bibliographiques**

**395, rue Wellington  
Ottawa ON K1A 0N4  
Canada**

*Your file Votre référence*

*Our file Notre référence*

**The author has granted a non-exclusive licence allowing the National Library of Canada to reproduce, loan, distribute or sell copies of this thesis in microform, paper or electronic formats.**

**The author retains ownership of the copyright in this thesis. Neither the thesis nor substantial extracts from it may be printed or otherwise reproduced without the author's permission.**

**L'auteur a accordé une licence non exclusive permettant à la Bibliothèque nationale du Canada de reproduire, prêter, distribuer ou vendre des copies de cette thèse sous la forme de microfiche/film, de reproduction sur papier ou sur format électronique.**

**L'auteur conserve la propriété du droit d'auteur qui protège cette thèse. Ni la thèse ni des extraits substantiels de celle-ci ne doivent être imprimés ou autrement reproduits sans son autorisation.**

0-612-72899-4

**Canada**

## **ABSTRACT**

# **AN INVESTIGATION OF THE PERFORMANCE OF TRICKLE VENTILATORS**

**Panagiota Karava**

Prediction of the air flow rate in naturally ventilated buildings is very important for the calculation of the thermal response of the buildings, as well as for ensuring appropriate air renewal rates for a healthy building environment. Due to its importance, this issue has been given a lot of attention, and significant effort has been put into the development of theoretical models and experimental techniques for the evaluation of the air flow rate in natural ventilation configurations.

In naturally-ventilated buildings, fresh air is provided through openings, and there is a wide range of possibilities regarding the selection of the opening type and the position in the façade. Different flow patterns are developed for various opening types and positions resulting in different values of ventilation capacity, controllability, impact on comfort, indoor air quality (IAQ) and security.

Trickle ventilators are commonly used means for natural ventilation, especially in Europe. These are manually operated air-inlets fitted to window openings (preferably at the top) to allow fresh, outside air passing through. This study presents a full-scale experimental investigation of the air leakage characteristics of two trickle ventilator types, namely slot and pressure-controlled. Furthermore, the performance of trickle ventilators under the influence of the wind, which is the main driving force of the air flow

through low-rise buildings, and the validity of the orifice equation to represent their behaviour have been assessed. Finally, the potential of trickle ventilator integration in ventilation design of office buildings is investigated through flow network simulations and design solutions for the opening area of trickle ventilators to satisfy the fresh air requirements, as recommended by ASHRAE, are presented.

It was found that the air flow through trickle ventilators may be modelled / predicted accurately and utilized in the design of natural / hybrid ventilation systems. However, the pressure-controlled ventilator appears to be preferable since it provides for better IAQ, and its performance is better than that of the slot ventilator with respect to comfort and energy use to warm up the ventilated air during the heating season.

## **ACKNOWLEDGMENTS**

I would like to express my deepest gratitude to my supervisors Dr. T. Stathopoulos and Dr. A. K. Athienitis for their continuous encouragement and support during my graduate studies and provision of critical thinking in building engineering issues.

I thank Mr. Payer, Mr. Zilka and Mr. Demers for the technical help in the experimental setup.

The provision of the trickle ventilators by Titon Inc. is acknowledged with thanks.

Special thanks to Thanos for his understanding and support throughout my studies. I am thankful to all my friends in Montreal and of course my family for their help and psychological support.

## TABLE OF CONTENTS

<b>LIST OF FIGURES</b> .....	
<b>NOMENCLATURE</b> .....	
<b>CHAPTER 1 INTRODUCTION</b> .....	1
1.1 Background.....	1
1.2 Motivation.....	2
1.3 Objectives.....	4
1.4 Thesis orientation.....	4
<b>CHAPTER 2 BACKGROUND KNOWLEDGE AND LITERATURE REVIEW</b> .....	6
2.1 Introduction.....	6
2.2 Natural ventilation assessment.....	6
2.3 Natural ventilation strategies.....	8
2.4 Driving mechanisms.....	11
2.4.1 Wind pressure.....	11
2.4.2 Stack pressure.....	15
2.4.3 Combining driving forces.....	17
2.5 Air flow through openings.....	19
2.6 Mathematical models.....	20
2.6.1 Basic equations.....	20
2.6.2 Empirical models.....	23
2.6.3 Network models.....	25
2.6.4 CFD models.....	28
2.7 Experimental techniques.....	30



2.8 Recent development in natural ventilation – Controls.....	32
2.9 Hybrid ventilation systems.....	34
2.10 Trickle ventilators and research needs.....	38
<b>CHAPTER 3 EXPERIMENTAL MEASUREMENTS.....</b>	<b>40</b>
3.1 Introduction.....	40
3.2 The outdoor test-room.....	41
3.3 Description of trickle ventilators.....	41
3.4 Sensors and measurements.....	44
3.5 The data acquisition system.....	47
3.6 Leakage characteristics of the ventilators – experimental methodology.....	48
3.7 Wind study.....	52
<b>CHAPTER 4 EXPERIMENTAL RESULTS AND DISCUSSION.....</b>	<b>54</b>
4.1 General.....	54
4.2 Air flow through the slot ventilator by using the fan depressurization technique.....	54
4.2.1 Repeatability of the results.....	57
4.2.2 Comparison with literature sources.....	59
4.2.3 Comparison with manufacture’s data and the orifice equation.....	60
4.2.4 Effective area of the slot ventilator.....	62
4.3 Air flow through the pressure-controlled ventilator by using the fan depressurization technique.....	63
4.3.1 Repeatability of the results.....	64
4.3.2 Comparison with manufacture’s data and literature sources.....	65
4.4 Sensitivity of the results to wind effect.....	66

4.5 Discussion of the fan depressurization results.....	68
4.6 Wind effect on trickle ventilators performance.....	69
4.6.1 Experimental results.....	69
4.6.2 Discussion.....	73
4.6.3 Comparison with literature sources.....	75
4.6.4 Sensitivity of the results to the background leakage.....	77
4.7 Comparison between the fan depressurization and the wind study results.....	78
4.8 Selection criteria.....	83
<b>CHAPTER 5 INVESTIGATION OF THE INTEGRATION OF TRICKLE VENTILATORS IN OFFICE BUILDINGS THROUGH FLOW NETWORK SIMULATIONS.....</b>	<b>86</b>
5.1 Introduction.....	86
5.2 Simulation study.....	87
5.2.1 Leakage characteristics.....	88
5.2.2 Stack pressure.....	89
5.2.3 Wind pressure.....	89
5.2.4 Opening area calculation.....	89
5.3 Case study.....	91
5.3.1 The building and its design environment.....	91
5.3.2 Sensitivity analysis.....	94
5.3.3 Simulation results.....	98
5.4 Limitations of the proposed methodology-Further study.....	100
<b>CHAPTER 6 CONCLUSIONS AND RECOMMENDATIONS.....</b>	<b>102</b>

6.1 Conclusions.....	102
6.2 Recommendations and possible extensions of current work.....	105
<b>REFERENCES.....</b>	<b>107</b>
<b>APPENDIX.....</b>	<b>116</b>

## LIST OF FIGURES

1.1 A trickle ventilator.....	2
2.1 Energy savings by using natural ventilation .....	8
2.2 Natural ventilation configurations.....	10
2.3 Wind-induced pressure .....	12
2.4 Mean internal pressures in buildings with various opening distributions .....	13
2.5 Mean internal pressure coefficient as a function of the opening area for different background porosities .....	15
2.6 Stack-induced pressure .....	17
2.7 Fan pressure .....	19
3.1 Installation of a trickle ventilator .....	41
3.2 Slot ventilator and exterior canopy .....	42
3.3 Pressure-controlled ventilator.....	43
3.4 Depressurization equipment inside the test-room.....	45
3.5 Experimental set-up in outdoor test-room .....	45
3.6 The flow network model .....	50
3.7 Air flow as a function of the inside-outside pressure difference .....	52
4.1 Airflow through the test-room envelope cracks .....	55
4.2 Exhaust flow rate, air flow through the test-room envelope cracks and air flow through the slot ventilator.....	56
4.3 Airflow through the slot ventilator .....	56
4.4 Repeatability of the results for the air flow through the test-room envelope cracks.....	58

4.5 Air flow through the slot ventilator - repeatability of the results .....59

4.6 Comparison of the air flow through the slot ventilator by using field data (present study), the orifice equation, wind tunnel data and data by applying ASTM E283 method .....61

4.7 Air flow through the pressure-controlled ventilator .....63

4.8 Airflow through the pressure-controlled ventilator - repeatability of the results.....65

4.9 Comparison of the air flow through the pressure-controlled ventilator by using field and manufacturer’s data .....66

4.10 Overestimation and underestimation of the air flow through the slot ventilator due to the wind.....67

4.11 Comparison between the airflow through the slot and the pressure-controlled ventilator.....68

4.12 Internal pressure coefficient variation with the ventilator closed (no opening).....71

4.13 Internal pressure coefficient variation with the rectangular slot open .....72

4.14 Internal pressure coefficient variation with the slot ventilator open .....72

4.15 Internal pressure coefficient variation with the pressure-controlled ventilator open.....73

4.16 Standard deviation of the internal pressure coefficient .....75

4.17 Internal pressure coefficient - comparison between field and wind tunnel .....77

4.18 Comparison between wind and fan depressurization data for the slot ventilator ....80

4.19 Comparison between wind and fan depressurization data for the pressure-controlled ventilator.....81

4.20 Admittance function (air flow through the pressure-controlled ventilator/airflow through the slot ventilator) for wind and fan depressurization data.....	82
5.1 Schematic of the simulated office .....	87
5.2 Hybrid ventilation strategy .....	92
5.3 Stack pressure at the location of slot ventilators ( $T_o = 15^{\circ}\text{C}$ ).....	94
5.4 Effect of wind speed on total pressure for different outside temperatures ( $C_{pe}=0.6$ ). 95	
5.5 Effect of external pressure coefficient on total pressure for different outside temperatures ( $V=2.5$ m/s).....	96
5.6 Effect of opening height on total pressure.....	97
5.7 Effect of outside temperature on total pressure.....	98
5.8 Opening area as a function of the outside temperature .....	100

## NOMENCLATURE

$A$	<i>opening area</i>
$A_o$	<i>effective area</i>
$C$	<i>flow coefficient</i>
$C_d$	<i>discharge coefficient</i>
$C_{pe}$	<i>external pressure coefficient</i>
$C_{pi}$	<i>internal pressure coefficient</i>
$\Delta P$	<i>pressure differential</i>
$\Delta T$	<i>temperature differential</i>
$\theta$	<i>wind incidence angle</i>
$g$	<i>gravitational acceleration</i>
$h$	<i>opening height</i>
$H_{NPL}$	<i>neutral pressure level height</i>
$K$	<i>flow coefficient per unit area</i>
$\mu$	<i>dynamic viscosity</i>
$n$	<i>flow exponent</i>
$O$	<i>occupancy</i>
$P_i$	<i>internal pressure</i>
$P_o$	<i>reference pressure</i>
$P_s$	<i>stack pressure</i>
$P_w$	<i>wind pressure</i>
$\rho$	<i>air density</i>

$Q$      *air flow*  
 $T_i$     *inside temperature*  
 $T_o$     *outside temperature*  
 $V$      *wind speed*



# CHAPTER 1

## INTRODUCTION

### **1.1 Background**

Building ventilation is the intentional movement of air through a space so as to provide acceptable indoor air quality and, at times, to regulate thermal comfort. Ventilation may be forced or natural. Forced ventilation uses mechanical means, such as fans, to drive air through a building. On the other hand, natural ventilation makes use of natural forces such as density differences due to temperature (also known as buoyancy or stack effect) and wind to induce air flow.

Prior to the oil embargo (1970), the availability of the inexpensive fuels led to the use, virtually exclusively, of mechanical heating, cooling and ventilating systems. Many buildings became entirely dependent upon these artificial systems for maintenance of the indoor environment. Since the mid 1970s and the energy crisis, there has been an urgent need to reduce the use of energy for the indoor air-conditioning worldwide. The shortage of energy supplies and related costs have recently forced architects and builders to evaluate most building components from the standpoint of energy conservation. Fenestration products have been designed to fit into the "energy conservation" concept.

The concept of additional natural, background or passive ventilation into specified tightly constructed buildings or houses originated in Scandinavian countries more than twenty five years ago. Window manufacturers in these countries developed what have been known as "trickle" ventilators, which are integral ventilating systems/devices

designed to fit into the “energy conservation” concept. Trickle ventilators are manually operated air-inlets fitted to window openings (preferably at the top) to allow a controlled flow of air to trickle in. The amount of air is usually sufficient to improve indoor air quality without significantly affecting energy costs. Figure 1.1 shows a trickle ventilator installed at the top of a window frame.

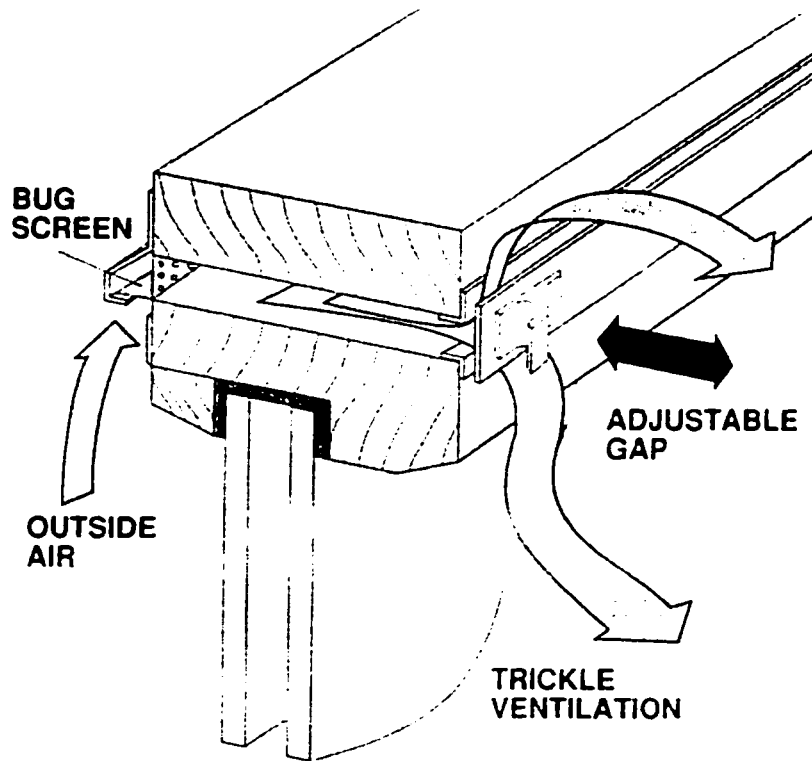


Fig. 1.1. A trickle ventilator (manufacturer’s manual).

## **1.2 Motivation**

In recent years, there are many companies manufacturing and/or marketing these products. Trickle ventilators are widely used in European countries and have become part of many Building Standards such as those of Building Research Establishment (BRE),

CIBSE, etc. For example, design guidelines regarding natural ventilation in non-domestic buildings as defined in BRE Digest 399 (1994) read as follows: “ Trickle ventilators of 400 mm<sup>2</sup> operable area per m<sup>2</sup> of floor area are required to provide controllable background ventilation”. This concept is relatively new in North America but during the last few years, trickle ventilators have been installed in commercial and domestic buildings. A large variety of trickle ventilators exist to suit almost all window types. Some innovative components intended to provide a constant natural supply of air flow independent of wind and temperature induced pressures have also been developed. Controlled air-inlets may help to overcome problems of draft and stuffiness that sometimes appear when fixed openings are used.

Despite the fact that trickle ventilators are presently used, their manufacturers provide very limited information about their actual performance or differences in performance between several types, since most of them have never been tested according to standards. As a result, their leakage characteristics are not well known and the air flow through them cannot be modelled/predicted accurately. Furthermore, trickle ventilators have not been tested in the Canadian climate in order to see how they perform under actual weather conditions, and reliable selection criteria are not available so far. Therefore, appropriate research is required with the objective to investigate their flow characteristics, to improve their integration in ventilation systems, and to develop, in the long run a central control strategy including several aspects as heating, cooling, lighting and ventilation.

### **1.3 Objectives**

The main objectives of this thesis are the following:

- To determine the leakage characteristics of two trickle ventilator types: a slot (fixed) and a pressure-controlled ventilator.
- To investigate the trickle ventilators' actual performance under the influence of the wind, by measuring the internal pressure coefficient for different locations of the ventilators with respect to wind.
- To check the degree of validity of the orifice equation for application in the case of trickle ventilators.
- To establish selection criteria in order to determine the suitability of each ventilator type and the conditions, under which, it should be used.
- To investigate the potential integration of trickle ventilators in ventilation design of office buildings, through flow network simulations.

### **1.4 Thesis organization**

Chapter 2 reviews the related literature. Several ventilation strategies are presented as well as theoretical/empirical models and experimental techniques for investigation of the effectiveness of various natural ventilation configurations. Emphasis is placed on recent developments related to trickle ventilators and controllable openings.

In chapter 3 the two trickle ventilator types considered in this work are described and the experimental procedure with the corresponding instrumentation is presented.

In chapter 4 the experimental results are presented and analyzed. The leakage characteristics of the two ventilators are determined. The performance of trickle

ventilators under the influence of the wind, which is the main driving force of the air flow through low-rise buildings, is investigated and compared to that of a simple rectangular opening that covers the same slot. The validity of the orifice equation to represent their behaviour has been assessed and a comparison between the two ventilator types is carried out, in order to establish appropriate selection criteria and to determine which type is better with respect to thermal comfort and IAQ.

Chapter 5 presents a simulation flow network model considering the integration of a hybrid ventilation system, which includes trickle ventilators, in a high-rise building. A sensitivity analysis has been carried out and several design solutions regarding the required opening area of trickle ventilators to ensure an acceptable comfort level for occupants, are discussed.

Chapter 6 presents the conclusions of this study and recommendations for future work.

## CHAPTER 2

### BACKGROUND KNOWLEDGE AND LITERATURE REVIEW

#### **2.1 Introduction**

This chapter presents basic background knowledge regarding the natural ventilation of buildings and reviews the related literature. Since this work includes an experimental and a simulation part (flow network model), emphasis is placed on similar experimental studies and flow network developments.

#### **2.2 Natural ventilation assessment**

Ventilation is considered an essential aspect of building design in most countries whereas in the past, ventilation used to characterize only the air infiltration through cracks in the building envelope and airing through the windows. Since the energy crisis in the mid 1970s, the growing concern for energy consumption and the relevant environmental impacts, have led to tighter construction standards aiming at the reduction in the supply rate of outdoor air in buildings. The “build tight” concept in many instances has ignored proper natural ventilation (Musser and Yuill, 1999). Consequently, problems associated with insufficient background ventilation have surfaced. The much-published “sick building syndrome” is fundamentally a complaint about the indoor air quality of a building. Building sickness comprises the sensation of stuffy, stale and unacceptable indoor air, headache, lethargy and so for (Awbi and Allwinkle, 1986). Well designed and

energy efficient natural ventilation systems are essential to create a healthier, stimulating environment for the building occupants.

In developing countries, the energy consumption for maintaining an acceptable environment in building constitutes by far the largest portion of the total energy demand. In Europe, buildings represent almost 40% of the total energy consumption. A high percentage of the energy consumed is used to cover cooling needs (Tsangrassoulis et al, 1997). Furthermore, according to a survey published by Jones and West (2001), the energy cost of air-conditioned buildings is 40% more than for non-air-conditioned buildings. As a result there is a growing interest in ventilation as part of an energy strategy for achieving thermal comfort in summer.

Natural ventilation is used to provide acceptable IAQ and summer comfort. This can be achieved by diluting the indoor concentration of pollutants and renewing the building air or cooling down the thermal mass.

As an illustration of the potential annual energy cost reduction, data from CIBSE (CIBSE, 1998) can be used: in a well-designed building making use of natural ventilation, substantial energy savings can be expected because energy consumption for refrigeration is avoided and a substantial reduction in energy use for fans and pumps - see Figure 2.1.

Several studies related to health costs and productivity benefits of improved IAQ have also been carried out (Dorgan et al, 1999). Quantification of the impact on productivity is less evident. However data from CIBSE (1998) shows that perceived productivity can be increased by 30% for a high degree of control. Occupants in naturally-ventilated buildings have a higher degree of perceived control over the environment compared to

occupants in buildings with only mechanical ventilation (Jones and West, 2001). Moreover, it has been shown (Kosik, 2001) that people prefer a wide range of indoor temperatures that have a direct correlation to outdoor temperatures. People also have less tolerance to temperature deviations in sealed, air-conditioned buildings: in fact, they tend to be two times as sensitive to temperature fluctuations.

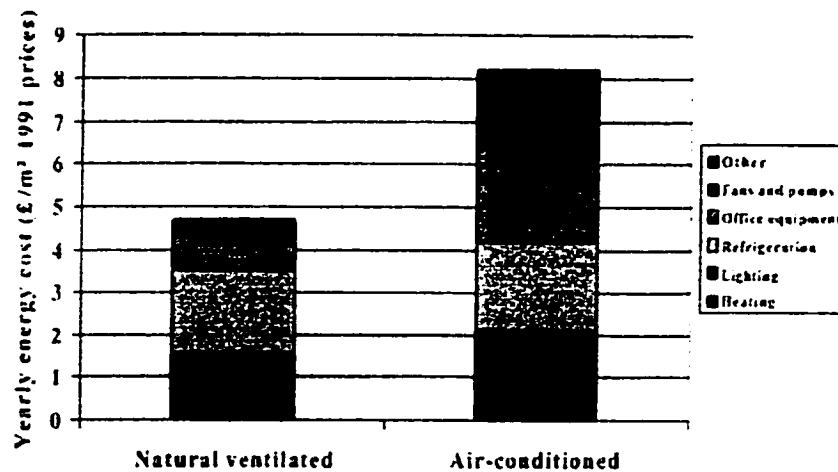


Fig. 2.1. Energy savings by using natural ventilation (CIBSE, 1998).

### 2.3 Natural ventilation strategies

There are two major natural ventilation types, namely: single-sided and cross natural ventilation. Single-sided natural ventilation occurs when the building communicates with the outdoor environment through one or more openings located on the same exterior wall; cross ventilation occurs when there are openings on opposite building walls. When employing natural ventilation, the building form is an important consideration. For example, according to CIBSE (1997) and Gan (2000), single-sided ventilation can be effective to a room depth of about two to two and half times the height of the space.



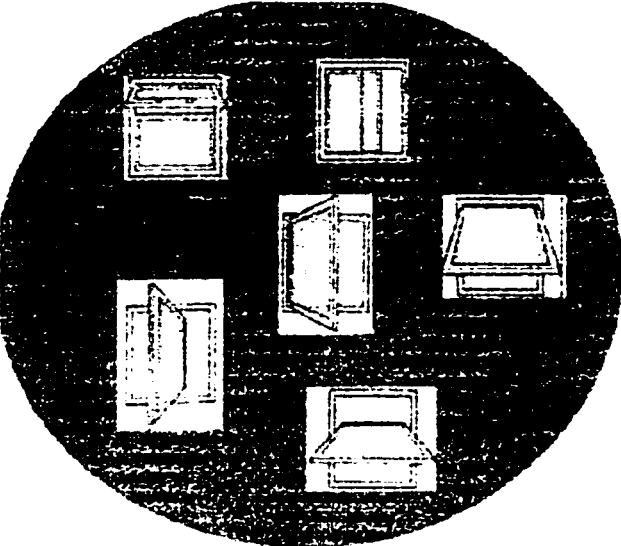
Cross ventilation is effective to a depth of about five times the height of the space, suggesting the need for a spatial arrangement and building plan depth consistent with these dimensions.

In natural ventilation systems, fresh air is provided through openings, and there is a wide range of possibilities with regard to selection of opening type and position in the façade. The most common, are different window types (e.g. simple opening, vertical-vane opening, horizontal-vane), fixed and operable screens such as grills, louvres, rolling and venetian blinds, exhaust chimneys, shafts and ducts, envelope and door vents, trickle ventilators. Different flow patterns are developed for various opening types and positions resulting in different values of ventilation capacity, controllability, impact on comfort, security and integration with solar control strategies (CIBSE, 1997).

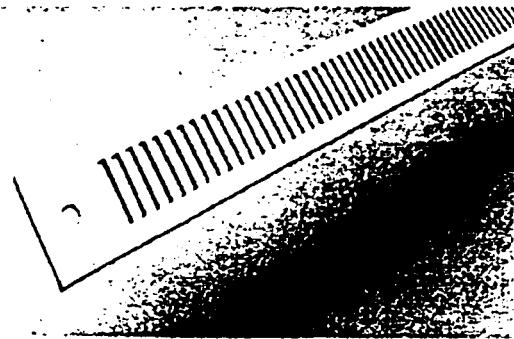
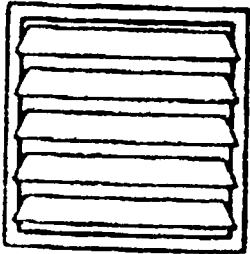
The use of openings as inlets and outlets suggests the need for proper design, sizing and placement. Operable windows with appropriate selection of size and type is a widely used solution, but drafts, building security and noise are disadvantages. Therefore, to avoid the previous concerns a carefully designed opening in a wall should be as small as possible (Jones, 2001).

As pointed out by Wouters et al (1999), the devices to be used for IAQ and summer comfort control are quite different. Effective night ventilation, which is used for cooling in most of the cases, requires rather high air flow rates in comparison with ventilation for IAQ control. Ventilation stacks or chimneys are currently a popular inclusion in modern, low energy ventilation design (Riain and Kolokotroni 2000, Battle et al 2000). Ventilation stacks (wind and thermal chimneys) exist in various forms with the purpose of increasing ventilation during summer months, so that some cooling is provided during

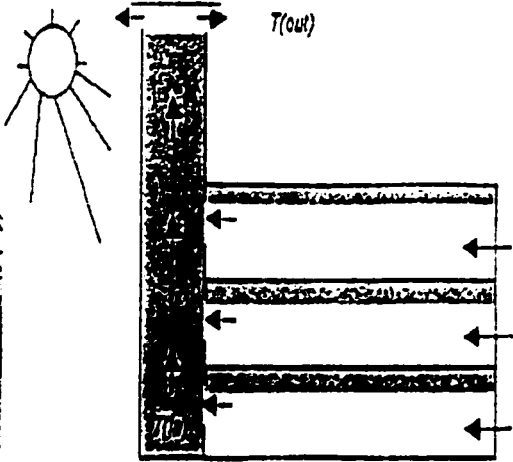
the day or by utilizing night ventilation. Figure 2.2 illustrates several types of openings that are utilized for IAQ or passive cooling purposes.



*Louvres*



Grills



Solar chimney

Fig. 2.2. Natural ventilation configurations (CIBSE, 1997)

## **2.4 Driving mechanisms**

Utilization of natural ventilation requires an appropriate understanding of principles of building pressurization. Two pressure-driving mechanisms must be considered for the natural ventilation to perform properly: the temperature difference across the opening (buoyancy or stack effect) and the wind. The interaction of these parameters creates pressure differences across the openings driving the air inside/outside the ventilated space. The indoor-outdoor pressure difference at a location depends on the magnitude each of the driving mechanisms as well as on the characteristics of the openings in the building envelope i.e. their locations and the relationship between pressure difference and air flow for each opening.

### **2.4.1 Wind pressure**

With reference to the static pressure of the wind upstream of an opening, the time-average pressure due to the wind flow,  $P_w$  (Pa), on a surface is given by Bernoulli's equation:

$$P_w = \frac{1}{2} \cdot C_{pe} \cdot \rho \cdot V^2 \quad (2.1)$$

where  $C_{pe}$  is the mean external pressure coefficient,  $\rho$  ( $\text{kg/m}^3$ ) the air density and  $V$  (m/s) the mean wind speed at the height of the building or the opening. The pressure coefficient is normally derived from pressure measurements in wind tunnels using reduced-scale models of buildings or by field experiments. The value of  $C_{pe}$  at a point on the building surface is determined by the building geometry, the wind velocity (speed and direction) relative to the building, the location of the building relative to other buildings, the topography and roughness of the upstream terrain in the wind direction. In general  $C_{pe}$  is

positive on the windward side of a building and negative on the leeward side. Figure 2.3 illustrates the pressure induced on the building envelope due to the wind. In reality the pressure distribution in the building envelope due to the wind is not uniform and what is shown in figure 2.3 is a simplified version. The magnitude of the pressure differences found on the surfaces of buildings varies rapidly with time because of turbulent fluctuations in the wind and the wake of the flow structure. The phenomenon of air exchange rate due to turbulent wind pressure has been observed by many researchers and it was found that this is due to pulsating flow, penetration of eddies and static or molecular diffusion. The effect of fluctuating air flow is especially significant when the mean pressure differences across openings are low while their turbulent components are large. An approach using the spectrum analysis technique was proposed by Haghight et al (1991) to model the pulsating flows through openings of a building. However, the use of average wind pressures to calculate pressure differences is usually sufficient for the evaluation of average air flow rates (Etheridge and Sandberg, 1996).

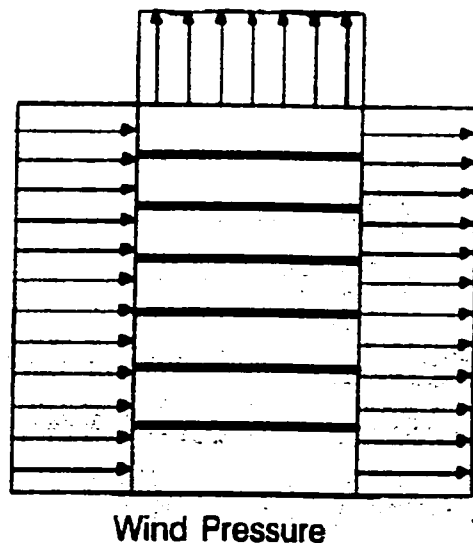


Fig. 2.3. Wind-induced pressure (ASHRAE, Fundamentals, ch.26, 2001).

The wind-induced indoor-outdoor pressure difference can be found using the coefficient  $C_{p(in-out)}$ , which is defined as:

$$C_{p(in-out)} = C_{pe} - C_{pi} \quad (2.2)$$

where  $C_{pe}$  is the external pressure coefficient and  $C_{pi}$  the internal pressure coefficient. The magnitude of the internal pressure depends primarily on the distribution of vents or openings in relation to the external pressure distribution. In the ideal case of a hermetically sealed building, the internal pressure is not affected by the external wind flow (Figure 2.4a). In most cases the opening or porosity distribution over the building envelope is not known and internal pressures could be either positive or negative (Figure 2.4d). For a building with uniformly distributed air leakage sites in all the walls  $C_{pi}$  is about  $-0.2$  (ASHRAE, Fundamentals, ch.16, 2001). A building with dominant venting on the windward side is under positive pressure (Figure 2.4 b), while building pressures are negative with dominant venting within the wake region (Figure 2.4c) (Simiu and Scanlan, 1977).

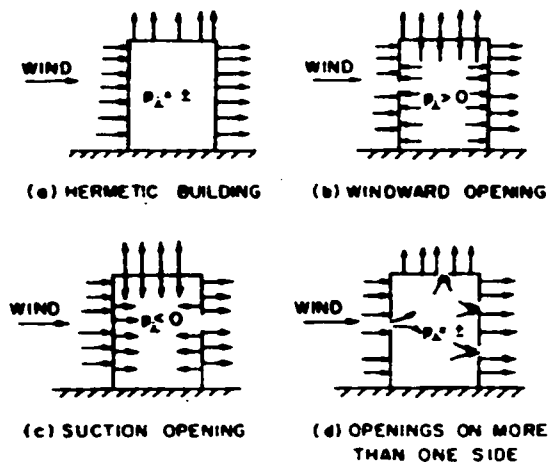


Fig. 2.4. Mean internal pressures in buildings with various opening distributions (Liu and Saathoff, 1982).

In a steady state the internal pressures can be computed from knowledge of the external pressure distribution and the size, shape and distribution of vents or openings. In the steady state, the inflow and outflow must balance. The flow through a wall of total open area  $A$ , subject to some uniform external pressure  $P_e$  and internal pressure  $P_i$  is given by:

$$Q = C_D \cdot A \cdot \left[ \frac{2 \cdot (P_e - P_i)}{\rho} \right]^{0.5} \quad (2.3)$$

where  $C_D$  is the discharge coefficient. If the pressures are expressed in terms of coefficients using equation (2.1), then:

$$Q = C_D \cdot A \cdot V \cdot (C_{pe} - C_{pi})^{0.5} \quad (2.4)$$

The value of  $C_{pi}$  can be computed from a knowledge of the values  $C_D$ ,  $A$  and  $C_{pe}$  for each external surface by use of the mass balance equation (Aynsley et al. 1977):

$$\sum Q = 0 \quad (2.5)$$

The effect of various opening configurations in the internal pressure was investigated in an extensive experimental wind tunnel study that was carried out by Stathopoulos et al (1979). Figure 2.5 shows the variation of the internal pressure coefficient with the opening area of a windward wall opening for different values of the background porosity. The opening area is expressed as a percentage of the surface area of the windward wall. It was found that for background porosity 0%, the internal pressure coefficient is about 0.7 for any opening area, while for background porosity 0.5%, the internal pressure coefficient is constant at value of about 0.7 for any opening area more than 10%.

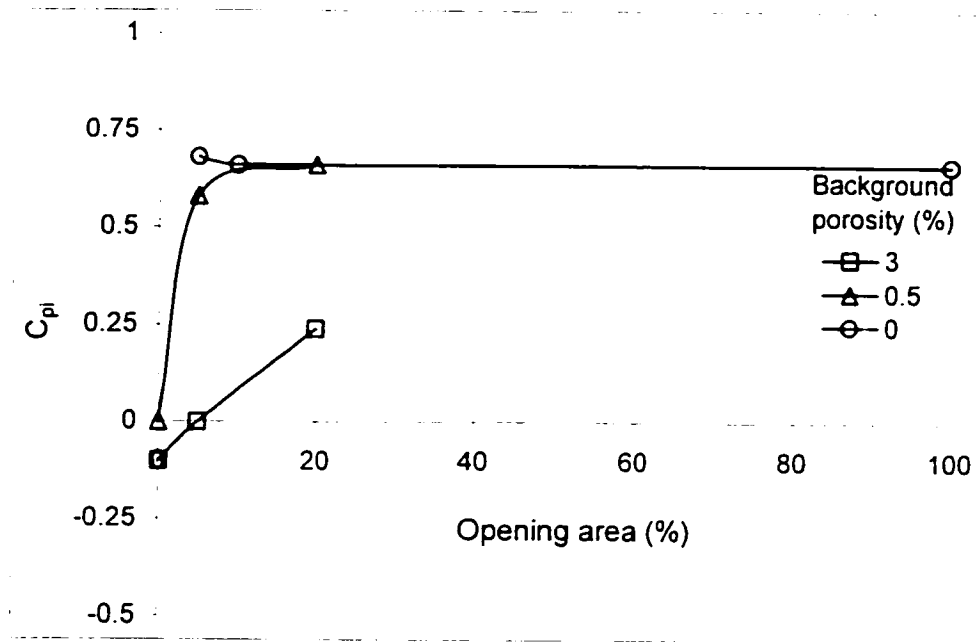


Fig. 2.5. Mean internal pressure coefficient as a function of the opening area for different background porosities in the case of suburban exposure (Stathopoulos et al. 1979).

#### 2.4.2 Stack pressure

The pressure due to buoyancy (stack effect) arises from the difference in temperature, hence density, between the air inside and outside of an opening. The variation of air density with temperature produces pressure gradients both within the internal and external zones. During the heating season, the warmer inside air rises and flows out of the building near its top and it is replaced by colder outside air that enters the building near its base. During the cooling season the flow directions are reversed. Figure 2.6 shows the pressure distribution over the building due to stack effect during the heating season, assuming uniformly distributed openings of the same air flow resistance, and no resistance to vertical air flow within the building.

The height at which transition between inflow and outflow occurs is the neutral plane where the pressures inside and outside are equal. In practice, the position of the neutral plane level (NPL) at zero wind speed is a structure-dependent parameter that depends only on the vertical distribution of openings in the envelope, the resistance of the openings to air flow, and the resistance to vertical air flow within the building. If the openings are uniformly distributed vertically, they have the same resistance to air flow, and there is no internal resistance, the NPL is at the mid-height of the building. The NPL in tall buildings varies from 0.3 to 0.7 of the total building height. For small buildings and especially buildings with chimneys, the NPL is usually above mid-height. Internal partitions, stairwells, elevator shafts, utility ducts, chimneys and mechanical supply and exhaust systems complicate the analysis of NPL location (ASHRAE, Fundamentals, ch.26, 2001). In general, exhaust systems increase the height of the NPL and outdoor air supply systems lower it (Etheridge and Sandberg, 1996). The pressure difference due to buoyancy (Pa) is given by:

$$\Delta P_s = \rho \cdot g \cdot (H_{NPL} - h) \cdot \frac{T_i - T_o}{T_i} \quad (2.6)$$

where  $\rho$  is the air density ( $\text{kg/m}^3$ ),  $g$  the gravitational acceleration ( $\text{m/s}^2$ ),  $H_{NPL}$  the height of the neutral pressure level (m),  $T_i$  the internal temperature,  $T_o$  the external temperature ( $^{\circ}\text{K}$ ) and  $h$  the height from ground level (m). Equation (2.6) provides a maximum stack pressure difference, given no internal resistance. In a building with airtight separations at each floor, each floor acts independently, with its own stack effect being unaffected by that of any other floor. Real multi-storey buildings are neither open inside nor airtight between stories. Vertical air passages, stairwells, elevator shafts, etc, allow air flow between floors. In that case the total stack effect of the building remains the same as that



with no internal flow resistance, but some of the total pressure difference maintains flow through openings in the floors and vertical shafts. As a result, the pressure difference across the exterior wall at any level is less than it would be with no internal flow resistance (ASHRAE Fundamentals, ch.26, 2001).

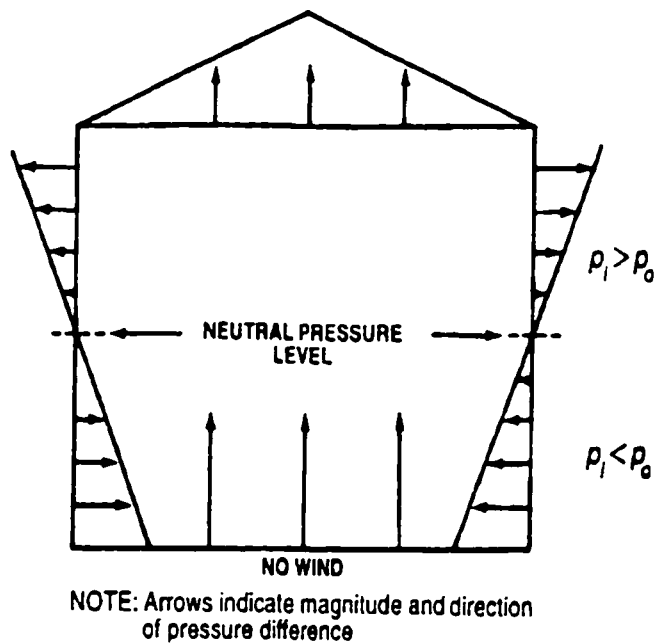


Fig. 2.6. Stack-induced pressure (ASHRAE, Fundamentals, ch.26, 2001).

### 2.4.3 Combining driving forces

The pressure fields illustrated in Figures 2.3 and 2.6 indicate that the wind and stack effects can be combined by simply adding the pressures. Because this pressure addition can cause directional changes in the resulting flow, the flows cannot be combined as simply. An accurate superposition of the two effects requires detailed knowledge of the two pressure fields (Hutcheon, 1983). For typical buildings the following equation can be used to combine wind and stack effects:

$$Q_{ws} = \sqrt{Q_w^2 + Q_s^2} \quad (2.7)$$

where  $Q_w$  ( $\text{m}^3/\text{s}$ ) is the air flow due to the wind assuming zero temperature difference,  $Q_s$  ( $\text{m}^3/\text{s}$ ) the flow due to stack effect assuming zero wind speed, and  $Q_{ws}$  ( $\text{m}^3/\text{s}$ ) the combined air flow. Equation (2.7) is derived using the orifice equation (2.3) considering that the total pressure difference is equal to the summation of the wind and stack pressure. This equation should be used only for turbulent flow; for laminar flow, the flow exponent is equal to one – see equation (2.11) and the combined air flow can be found by simply adding the flow due to the wind and the stack effect. Another way to calculate the air flow due to the combined effect is to calculate the air flow rates when the wind and stack effect act separately and take the larger of the two values. According to Etheridge and Sandberg (1996), the first way is more accurate.

The relative importance of the wind and stack pressures in a building depends on building height, internal resistance to vertical air flow, location and flow resistance characteristics of envelope openings, local terrain, and the immediate shielding of the building. The taller the building and the smaller its internal resistance to air flow, the stronger the stack effect will be. The more exposed the building, the more susceptible it will be to wind (Wagdy, 2001).

Equation (2.7) provides the combined air flow due to the wind and stack effect assuming no operation of mechanical equipment in the building. The operation of mechanical equipment, such as supply/exhaust systems and vented combustion devices, affects pressure differences across the building envelope. Mechanical systems can change the flow through envelope openings by affecting the internal pressure. The effect of mechanical ventilation on envelope pressure differences is complex and depends on both

the direction of the ventilation flow (exhaust or supply) and the differences in these ventilation flows among the zones of the building. In general, supply fans create positive pressure inside the building while exhaust fans create negative internal pressure. Figure 2.7 illustrates the fan pressure in the building envelope when the interior of the building is pressurized due to the mechanical system. When both supply and exhaust fans are present, the mechanical ventilation can be broken up into the amount of ventilation flow that creates no change in pressure distribution, or the balanced part:

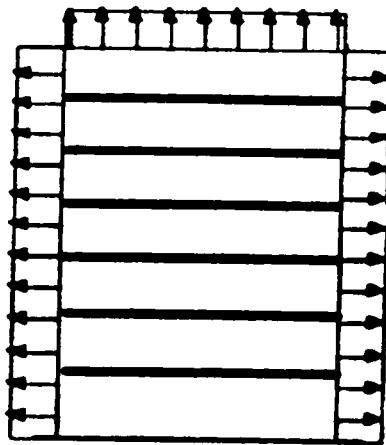
$$Q_{bal} = \text{Minimum}(Q_{sup}, Q_{exh}) \quad (2.8)$$

and an unbalanced part that does affect the pressure distribution (Awbi, 1991):

$$Q_{unbal} = \text{Maximum}(Q_{sup}, Q_{exh}) - Q_{bal} \quad (2.9)$$

In that case the total flow is given by the following equation:

$$Q_{total} = Q_{bal} + \sqrt{Q_w^2 + Q_s^2 + Q_{unbal}^2} \quad (2.10)$$



**HVAC Fan Pressure**

Fig. 2.7. Fan pressure (Wadgy, 2001).

## **2.5 Air flow through openings**

At present most standards are descriptive and there is no direct specification of the required air quality; only indirectly by specifying the required flow rates. The primary requirement of a ventilation system is to realise an acceptable indoor air quality or, if the air flow rates are specified, to meet the specified air flow rates (Wouters et al, 1999). In general, the air flow through an opening is dependent on: (i) the size of the opening, (ii) the leakage characteristics of the opening and (iii) the pressure difference across it. For the evaluation of the air flow through an opening it is essential that all these three influential factors be known.

Prediction of the air flow rate in naturally-ventilated buildings is very important for the calculation of the thermal response of the buildings, as well as for ensuring appropriate air renewal rates for a healthy building environment. Due to its importance, this issue has been given a lot of attention and significant effort has been put into the development of theoretical models and experimental techniques for the evaluation of the air flow rate in natural ventilation configurations.

## **2.6 Mathematical models**

Mathematical models for the air flow prediction include empirical, network and CFD models.

### **2.6.1 Basic equations**

The most common equation describing the air flow through an opening is the orifice equation, which is based on the Bernoulli equation with steady incompressible flow. This

equation can be used for a relatively large opening area (typical dimension larger than 10 mm), such as a vent or a large crack. In that case, the flow tends to be turbulent under normal pressures and the flow rate,  $Q$  ( $\text{m}^3/\text{s}$ ), is proportional to the square root of the pressure difference as already mentioned in section 2.4.1:

$$Q = C_D \cdot A \cdot \left( \frac{2 \cdot \Delta P}{\rho} \right)^{0.5} \quad (2.3)$$

where  $C_D$  is the discharge coefficient of the opening,  $A$  the flow area ( $\text{m}^2$ ),  $\Delta P$  the pressure difference across the opening (Pa) and  $\rho$  the air density ( $\text{kg}/\text{m}^3$ ). The discharge coefficient  $C_D$  is a dimensionless number that depends on the geometry of the opening and the Reynolds number of the flow, and includes the influence of contraction and friction. For turbulent flow,  $C_D$  is constant at a fixed Reynolds number and therefore, the flow is proportional to square root of  $\Delta P$ . For a sharp-edge orifice flow the discharge coefficient is almost independent on the Reynolds number and has a value between 0.6 and 0.65. However, in most of the cases  $C_D$  appears to be variable because of the geometry of the openings and the variation in pressure difference with the environmental conditions inside and outside the building (Awbi, 1991).

For extremely narrow openings (cracks) the flow within the opening is essentially laminar. In such cases the flow rate ( $\text{m}^3/\text{s}$ ) is given by the Couette flow equation:

$$Q = \frac{b \cdot h^3}{12 \cdot \mu \cdot L} \cdot \Delta P \quad (2.11)$$

where  $b$  is the length of crack (m),  $h$  the height of crack (m),  $L$  the depth of crack in flow direction (m) and  $\mu$  the dynamic viscosity of air (Pa.s). This equation is derived from the so-called Hagen-Poiseuille law for laminar flow in tubes:

$$h_L = 32 \cdot \frac{\mu}{g \cdot \rho} \cdot \frac{L}{D^2} \cdot V \quad (2.12)$$

where  $h_L$  is the head lost in friction,  $V$  the velocity,  $g$  the gravitational acceleration,  $\rho$  the air density, and  $L$  and  $D$  the length and the diameter of the pipe respectively. For laminar flow, the discharge coefficient is dependent on the Reynolds number ( $Re = \rho \cdot V \cdot L / \mu$  or  $Re = \rho Q / \mu \cdot L$ ); for that reason the dynamic viscosity  $\mu$  appears on the right side of equation (2.11). The influence of viscosity and the dependence on Reynolds number arise from the passage of the flow between the walls of the openings. Increasing the flow rate, the Reynolds number increases and leads to a reduced dependence of  $C_D$  on Reynolds number. This is partly due to the pressure changes in the inlet region, but also due to the turbulence. When turbulence exists, the wall shear stress is largely determined by the apparent stresses arising from turbulent momentum transport and the effect of viscosity is reduced (Etheridge and Sandberg, 1996).

For wider cracks the flow is usually neither laminar nor fully turbulent but in the transition region. The flow ( $m^3/s$ ) is given by a power-law equation of the form:

$$Q = C \cdot (\Delta P)^n \quad (2.13)$$

Where  $C$  is the flow coefficient ( $m^3/s/Pa^n$ ),  $\Delta P$  the pressure difference across the opening (Pa) and  $n$  a dimensionless flow exponent. The flow coefficient is dependent on the opening geometry. The flow exponent is dependent on the flow regime and acquires a value of 0.5 for fully turbulent flow and 1 for laminar flow. However, in practice the value of  $n$  for several types of openings tends to be between 0.5 and 1. Assuming turbulent flow ( $C_D = \text{constant}$  and  $n = 0.5$ ), comparison between the equations (2.3) and (2.12) leads to the following equation:

$$C = C_D \cdot A \cdot \sqrt{\frac{2}{\rho}} \quad (2.14)$$

### 2.6.2 Empirical models

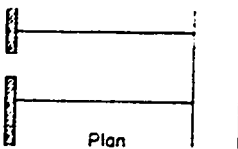
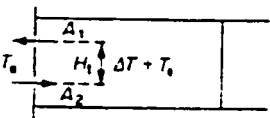
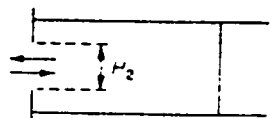
These are simplified procedures based on empirical data which can produce estimates of air flow rates and calculation of natural ventilation in single-zone buildings. Assuming a two-dimensional flow through a building and ignoring internal partitions, B.S 5925 (1980) gives tables of formulas for calculating the air flow rate due to the wind and buoyancy for openings on the same wall (single-sided ventilation) and openings on opposite walls (cross ventilation). Tables 2.1 and 2.2 show schematically the expected air flow patterns for different conditions and give the formulas used for calculating the air flow rate for each case.

Table 2.1. Formulas for cross ventilation (Awbi, 1991).

Conditions	Schematic representation	Formula
a) Wind only		$Q_w = C_d A_w V \sqrt{\Delta C_p}^{1/2}$ $\frac{1}{A_w^2} = \frac{1}{(A_1 + A_2)^2} + \frac{1}{(A_3 + A_4)^2}$
b) Temperature difference only		$Q_b = C_d A_b \left( \frac{2 \Delta T_g H_1}{\bar{T}} \right)^{1/2}$ $\frac{1}{A_b^2} = \frac{1}{(A_1 + A_2)^2} + \frac{1}{(A_3 + A_4)^2}$ $\bar{T} = \frac{1}{2} (T_e + T_i)$
c) Wind and temperature difference together		$Q = Q_b$ <p>for <math>\frac{V}{\sqrt{\Delta T}} &lt; 0.26 \left( \frac{A_b}{A_w} \right)^{1/2} \left( \frac{H_1}{\Delta C_p} \right)^{1/2}</math></p> $Q = Q_w$ <p>for <math>\frac{V}{\sqrt{\Delta T}} &gt; 0.26 \left( \frac{A_b}{A_w} \right)^{1/2} \left( \frac{H_1}{\Delta C_p} \right)^{1/2}</math></p> $\Delta T = T_i - T_e$

In Tables 2.1 and 2.2  $C_d$  is the discharge coefficient,  $V$  is the wind speed,  $\Delta C_p$  is equal to  $|C_{p1} - C_{p2}|$ ,  $\Delta T$  is the inside-outside temperature difference and  $g$  the gravitational acceleration. In the Table 2.2, it is assumed that when the wind and stack effect are of the same order of magnitude, to a first approximation, the larger of the two rates may be taken. As has been already discussed in section 2.4.3, it is more accurate to calculate the combined effect by using the equation (2.7).

Table 2.2. Formulas for single-sided ventilation (Awbi, 1991).

Conditions	Schematic representation	Formula
a) Due to wind		$Q = 0.025 AV$
b) Due to temperature difference with two openings		$Q = C_d A \left[ \frac{\epsilon \Delta T}{1 - \epsilon; 1 + \epsilon^2} \right] \left[ \frac{\Delta T g H_{eq}}{T} \right]^{1/2}$ $\epsilon = \frac{A_1}{A_2}; A = A_1 + A_2$
c) Due to temperature difference with one opening		$Q = C_d \frac{A}{3} \left[ \frac{\Delta T g H_{eq}}{T} \right]^{1/2}$

There are many other models e.g. the Building Research Establishment (BRE) model, 1980, the Lawrence Berkeley Laboratory (LBL) model, 1982 etc. All these provide estimations of the global air flow rate, using correlation equations but they give no information on the individual flow rates or the air velocity fields in the ventilated spaces.



Furthermore, the fact that the proposed formulas referred to specific geometrical configurations and were derived from a certain number of experiments in wind tunnels or in the field but under specific conditions restricts their applicability.

### 2.6.3 Network models

Network modelling is based on the solution of the mass balance equation for the calculation of the pressure at discrete nodes representing the simulated zones. Two basic types have been developed: single-zone and multi-zone models. In the single-zone modelling approach, the interior of the building is considered as one zone and it is represented by a single node; in the multi-zone approach, the building is subdivided into a number of zones represented by an equivalent number of nodes. Models of this category can be used for simulations of naturally-ventilated buildings to provide information on the individual air flows in each simulated zone, as well as through each opening. In a multi-zone model, the mass balance equation assuming  $j$  flow paths may be written as follows:

$$\sum_{i=1}^j \rho_i \cdot Q_i = 0 \quad (2.15)$$

where  $Q_i$  ( $\text{m}^3/\text{s}$ ) is the volumetric flow rate through  $i$ th path, and  $\rho_i$  ( $\text{kg}/\text{m}^3$ ) the density of air flowing through  $i$ th path. Equation (2.14) is a generalization of equation (2.5), which assumes incompressible flow ( $\rho = \text{constant}$ ).

Many models of this type have recently been developed because they are easy to use and require simple input data. Some of them are: NatVent (Svensson and Aggerholm, 1998), COMIS (Feustel et al, 1990), AIRNET (Walton, 1988), BREEZE (BRE, 1992).

ESP (Clarke, 1993), NORMA (Santamouris, 1994), PASPORT-AIR (Dascalaki and Santamouris, 1995), CONTAM93 (Walton, 1993), DOE-2 (Lawrence Berkeley Laboratory, 1993).

Kronvall et al (1998) using the NatVent program determined the parameters that have the largest influence on the performance of natural ventilation. The interaction between different parameters is also discussed. An air flow and thermal model are coupled together in this model, which can be used in the early design process, to determine possible restrictions in the use of natural ventilation in an office building. The study concluded that the natural ventilation performance is better for:

- Tall buildings
- Airtight buildings
- Well insulated envelopes
- High thermal mass
- Large area of adjustable façade vents
- Limited internal heat loads
- Night ventilation
- Active use of windows
- Effective solar shading.

Ajiboye (1998a and 1998b) using NatVent, developed a design tool to suggest suitable air inlets for buildings in polluted urban areas, in order to reduce the impact of external pollution on air quality within buildings. These involve selection and suitable location of intakes to office buildings. Several types of openings, like inlets with noise and particle attenuation, and inlets that can be closed during peak traffic periods were considered.

Ternoveanu (1998) using the TRNSYS software developed two multi-zone natural ventilation models for dwellings to investigate the impact of different ventilation strategies on the building cooling load. The first model used for simulating natural ventilation was based on a default air change rate for one zone which is adjusted as a function of wind speed and zone occupancy in order to simulate buildings minimum hygienic air renewal requirements. In the second model the stack effect is also considered and the two driving forces (wind and stack effect) are related to the zone temperature. It was found that an unacceptable overheating in the occupied zone occurs by using the first model, while the second model provides an efficient natural cooling. It was also shown that the cooling effect is 5 to 6 times higher using the second model and an adequate strategy (night cooling). A sensitivity analysis was carried to study the influence of different parameters of the second model. Although, the stack effect was the main driving force, the wind smaller influence cannot be generalized, as it is varying for different building types and environmental conditions.

Haghighat and Megri, 1996 carried out a comprehensive validation of two models: COMIS and CONTAM. The validation processes was carried out at three different levels: inter-program comparison, validation with experimental data, which was collected in a controlled environment, and finally, validation with field measurement data. At the inter-program level, the air flow rates and pressure values predicted by COMIS and CONTAM for a four-zone paper building were compared with the air flow rates and pressures predicted by CBSAIR, AIRNET and BUS. The results showed good agreement between these software programs. Fan depressurization, smoke and tracer gas tests were conducted to estimate the permeability of building envelope components, to locate the

cracks, and to determine the interzonal air flow rates between rooms. The results confirm that there is a good agreement between predictions made by COMIS and CONTAM; there are, however, some differences between these models' predictions and the measured data. The predictions made by these models were also compared with the results of a tracer gas measurement carried out in a residential building and the predicted and measured values were in good agreement.

Dascalaki et al (1995) compared the results of a full experimental study on the performance of single-sided natural ventilation configurations with the predictions of existing network models like AIRNET, BREEZE, COMIS, ESP, NORMA, and PASSPORT-AIR. Totally 52 single-sided ventilation configurations were tested and the measured flow rates were compared with those predicted by using the network tools. Similar values were predicted by all tools for each experiment, since all tools use the same technique and equations to predict the air flow, but the predicted flow rates were far from the mean measured values due to the use of the same discharge coefficient for any opening configuration ( $C_D = 1$ ). Thus, for each experiment and tool, a correction coefficient  $CF$ , defined as  $CF = \text{Mean measured air flow}/\text{predicted air flow}$ , was calculated. The calculated correction coefficient for each experiment and tool is equal to the value of the discharge coefficient necessary to make equal predicted and measured air flow rates.

In general, the network modelling approach assumes that the pressure in each of the simulated zones varies almost linearly around a reference value. In the case of single-sided natural ventilation, where the non-uniform and almost random pressure difference caused by the wind is a very important characteristic, this assumption is not valid; this is

why common network models fail to predict with accuracy the air flow rate (Dascalaki et al, 1999).

Herrlin (1999) discusses the importance of any model validation by comparing the values produced against actual measurements. A major obstacle in validating a model is that dynamic effects cannot be modeled. Dynamic effects are typically caused by changes in wind velocity and/or direction and doors that are opened or closed.

#### 2.6.4 CFD models

Prediction of the air velocity field in a naturally-ventilated space is an important issue, when one addresses the problems of thermal comfort or the removal of the indoor air pollution. In most of the studies involving the determination of an air velocity field, the adopted mathematical approach is that of computational fluid dynamics (CFD). Computerized methods based on numerical fluid dynamics methods, widely referred to as CFD models, represent the ultimate deterministic approach and permit calculation of the air velocity and temperature in the studied zones by solving the system of Navier-Stokes equations combined with an appropriate turbulence model that best describes the problem. Navier-Stokes (NS) equations are analytical expressions in partial differential form (PDE), describing the basic space-time relationships between mass, velocity and temperature. The PDE system may be directly applied to description of laminar flow fields only, however, almost all room air flows are at least locally turbulent. For predicting turbulent flow, a mathematical manipulation on the NS equations, called Reynolds-averaging, is required.

CFD can be used to predict the air movement and temperature distribution arising from sources of momentum (i.e. jets), surface heat transfer and pressure boundaries (i.e. natural ventilation) and can account for the effects of blockages due to the geometry of the space and its contents. CFD can predict 3-dimensional effects that are either constant or variable over time (Clements-Croome, 1997). In fact, CFD can predict fluid levels and pressure differences to low levels that are essentially impossible to measure experimentally. However, a CFD model constitutes the culmination of a large number of assumptions and approximations, and the answer to the question of accuracy can be very dependent on the assumptions made and the boundary conditions selected. Therefore, since no CFD room air simulation can be exact, a range of CFD simulations must be conducted to verify solution sensitivity to closure model parameters and boundary conditions embedded in the selected system. Comparison with measured data is another mean of CFD validation (Baker et al, 1997).

Dascalaki et al (1999) compared the results of a full-scale experimental study on the performance of single-sided natural ventilation configurations with the predictions of the PHOENICS (Cham, 1995) CFD model. The experiments were carried out to measure the air velocity field inside the openings. It was shown that that the predicted and measured values were not in good agreement. The application of models of this type was found quite complex and requires detailed input data that are not always available.

## **2.7 Experimental techniques**

Measurement techniques are the fundamental means of acquiring a greater understanding of air flow and ventilation in existing buildings as they provide a

quantitative assessment of the air flow characteristics of several opening types. The most common methods used are tracer gas techniques, pressurization/depressurization techniques and smoke tests.

Full-scale ventilation measurements were carried out by Dascalaki et al (1995), (1996) using the single tracer gas decay technique. The air change rate of several single-sided ventilation configurations was measured under different weather conditions. Measurements of the air velocity were also carried out as an alternative way to measure the air flow rate through an opening.

Two types of shading devices and in particular, movable vertical and horizontal louvers were tested by Tsangrassoulis (1997). The ventilation effectiveness of these devices was investigated using the single tracer gas decay technique. Yakubu and Sharples (1991) investigated the air flow characteristics through a system of modulated louvers. They carried out experiments in a pressurization chamber and they studied the pressure drop due to the presence of louvers. Finally they proposed quadratic expressions to describe the relationship between the pressure drop and the air flow rate through the louver system.

A series of laboratory investigations to characterize three window types were carried out by Heiselberg et al (1999). Single-sided and cross ventilation configurations were tested under the influence of the stack effect. The air flow in a naturally-ventilated room was investigated by smoke tests for both single-sided and cross ventilation configurations, for all three window types. Another experimental study was carried out by Heiselberg et al (2002) with the purpose of investigating the impact of different opening strategies on thermal comfort conditions in the occupied zone. Velocity and

pressure measurements were carried out and the discharge coefficient values were calculated, for different window configurations and for two temperature differences (0 and 10 °C). It was found that the discharge coefficient varies with the configuration, the opening area, the temperature and the pressure difference. The study found that different window opening strategies result in quite different air flow and thermal comfort conditions, which are a result of a multivariable impact. Detailed descriptions of the flows involved are complex and the geometrical shape of the window opening is important for the flow characteristics. Finally, the study found that the Archimedes number describes the flow for a certain geometry (it should be mentioned that the Archimedes number describes the forces of buoyancy divided by the forces of inertia).

A field study was carried out by Kolokotroni et al (1995) during the heating season, to study the natural ventilation effectiveness of trickle ventilators when they are used in office buildings. Varying levels of occupancy were simulated by constant CO<sub>2</sub> injection (to simulate metabolic rate) and heat sources (lamps). Internal measurements were carried out, including the monitoring of CO<sub>2</sub> levels, air velocity and temperature. It was found that trickle ventilators with a minimum openable area of 400 mm<sup>2</sup> per m<sup>2</sup> of floor area can provide adequate fresh air during winter, in a typical office room with maximum occupancy density of 8 m<sup>2</sup> floor area per person. When the trickle ventilators were open the CO<sub>2</sub> level did not exceed 1000 ppm if the correct sized ventilator was used for the occupancy of the office. When the trickle ventilators were closed, the CO<sub>2</sub> level was higher. Cold drafts did not appear to be a problem since the measured velocities were below the accepted level for comfort (0.3 m/s).



## **2.8 Recent developments in natural ventilation - Controls**

Apart from the required air flow, in practice, a whole range of other “secondary” requirements have to be fulfilled before one can consider that a ventilation system has a good performance (Wouters et al. 1999). The secondary requirements include:

- Energy use: should be as low as possible for the required air flow rates
- Thermal comfort, which is dependent on the selected opening type and the available pressure across it, the natural ventilation strategy, and the outdoor conditions
- Acoustics: noise levels should be below acceptable limits
- Ease of operation and controllability
- Ease of maintenance
- Aesthetics: it must be possible to integrate the system in the building in an aesthetic way.

During the last two decades interesting new devices and controls have been developed in order to satisfy all the previous requirements. Size and control of inlets have become vital elements in design. Several types of passively controlled openings can be considered such as:

- Pressure-controlled
- Humidity-controlled
- Pollutant-controlled
- Temperature-controlled

The most commonly used are the pressure-controlled inlets which are designed to supply a constant natural air flow independent of wind and stack pressure differences. Depressurization tests carried out by de Gids (1997) showed that for different pressure-

controlled ventilator types, the pressure at which the air flow rate passing through becomes almost constant, varies from 1 to 20 Pa. Controllable air inlets that provide constant air flow even at values of  $\Delta P$  as low as 1 Pa are available in the market, and it appears that their performance is more satisfactory. The response time of the control of inlets has been found quite different. Some inlets respond almost immediately while others react only in a few minutes.

Apart from the passive controlled inlets that were discussed above, active controlled air inlets have been developed. With the help of a small motor the grid of the inlet is controlled. The advantage of this active type of control is of course the possibility of connection with a building management system (de Gids, 1997).

Knoll (1998) developed a system of Controlled Natural Ventilation (CNV program) based on a computer program that simulates ventilation. This program is based on a flow network model that simulates wind and stack effect, and calculates the air flow through various types of openings using the power-law equation and the mass balance equation. The control unit developed may control the air flow through grills and windows; while the main purposes are:

- to compensate for fluctuating forces (wind and temperature) so that the ventilation flows are kept near a set point value, independent of weather conditions;
- to optimize the air flow distribution in the building with the highest possible ventilation efficiency;
- to restrict ventilation openings when draft risks occur.

Evaluation of the system performance showed that the fully developed system has the potential to keep ventilation flows constant within 20% range, to improve IAQ and to prevent drafts.

## **2.9 Hybrid ventilation systems**

Mechanical and natural ventilation systems have been developed separately during many years. Mechanical ventilation has developed from constant air flow systems, through systems with extensive heat recovery, and demand controlled air flows to energy optimized low pressure ventilation systems. Natural ventilation has in the same period developed from being considered only as air infiltration through cracks and airing through windows, to be a demand controlled ventilation system with cooling capabilities, heat recovery and air cleaning possibilities. The focus in the development has for both systems been to minimize energy consumption while maintaining a comfortable and healthy indoor environment. The natural next step is to develop ventilation concepts that utilise and combine the best features from each system into a new type of ventilation system, the so-called Hybrid Ventilation.

Hybrid ventilation systems can be described as systems providing a comfortable internal environment using different features of both natural and mechanical ventilation systems at different times of the day or season or the year. In hybrid or two-mode systems the control is done automatically (Wouters et al. 1999). There are two main types of hybrid ventilation systems:

- Changeover (or Complementary) systems have spaces that are either totally in mechanical air conditioning or totally in natural ventilation mode.

- Concurrent or Zoned systems are designed to have concurrent operation of both the mechanical and natural ventilation systems. These systems are usually designed to have discrete zones that can either have mechanical or natural ventilation.

The main strategies in designing a hybrid ventilation system are Operable Windows, Integral Building Openings, Use of Atrium, Heat Stacks, Double-skin Glazing Systems, Fan Assist, and Low Pressure Air-Conditioning Components (Kosik, 2001).

Hybrid ventilation should be dependent on building design, internal loads, solar shading, exposed thermal mass, prevailing winds, life safety issues, control of infiltration, control of outdoor pollutants, natural driving forces, and season to fulfil the immediate demands to the indoor environment in the most energy-efficient manner (Heiselberg and Tjelflaat, 1999). A very robust building management system will be needed to control the operable windows, louvers, dampers, etc. and to integrate the operation of the mechanical system with the natural ventilation system (Kosik, 2001). As a result, the proper design of hybrid ventilation systems requires careful analysis and high level of systems integration. Moreover, for the design of a hybrid ventilation system the air flow rates should be simulated according to the climatic conditions and the building use.

Herrlin (1999) developed an air flow model that is capable of simultaneously assessing the air flows in a multi-zone building and its ventilation system under steady-state conditions. The performance of a typical hybrid ventilation system including inlet ventilation slots with fan assist was investigated and compared with that of a typical exhaust-supply ventilation system. It was found that the hybrid ventilation system allows a pressure hierarchy that is beneficial for controlling interzonal air flows and exfiltration. The system effectively isolates a contaminant source in an apartment. This hierarchy,

however, turns into a disadvantage since by closing ventilation slots, the air exchange rates for apartments on the upper floors can be substantially decreased. It was also found that closed ventilation slots elevated the pressure differences without reaching extreme values. The exhaust-supply ventilation system has the advantage of guaranteeing a minimum air exchange rate under all conditions: the stability of the air exchange rates, therefore, is higher for this system. The drawback of this system is that the air flows from apartments on the lower levels to apartments on the upper levels via a staircase.

Ad van der Aa (2002) carried out field measurements to evaluate the performance of a hybrid ventilation system including controllable air inlets and fan assistance, in a school building in Netherlands. The experiments were carried in two classrooms, including CO<sub>2</sub> and temperature monitoring, as well as depressurisation tests to evaluate the capacity of the installed inlets. In the first classroom only natural ventilation had applied while the second classroom was equipped with a hybrid ventilation system. It was found that the CO<sub>2</sub> concentration in the room with natural ventilation inlets was about 2000 ppm while the automatic control of the inlet grilles was not sufficient to keep the concentration below 1500 ppm. The hybrid-ventilated room did not exceed a CO<sub>2</sub> level of 1500 ppm due to the operation of the fan. The fan was switched on a CO<sub>2</sub> level of 1300 ppm providing a significantly better IAQ. The relationship between the fan operation hours and the wind speed was also investigated and it was found that the operation hours are decreased when the average wind speed increases. Drafts problems especially near the inlets were appeared and velocity measurements carried out to investigate the problem. Therefore, some adjustments were tested to improve the situation; it was found that a

labyrinth construction increases the air flow resistance of the inlets and the air velocity is reduced by 30%.

The thermal and aerodynamic processes occurring in a hybrid ventilated building are difficult to represent by a simple analysis tool. In addition, hybrid ventilation always stands for an interaction with a mechanical system in an intelligent way. Albrecht et al (2002) carried out an evaluation study of a coupled calculation for a hybrid ventilated school building in German. The main hypothesis behind was to use building simulation or zonal modelling (coupled thermal and air flow modelling) where it is sufficient (classrooms), and to use CFD for large spaces with complicated flow structures (e.g. atria). A night cooling situation, which was part of the ventilation strategy, was selected as fully coupled simulation case, e.g. all the models interactively work together within one calculation. The investigations showed satisfactory results for the classrooms but some uncertainties were observed in the atria. It was also found that a fully coupled calculation is the best way to represent all the phenomena and processes in a hybrid ventilated building. However, the expenses are very high and only a team of experts can handle such a simulation tool.

### **2.10 Trickle ventilators and research needs**

As mentioned previously (see section 2.3), different opening types have a variety of characteristics and different impact on the thermal conditions in the occupied zone and IAQ. It has been established that an opening should have the following characteristics for a satisfactory performance:

- It should provide adequate air flow even at low values of the pressure differential (the pressure differential across the building envelope is most of the time less than 5 Pa) to improve IAQ without significantly affecting the energy use to warm up the ventilated air.
- Good performance in terms of thermal comfort, preventing from drafts and potential discomfort of the occupants.
- Opening area as small as possible to avoid building security and noise problems.

In the previously mentioned studies of the ventilation performance of several inlet openings, very few are related to trickle ventilators (Kolokotroni et al 1995, de Gids, 1997). A field study has been performed to investigate trickle ventilators effectiveness by monitoring temperature and CO<sub>2</sub> concentration (Kolokotroni et al, 1995), but the results cannot be generalized because the experiments were carried out under specific climatic conditions (UK climate) and for a given building. An overview of the availability, performance and application of existing air flow inlets (fixed and controllable) has been carried out by de Gids (1997) but it provides only general information.

Therefore, an extensive experimental study to determine the leakage characteristics of regular (fixed) and pressure-controlled trickle ventilators, and to investigate their actual performance under the influence of the wind (full-scale measurements) is essential. In this way, appropriate selection criteria can be established to determine which type is better, and under which conditions it should be used, in order to improve the ventilation capacity, thermal comfort and IAQ.

Since experimental values for the leakage characteristics of trickle ventilators are not, so far, available in the literature, the orifice equation (2.3) is used for the calculation of

the air flow. For that reason, most of the existing air flow models fail to predict with acceptable accuracy the air flow through various types of openings (Dascalaki et al, 1999). Therefore an evaluation of the orifice equation with experimental values is essential.

Finally, by performing full-scale experiments it is impossible to investigate all the parameters (temperature, wind speed and direction, building location, opening height) that affect the trickle ventilators performance. Therefore, the development of a flow network model is required, which based on experimentally-deduced inputs (leakage characteristics), can be used to investigate the system integration in ventilation design of buildings.



## **CHAPTER 3**

### **EXPERIMENTAL MEASUREMENTS**

#### **3.1 Introduction**

In this chapter the experimental measurements are described. It was decided to carry out field instead of wind tunnel tests because the trickle ventilators are too large to be tested in a wind tunnel and therefore, similarity problems could have affected the results. As far as the CFD approach is concerned, the solution of Navier-Stokes equations can provide information about the air velocity distribution in a naturally-ventilated space but cannot provide information about the leakage characteristics of an opening. Furthermore, the required detailed input data are not available, and the accuracy can be dependent on the selected partial differential (PDE) form of Navier-Stokes equations and the boundary conditions. On the other side, field tests are closer to the real case in comparison to wind tunnel tests and the CFD approach; however, practical difficulties and time delays are possible to be faced during their performance since experiments have to be carried out under specific weather conditions. Moreover, the accuracy of the results can be affected by the weather conditions, since most of the time weather is not stable or cannot be controlled.

Two types of experiments were carried out. First, a fan depressurization test was performed to determine the leakage characteristics of two trickle ventilator types, i.e. slot and pressure-controlled. This was followed by internal pressure measurements carried out to investigate the actual performance of the trickle ventilators under the influence of the wind and compare it with the performance of a simple rectangular slot.

### **3.2 The outdoor test-room**

The experimental measurements took place in an outdoor test-room placed on the roof of the Concordia University BE building (SE corner of Guy and St. Catherine streets) in Montreal (latitude 45°N, longitude 74°W), during the period September 2001 to February 2002. The interior dimensions of the test-room are 2.5 m × 2.25 m × 2.25 m. The trickle ventilators were installed in the upper part of a door at 1.75 m height from the floor. Figure 3.1 shows a trickle ventilator inserted in their location. The door is facing North.



Fig. 3.1. Installation of a trickle ventilator.

### **3.3 Description of the trickle ventilators**

Two different types of trickle ventilators provided by TITON Inc. were studied: (i) the regular type called slot ventilator (fixed opening) and (ii) the pressure-controlled type (controllable opening). Both ventilators are designed to be mounted at the top of a

window frame covering a slot. For the purpose of the experiment the ventilators were covering a slot on the door. Both ventilators are manually operated.

As shown in Figure 3.2, the slot ventilator consists of a movable interior part (ventilator) and a fixed exterior canopy. The exterior canopy has a metal mesh used to prevent the intrusion of dust, rain and insects. The slot ventilator covers a slot with dimensions 37.1 cm × 1.6 cm while the length of the exterior canopy is 37 cm. The trickle ventilator (interior part) and the exterior screen have the same opening area (40 cm<sup>2</sup>), which is given by the manufacturer.

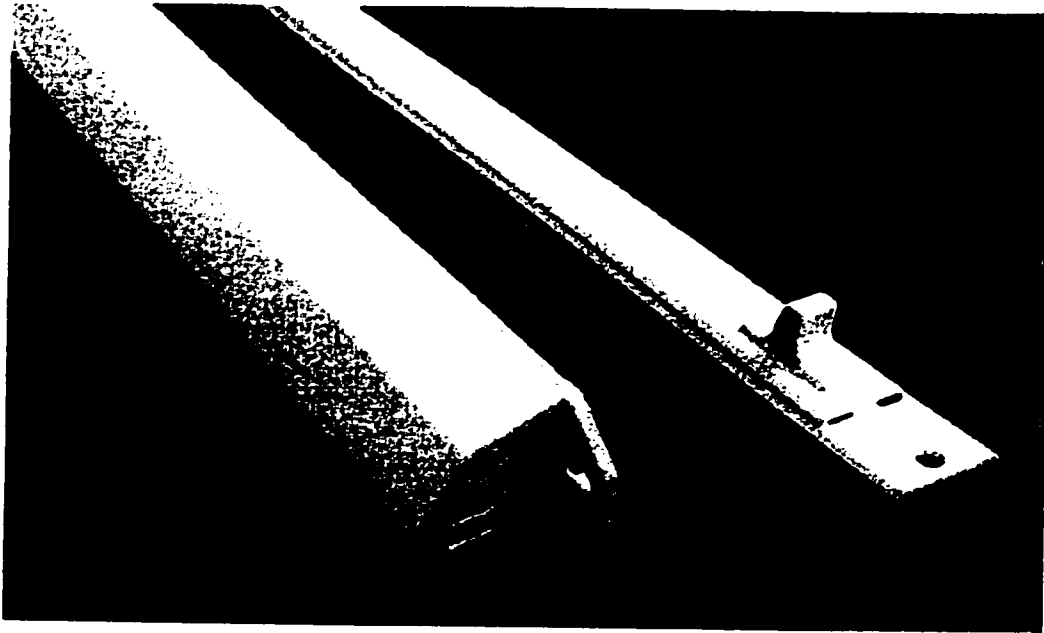


Fig. 3.2. Slot ventilator and exterior canopy.

The pressure-controlled ventilator also consists of an interior and an exterior part. As shown in Figure 3.3 (see Figure 1.1 also), the exterior part consists of a screen to prevent

the intrusion of dust, rain and insects, and a flap to control the exact amount of air passing through. The flap is moving according to the pressure differential across it. For low pressure differential, the flap moves to create a larger inlet area; for high pressure differential, the flap moves and reduces the inlet area, thus restricting the air from passing through. In that way the air flow is passively controlled and a pre-specified amount of air is passing through the ventilator. The interior part covers a slot with dimensions 30.3 cm  $\times$  1.6 cm while the exterior canopy is 33.5 cm long. The opening area of the interior part given by the manufacturer is 18.93 cm<sup>2</sup>.

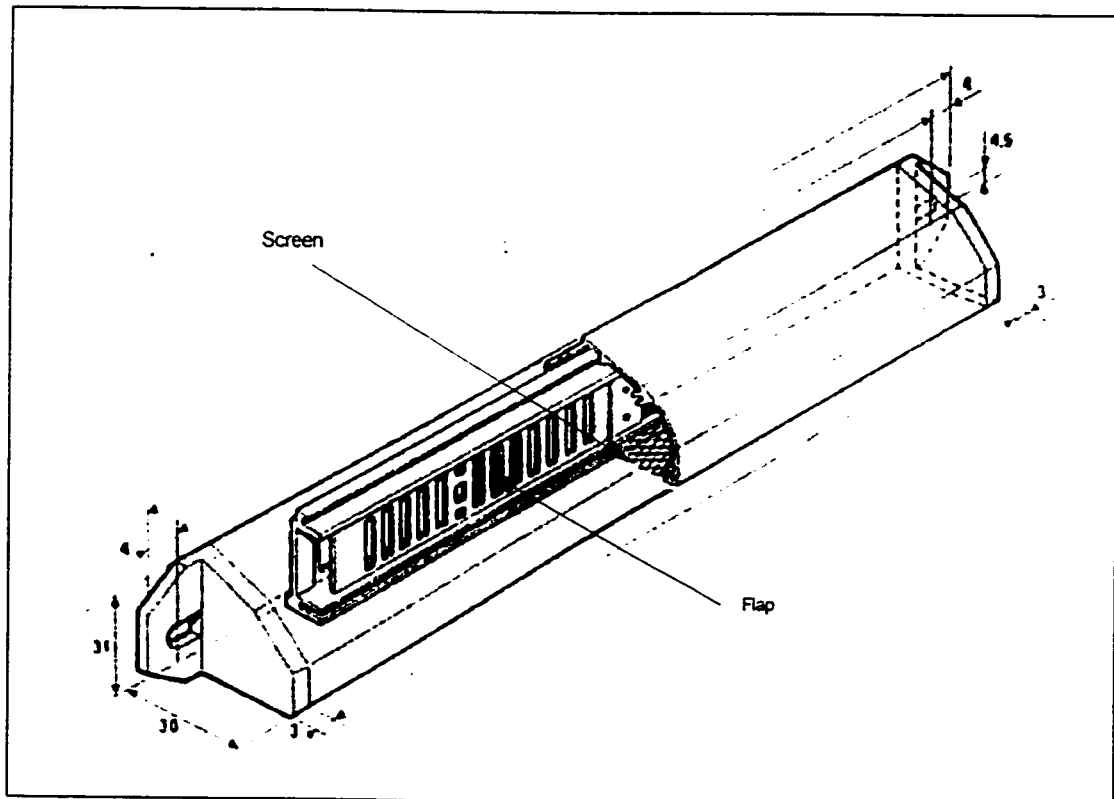


Fig. 3.3. Pressure-controlled ventilator.

### **3.4 Sensors and measurements**

In the first part of the experiment, a fan depressurization test was carried out to determine the leakage characteristics (C and n value) of the trickle ventilators (see equation (2.12)). In the second part of the experiment, the wind effect on trickle ventilators performance was tested; in this part, the fan was not used. The ventilators were installed in the same location on the door.

For the depressurization technique, an exhaust fan was used to extract air through a 7.6 cm diameter duct from the room to the outside and to create negative pressure in the test-room. The air flow was measured by a standard TSI flow meter. Inside the exhaust duct at 10 cm distance from the fan, a number of straws were fitted across the duct diameter in order to create uniform flow and to reduce possible fluctuations during the measurements. At 6 cm distance from the straws a flowmeter was inserted in the duct at a direction perpendicular to the flow. The average of 6 readings along the duct diameter constituted a measurement value. The output of the flowmeter, which is velocity, was multiplied by the area of the duct to get the volumetric flow rate of the air extracted to the outside. A valve was also installed to control the exhaust air flow rate. Figure 3.4 shows the fan, the exhaust duct and the valve in the interior of the test-room, while Figure 3.5 shows a schematic of the experimental set up with the trickle ventilator, the fan, the exhaust duct and the instrumentation.

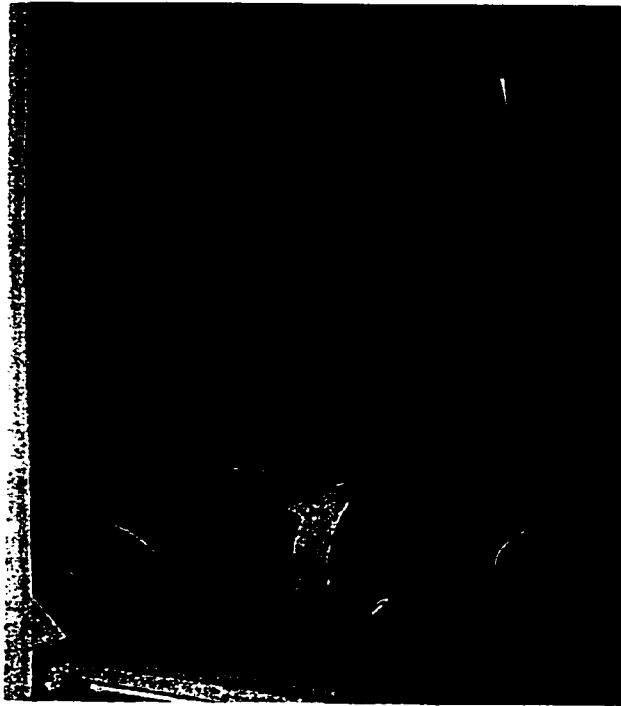


Fig. 3.4. Depressurization equipment inside the test-room.

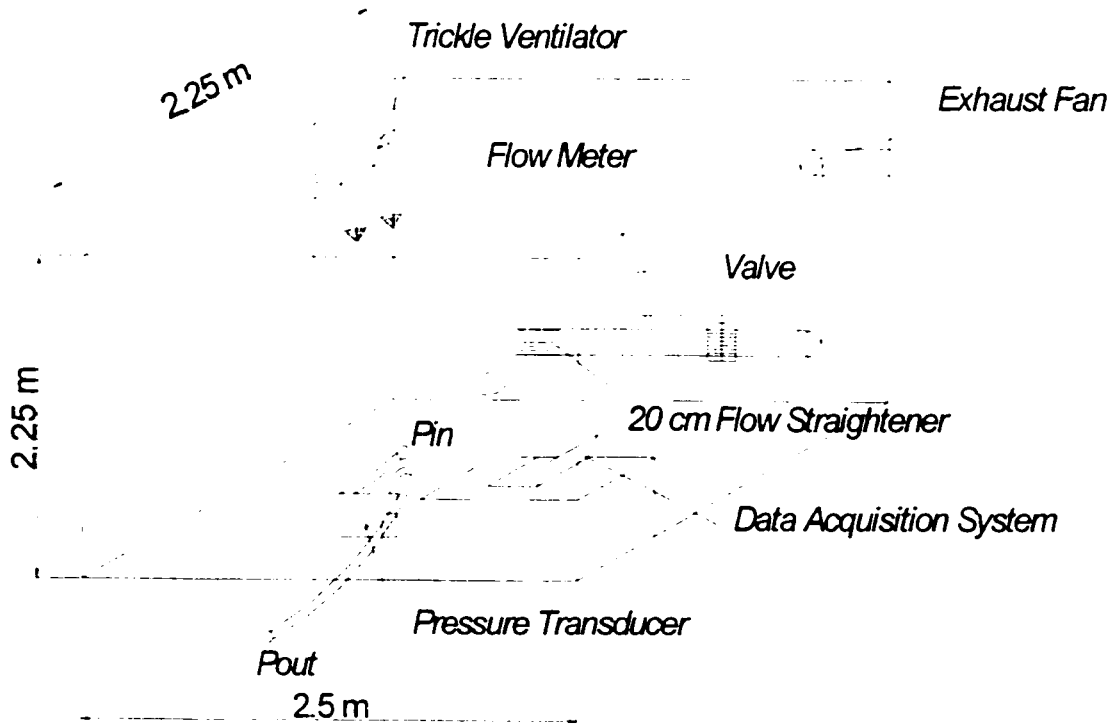


Fig. 3.5. Experimental set-up in outdoor test-room.

The inside-outside pressure difference, which is the driving force of the air flow, was measured by an Air Neotronics MP6KP pressure transducer. The range of this transducer is from 0 to 200 Pa. The transducer was calibrated with a standard manometer (Microtector 1430) in the range between 0 and 30 Pa, i.e. the expected range of the pressure differential in this experiment and the calibration curve was linear. Figure 1 in Appendix shows the calibration curve of the pressure transducer. According to manufacturer specifications the accuracy of the transducer is  $\pm 0.5$  Pa, which is enough for pressure differences higher than 5 Pa but it can cause some errors at lower values of pressure difference.

The pressure measurements can be taken either manually or electronically by connecting the transducer to a data acquisition system. The transducer was connected with two plastic tubes; one was inside and the other outside, positioned at the ground, to measure the inside static pressure relative to the outside. The inside tube was placed on the floor in the centre of the room while the outside tube was placed at a gap between the test-room and the ground in order to be protected by the rain, the snow and the wind. To ensure that the inside-outside pressure difference was not affected by any local conditions, several positions for the inside and outside tube were tested: 1m, 5m far from the test-room for the outside tube, and on the floor, in the mid-height of the building, near the ceiling, etc for the inside tube. No significant differences were noticed and, therefore, it was decided that one pressure transducer, located as described previously, was sufficient to measure the pressure difference in that small room accurately.

The wind was measured using a 3-cup anemometer installed on the roof of another roof structure at a height equal to the test-room height. Since the distance between the test-

room and this building is 10 m and both have the same height, no corrections in the measured speed were made. The wind direction was measured using a vane installed at the same position with the anemometer. The anemometer was calibrated with a standard TSI velocity meter, in a 12 m long, 1.8 m wide and 1.8 m high, wind tunnel. Figures 2 and 4 in Appendix show the calibration curves for the anemometer and the vane. The inside and outside temperatures were also monitored with several thermocouples during the tests in order to investigate temperature (stack) effect on the results, if any.

### **3.5 The data acquisition system**

The data acquisition system used for the tests was a DaqView 7.0 with a specially developed Visual C++ acquisition and control program interface. It displays the readings of all installed sensors, which are the pressure transducer, the 3-cup anemometer, the vane and the thermocouples. Data were sampled at a specified by the program frequency of 100 Hz and averaged at a pre-specified by the user scan rate, depending on the desired detail for the analysis of the data.

During the fan depressurization test the data acquisition was used to display only the wind speed, direction and temperature data. The scan rate used was 0.05 Hz (3 scans per min) because in this study only typical, average values of the wind speed, direction and temperature are required. The pressure and air flow measurements were carried out manually to avoid time delays and practical difficulties as far as the sealing of the door. For the wind study of the trickle ventilators, the data acquisition system was used to display the wind speed, direction, temperature and pressure data. By trying different scan rates from 0.017 Hz (1 scan per min) to 1 Hz (1 scan per sec), it was established that the



measurements under the same conditions, are not sensitive to the scan rate that is used, since the purpose of the experiment is to measure mean values. However, in this study wind speed and pressure variations in smaller time scale (in comparison to the depressurization test) are required in order to investigate their correlation, as well as differences in performance between the two ventilators and the rectangular opening. Therefore, a scan rate equal to 0.17 Hz (10 scans per min) was decided that is appropriate for the wind study.

### **3.6 Leakage characteristics of the ventilators – experimental methodology**

As mentioned in section 2.6.1, the air flow through an opening, as a function of the pressure difference across it, may be written as follows:

$$Q = C \cdot (\Delta P)^n \quad (3.1)$$

where  $C$  ( $\text{m}^3/(\text{sPa}^n)$ ) is the flow coefficient and  $n$  the flow exponent (dimensionless) of the opening. Therefore, if the leakage characteristics ( $C$  and  $n$ ) of the opening are known, the air flow passing through can be predicted by using equation (3.1).

The  $C$  and  $n$  values of a particular opening depend on the range of  $\Delta P$  over which equation (3.1) is applied (ASHRAE Fundamentals Handbook, 2001, ch.26, Heiselberg et al 2002, Etheridge 1996). Under normal conditions, the average pressure differential across the building envelope is between 0 and 5 Pa but the predicted air flow rates in this range are subject to uncertainty due to lower accuracy of pressure transducers measuring at low values of pressure difference. Apart from that, at low pressure differentials the results are affected by the wind speed and inside-outside temperature difference because the pressure differences they induce during the test interfere with the test pressures and

cause measurements errors. Fan depressurization tests are usually carried out at pressure differences from 10 to 60 Pa in order to avoid these errors (ASHRAE Fundamentals Handbook, 2001, ch.26). However, these values are generally far from the actual pressure differences applied in the building envelope. For these reasons, it was decided that the depressurization test should be carried out for pressure differences between 0 and 25 Pa, which reflects the actual pressure differences that exist most of the time across the building envelope, and the results are not subject to significant errors due to instrumentation. In practice, the errors due to weather conditions cannot be avoided, unless the wind speed and inside-outside temperature difference during the measurements is low. In this study, the fan depressurization test measurements were carried out only during days with very light wind speeds, while the inside-outside temperature difference was kept at low values by controlling the heating system.

ASTM E783 (1993) is a standard method for measuring the air leakage associated with specific components of a building, by employing the so-called reductive sealing. A differential pressure is applied across the building envelope by using an exhaust or supply fan and the resulting air leakage of the whole building is measured at a known pressure differential. After that, the element of interest is sealed and the building is pressurized again. The flow difference between the unsealed and the sealed test provides a measure of air leakage associated with the sealed element. In this study, the experimental measurements (fan depressurization test) to determine the leakage characteristics of the ventilators were based on this method.

Prior each fan depressurization test, the door was sealed perimetrically to reduce the leakage. An exhaust fan was used to extract air from the room to the outside and create

negative pressure inside the test-room. A valve was also used to control the exhaust flow rate and thus, to create several inside-outside pressure differentials. According to the mass balance, the volume of air that is exhausted to the outside through the fan ( $Q_F$ ) is equal to the air flow coming into the room through the ventilator ( $Q_V$ ) and the building leaks ( $Q_L$ ):

$$Q_F = Q_V + Q_L \quad (3.2)$$

The model used is described with the flow network shown in Figure 3.6. In that model, the exhaust fan is a flow source with flow rate  $Q_F$ , measured with a standard flow meter (TSI), while  $P_{in}$  and  $P_o$  are the inside and outside pressure respectively measured with a pressure transducer.

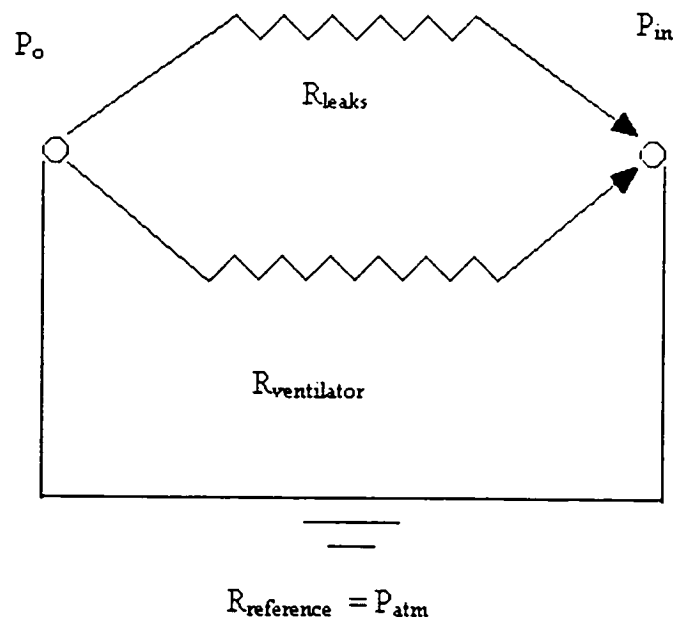


Fig. 3.6. The flow network model.

Two flow resistances are considered: the resistance of the ventilator and the resistance of the building leaks. Thus, there are two parallel flow paths: the ventilator ( $Q_v$ ) and the building leaks ( $Q_l$ ).

When the trickle ventilator is closed, according to equation (3.2)  $Q_f$  is equal to  $Q_l$  and therefore, for a particular position of the valve i.e. for a specified exhaust flow rate or pressure differential, the air flow through the building leaks is known. By changing the position of the valve, the exhaust flow rate is different and as a result another pressure differential is applied. The air flow through the leaks is a power-law function of the inside-outside pressure difference, and the corresponding plot is like that shown in Figure 3.7. Since the data follow a power law form, power regression techniques are applied and the leakage characteristics of the room,  $C_l$ ,  $n_l$  can be determined. When the ventilator is open, the inside-outside pressure difference  $\Delta P_l$  is different from that with the ventilator closed at the same exhaust flow rate. Since the leakage characteristics of the room have been determined, the air flow through the leaks is given by the following equation:

$$Q_l = C_l \cdot (\Delta P_l)^{n_l} \quad (3.3)$$

Therefore, by subtracting the air flow through the leaks,  $Q_l$ , from the air flow exhausted through the fan,  $Q_f$ , the air flow rate through the ventilator,  $Q_v$  is calculated. By changing the position of the valve, the air flow through the ventilator can be calculated for several pressure differences. The air flow through the ventilator is plotted as a function of the inside-outside pressure differential and a curve like that shown in Figure 3.7 is drawn. Since the data follow a power form, power regression techniques are applied and the leakage characteristics of the ventilator,  $C_v$  and  $n_v$ , can be determined. Therefore, the air flow through the ventilator at a known pressure differential can be calculated as follows:

$$Q_v = C_v \cdot (\Delta P)^{0.5} \quad (3.4)$$

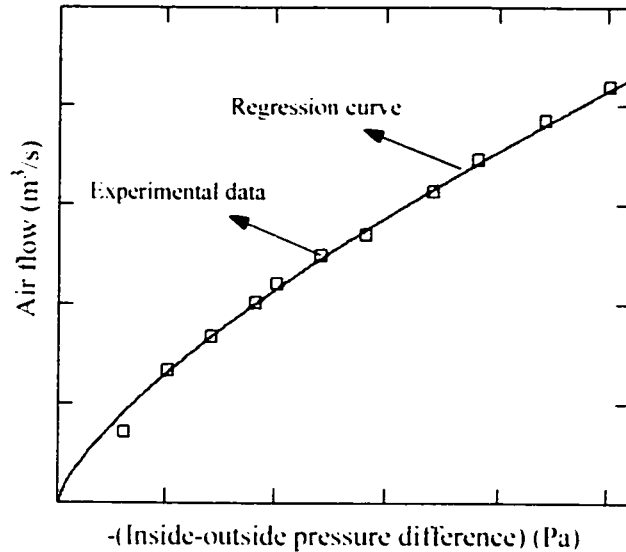


Fig. 3.7. Air flow as a function of the inside-outside pressure difference.

### **3.7. Wind study-experimental methodology**

The purpose of this experiment is:

- To investigate the trickle ventilators actual performance (without the fan) and to compare their performance with that of a simple rectangular opening that covers the same slot on the door.
- To confirm the reliability of the fan depressurization results.

The wind effect was studied as the only driving force, since the stack effect in this 2.25 m high test-room is small and cannot be accurately studied. Although the stack effect is very small, to avoid possible errors in the results, the measurements were carried out under conditions with small inside-outside temperature difference. Because of the reduced accuracy of the transducer when low pressures are measured, this experiment

was carried out only during windy days. The outlet of the fan used in the depressurization technique was sealed during the wind study in order to avoid possible leakage introducing further errors to the results. Again, a perimeter sealing of the door was applied before each experiment in order to reduce the leakage through the door.

The variation with time of the internal pressure, wind speed and direction was measured in this study. The internal pressure was measured relative to the outside static pressure (reference pressure). Data for the inside and outside temperature was also recorded in order to ensure that their difference is small, resulting to an insignificant stack effect. Data were scanned with the data acquisition system at a rate of 10 scans per min. Several measurements were taken for different wind directions since the location of the ventilator in relation to the wind direction (leeward or windward opening) or, in other words, in relation to the external pressure distribution, prescribes the magnitude of the internal pressure  $P_{in}$ . The following cases were studied for both the slot and the pressure-controlled ventilator:

- a. Trickle ventilator closed and wind perpendicular to one of the facades
- b. Trickle ventilator open and wind perpendicular to the façade with the ventilator (windward opening)
- c. Trickle ventilator open and wind from other directions (opening under suction)
- d. A simple rectangular opening with dimensions 37.1 cm length and 1.6 cm height (no ventilator) and wind perpendicular to the façade with the opening (windward opening)
- e. A simple rectangular opening with dimensions 37.1 cm length and 1.6 cm height (no ventilator) and wind from other directions (opening under suction).

## CHAPTER 4

### EXPERIMENTAL RESULTS AND DISCUSSION

#### **4.1 General**

In this chapter the experimental measurement results of the full-scale study are presented and discussed. The leakage characteristics of two ventilator types (slot and pressure-controlled) are determined, and the actual performance of the ventilators under the influence of the wind is analyzed. The degree of validity of the orifice equation for application in the case of trickle ventilators is also discussed. The fan depressurization data (artificial technique) are compared with data obtained under the influence of the wind (actual driving force). Finally, a comparison between the two ventilator types is carried out, in order to establish appropriate selection criteria and to determine which type is better with respect to thermal comfort and IAQ.

#### **4.2 Air flow through the slot ventilator by using the fan pressurization technique**

The results of the reductive sealing depressurization method are presented and analyzed in order to determine the leakage characteristics of the slot ventilator. As mentioned in section 3.6, the slot ventilator was first sealed and the test-room was pressurized. Thus, the air flow through the test-room envelope cracks was measured as a function of the inside-outside pressure difference; by applying regression analysis, the leakage characteristics of the room were determined. Figure 4.1 shows typical experimental measurement results of the air flow through the building cracks and the related empirical

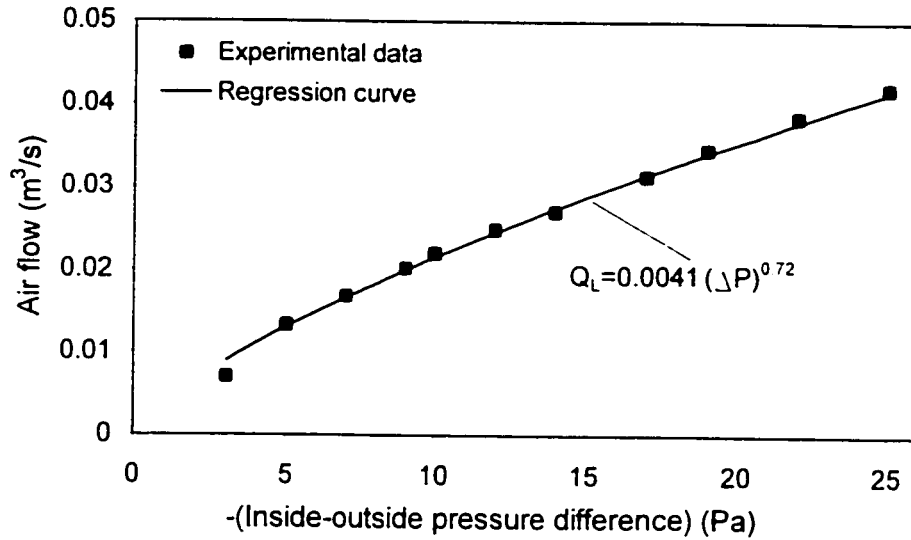


Fig. 4.1. Airflow through the test-room envelope cracks.

equation.

The air flow through the ventilator can be found by subtracting the air flow due to the leakage of the test-room envelope cracks from the total air flow exhausted through the fan. Figure 4.2 shows the total air flow exhausted through the fan  $Q_F$ , the air flow through test-room envelope cracks  $Q_L$ , and the air flow through the ventilator as a function of the inside-outside pressure differential.

Figure 4.3 shows experimental measurement results of the air flow through the slot ventilator as a function of the indoor-outdoor pressure difference and the related empirical equation derived by employing regression techniques.



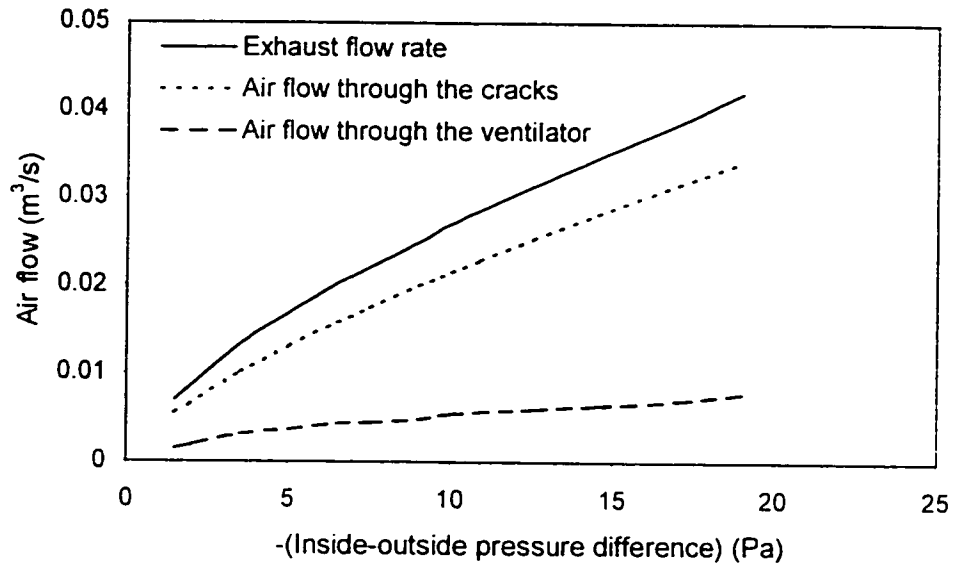


Fig. 4.2. Exhaust flow rate, air flow through the test-room envelope cracks and air flow through the slot ventilator.

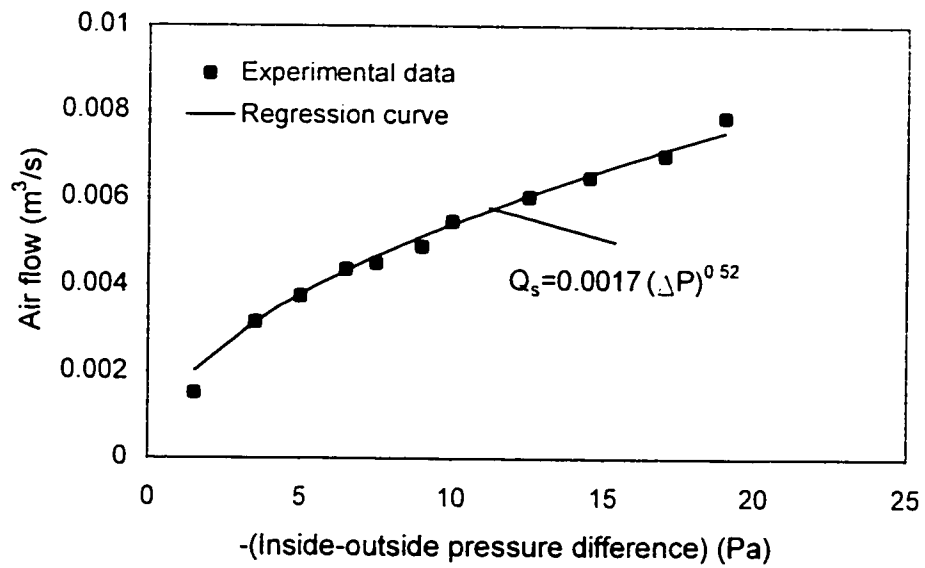


Fig. 4.3. Air flow through the slot ventilator.

#### 4.2.1 Repeatability of the results

The fan depressurization test was repeated several times during the period September-December 2001. Table 4.1 shows typical results regarding the leakage characteristics of the room and the ventilator, the wind speed, direction, inside and outside temperature during the measurements. It is observed that the flow coefficient for the test-room envelope cracks,  $C_L$ , varies between 0.0040 and 0.0043 while the flow exponent,  $n_L$ , is between 0.70 and 0.73. The coefficient of variation in the air flow through the cracks by using different pairs of  $C_L$ ,  $n_L$  values is small (2%) since it appears that when  $C_L$  increases,  $n_L$  decreases and the air flow remains about the same. The average  $C_L$ ,  $n_L$  values are  $0.0041 \text{ m}^3/\text{s}/\text{Pa}^{0.72}$  and 0.72 respectively and the air flow through the test-room envelope cracks ( $\text{m}^3/\text{s}$ ) can be written as follows:

$$Q_L = 0.0041 \cdot (\Delta P)^{0.72} \quad (4.1)$$

Table 4.1. Fan depressurization test results for the slot ventilator.

Date	$C_L$ [ $\text{m}^3/(\text{s}/\text{Pa}^{n_L})$ ]	$n_L$	$C_v$ [ $\text{m}^3/(\text{s}/\text{Pa}^{n_v})$ ]	$n_v$	$T_{in}$ ( $^{\circ}\text{C}$ )	$T_{out}$ ( $^{\circ}\text{C}$ )	V (m/s)	Wind direction
19/09/01	0.0041	0.73	0.0018	0.52	21.52	13.15	1.7	SW
25/09/01	0.004	0.72	0.0015	0.55	18.23	12.20	1.15	SW
6/10/01	0.0041	0.72	0.0017	0.52	16.45	10.29	1.07	SW
17/10/01	0.004	0.71	0.0017	0.5	16.82	9.57	1.5	SE
24/10/01	0.0043	0.70	0.0016	0.52	22.05	16.85	0.99	NE
29/10/01	0.0041	0.72	0.019	0.5	18.42	10.93	1.35	NE
02/11/01	0.0041	0.73	0.0016	0.51	21.48	16.59	1.44	SW
Average	0.0041	0.72	0.0016	0.53	-	-	-	-

Figure 4.4 shows the air flow through the test-room envelope leaks as a function of pressure difference for different pairs of  $C_L$ ,  $n_L$  values from Table 4.1.

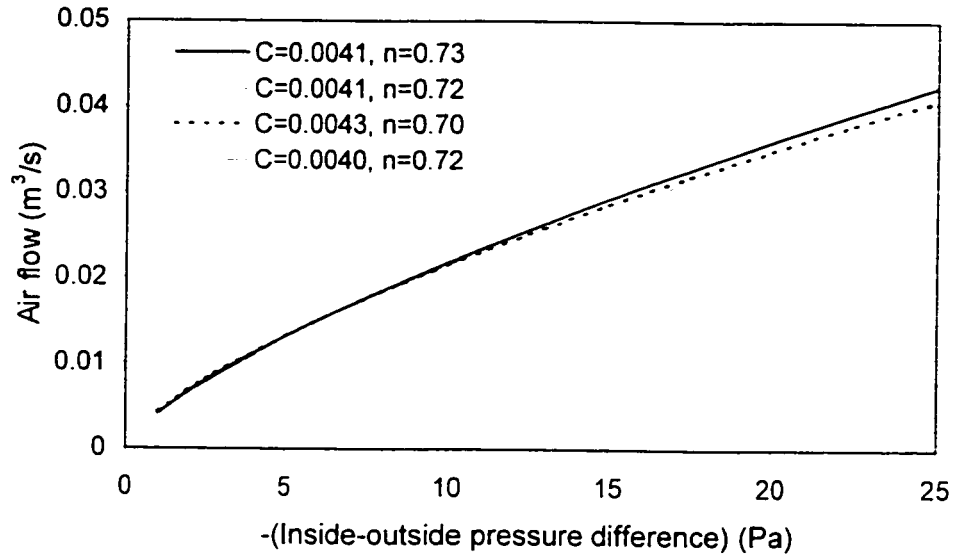


Fig. 4.4. Repeatability of the results for the air flow through the test-room envelope cracks.

Regarding the slot ventilator, the flow coefficient,  $C_v$ , ranges between 0.0015 and 0.0019, and the flow exponent,  $n_v$  between 0.50 and 0.55. However, the actual variation of the air flow is small since it appears that when  $C_v$  increases,  $n_v$  decreases and, as a result, the air flow through the slot ventilator, remains about the same. Figure 4.5 shows the repeatability of the results for different pairs of  $C_v$ ,  $n_v$  values from table 4.1. The coefficient of variation in the air flow through the ventilator for different  $C_v$ ,  $n_v$  values is about 7%. The average  $C_v$ ,  $n_v$  values are  $0.0016 \text{ m}^3/\text{s}/\text{Pa}^{0.53}$  and 0.53 respectively and the air flow through the slot ventilator ( $\text{m}^3/\text{s}$ ) is given by the following empirical equation:

$$Q_v = 0.0016 \cdot (\Delta P)^{0.53} \quad (4.2)$$

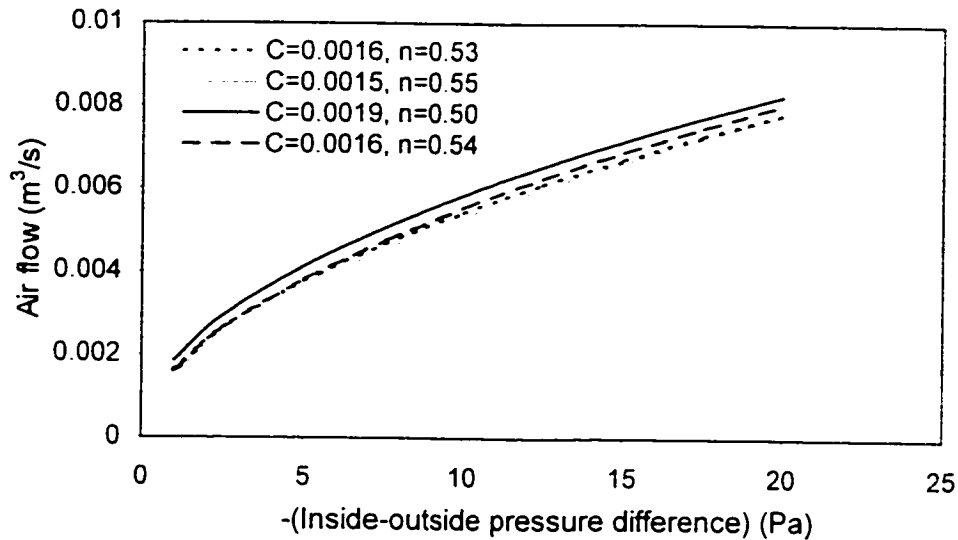


Fig 4.5. Air flow through the slot ventilator - repeatability of the results.

#### 4.2.2 Comparison with literature sources

The value of the flow exponent found for the test-room envelope cracks is consistent with that provided by several literature sources like ASHRAE (Fundamentals Handbook, ch.26, 2001), Awbi (1991), CIBSE (2000), and many others. According to these sources, the n value for cracks and openings in the building envelope is usually between 0.6 and 0.7. The normalized leakage area of the test-room envelope found to be around 0.7: thus, according to leakage classes given by ASHRAE Standard 119 (ASHRAE Fundamentals Handbook, ch.25, 1997), based on annual average building air exchange rate, the test-room belongs to class G, i.e. the test-room is quite leaky which was predictable. As far as the n value of the ventilator is concerned, this is in good agreement with data from CIBSE (2000) that give a value of n for trickle ventilators about 0.5. The flow exponent for the test-room envelope cracks and the ventilator show flow in the transition region through the test-room envelope cracks and almost turbulent flow through the ventilator.

#### 4.2.3 Comparison with manufacturers' data and the orifice equation

Two types of experimental data given by the manufacturer of the trickle ventilators (Titon Inc.) are compared with the field data presented previously. The results are also compared with theoretical estimation of the air flow by using the orifice equation. The first type of manufacturer's data are results of an experimental study carried out in a small wind tunnel with a fan at one end, a flow regulator in the middle, and a board including the ventilator at the other (Titon Inc., 2002). Different pressure differentials were applied and the resulting air flow through the ventilator was measured. For the second type of data the standard ASTM E283 (1991) method was applied and the results published by The American Architectural Manufacturers Association (2000). This method involves pressurization of individual components or elements of a building by containing them in a temporary enclosure and directly pressurizing the component. For the comparison with the orifice equation a value of the discharge coefficient equal to 0.6 (Fundamentals Handbook, ch.26, 2001) was used: the opening area of the ventilator given by the manufacturer is 40 cm<sup>2</sup>. It should be mentioned that this is the opening area of the interior part as well as the area of the exterior mesh (see Figure 3.2).

Figure 4.6 illustrates the air flow through the ventilator as a function of the pressure difference across it by using (i) the orifice equation (2.10), (ii) wind tunnel data (Titon Inc., 2002) (iii), field data (present study), and (iv) data obtained by employing the ASTM E283 method (The American Architectural Manufacturers Association 2000).

Examination of Figure 4.6 reveals that the particular wind tunnel measurements overestimate the air flow through the ventilator. This overestimation occurs because the wind tunnel used for the measurements was small, resulting to an unrealistic fully

developed uniform flow. On the contrary, the ASTM E283 method gives lower values of air flow in comparison to field measurements. It is observed also that the orifice equation with  $C_D = 0.6$  overestimates the air flow through the ventilator in comparison to different experimental results. In particular, the predicted values of the air flow are almost double compared to field measurements. This discrepancy can be explained by the value of the discharge coefficient,  $C_D$  that was used; this value is not constant in reality and depends on the opening geometry and the pressure difference across it (Heiselberg et al, 2002).

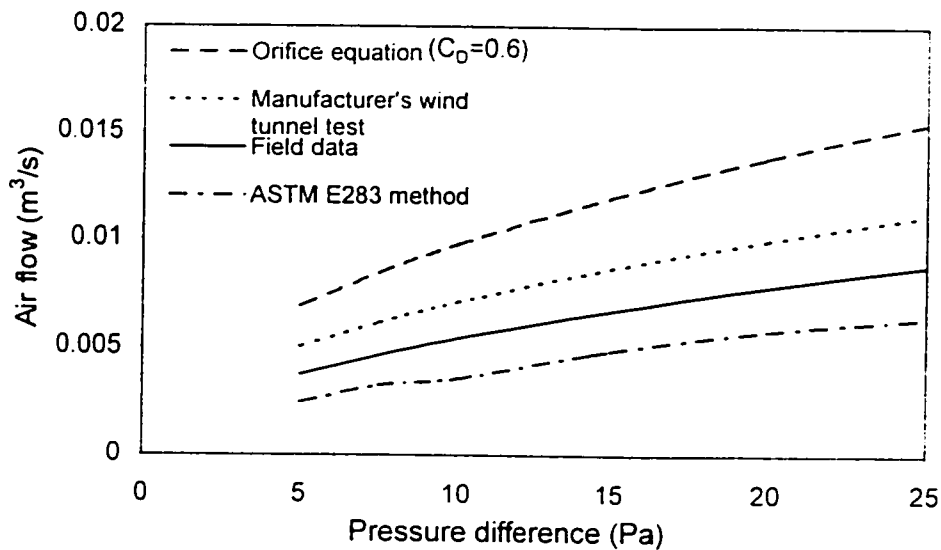


Fig. 4.6. Comparison of the air flow through the slot ventilator by using field data (present study), the orifice equation, wind tunnel data and data by applying the ASTM E283 method.

In general, there is a lot of disagreement in the literature about the value of discharge coefficient should be used for several opening types (see section 2.6.1). The actual value

of the discharge coefficient that should be used for openings such as trickle ventilators in order to achieve equal measured and predicted air flow rates, can be found by the ratio:

$$C_D = \frac{\text{measured air flow}}{\text{predicted air flow}} \cdot 0.6 \quad (4.3)$$

Therefore, the value of  $C_D$  that should be used for application of the orifice equation in the case of trickle ventilators is 0.34. As discussed by Dascalaki et al (1995), a correction coefficient as that in equation (4.3) should be calculated for the validation of a prediction model with experimental data. This coefficient should be equal to the input value of the discharge coefficient in the prediction model, in order to achieve equal predicted and measured values.

#### 4.2.4 Effective area of the slot ventilator

The quantity  $C_D \cdot A$  in the orifice equation (2.3) is known as effective leakage area  $A_0$  ( $\text{m}^2$ ) and can be determined by fan pressurization data using the following equation:

$$A_0 = \frac{Q_v}{(2 \cdot \Delta P_{ref} / \rho)^{0.5}} \quad (4.4)$$

where  $Q_v$  ( $\text{m}^3/\text{s}$ ) is the air flow through the slot ventilator calculated from fan depressurization test data (equation (4.2)),  $\rho$  the air density ( $1.2 \text{ kg}/\text{m}^3$ ), and  $\Delta P_{ref}$  a reference pressure (4 Pa). Reference pressure of 4 Pa is used because is closer to the pressure differences that actually induce the air flow and, therefore, better model the flow characteristics of the ventilator. By using the previous equation, the effective area of the ventilator found  $A_0 = 13 \text{ cm}^2$ , which is equal to one third of its geometric area ( $40 \text{ cm}^2$ ). This difference is due to the “trickle” design of the ventilator with air cavities and the exterior mesh that increase the flow resistance of the ventilator.

### 4.3 Air flow through the pressure-controlled ventilator by using the fan pressurization technique

The other ventilator type (pressure-controlled ventilator) was also tested by using the same methodology followed for the slot ventilator. Figure 4.7 shows typical experimental measurement results of the air flow through the pressure-controlled ventilator and the related empirical equation derived by employing regression techniques. The air flow through this ventilator type increases for values of pressure difference up to 12 Pa; for higher values of  $\Delta P$  it appears remaining almost constant at around 0.006 m<sup>3</sup>/s (or 6 L/s).

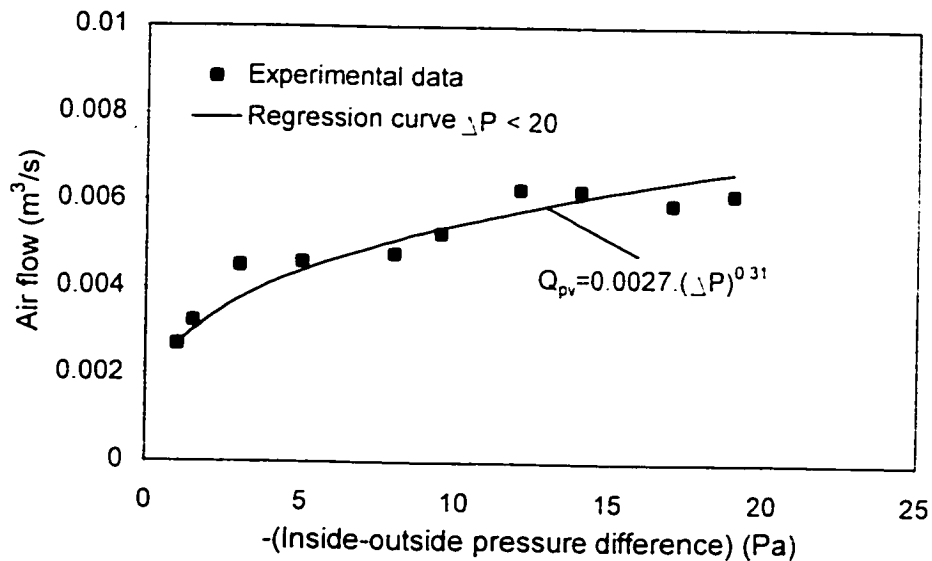


Fig. 4.7. Air flow through the pressure-controlled ventilator.

Therefore, by using this type of ventilator the flow is expected to be between 3 and 5 L/s for  $\Delta P$  from 2 to 5 Pa, which is a typical value of pressure difference across the building envelope under normal conditions, while for high values of  $\Delta P$  (load conditions) it remains constant at about 6 L/s.



### 4.3.1 Repeatability of the results

The fan depressurization test was repeated several times during the period September-December 2001. Table 4.2 shows typical results regarding the leakage characteristics of the test-room envelope cracks and the pressure-controlled ventilator, the wind speed, direction, inside and outside temperature during the measurements. It appears that the flow coefficient,  $C_v$ , ranges between 0.0024 and 0.0030, and the flow exponent,  $n_v$ , between 0.28 and 0.33. However, the actual variation of the air flow is small since it appears that when  $C_v$  increases,  $n_v$  decreases and, as a result, the air flow through the slot ventilator, remains about the same.

Table 4.2. Fan depressurization test results for the pressure-controlled ventilator.

Date	$C_L$ [ $m^3/(s/Pa^{n_L})$ ]	$n_L$	$C_v$ [ $m^3/(s/Pa^{n_v})$ ]	$n_v$	$T_{in}$ (°C)	$T_{out}$ (°C)	V (m/s)	Wind direction
6/10/01	0.0041	0.72	0.0025	0.32	16.45	10.29	1.07	SW
17/10/01	0.0040	0.71	0.0030	0.28	16.82	9.57	1.50	SE
24/10/01	0.0043	0.70	0.0027	0.31	22.05	16.85	0.99	NE
02/11/01	0.0041	0.73	0.0028	0.32	21.48	16.59	1.44	SW
06/11/01	0.0041	0.72	0.0025	0.33	17.22	11.5	1.65	SW
09/11/01	0.0041	0.73	0.0024	0.33	15.8	9.5	1.59	SW
Average	0.0041	0.72	0.0026	0.31	-	-	-	-

The average  $C_v$  and  $n_v$  values are  $0.0026 \text{ m}^3/\text{s}/\text{Pa}^{0.53}$  and 0.31 respectively and despite the fact that may not have any specific physical meaning, the air flow through the pressure-controlled ventilator ( $\text{m}^3/\text{s}$ ) is given by the following empirical equation:

$$Q_{pv} = 0.0026 \cdot (\Delta P)^{0.31} \quad (4.5)$$

Figure 4.8 shows the air flow through the pressure-controlled ventilator as a function of the pressure difference for different pairs of  $C_L$ ,  $n_L$  values from Table 4.2.

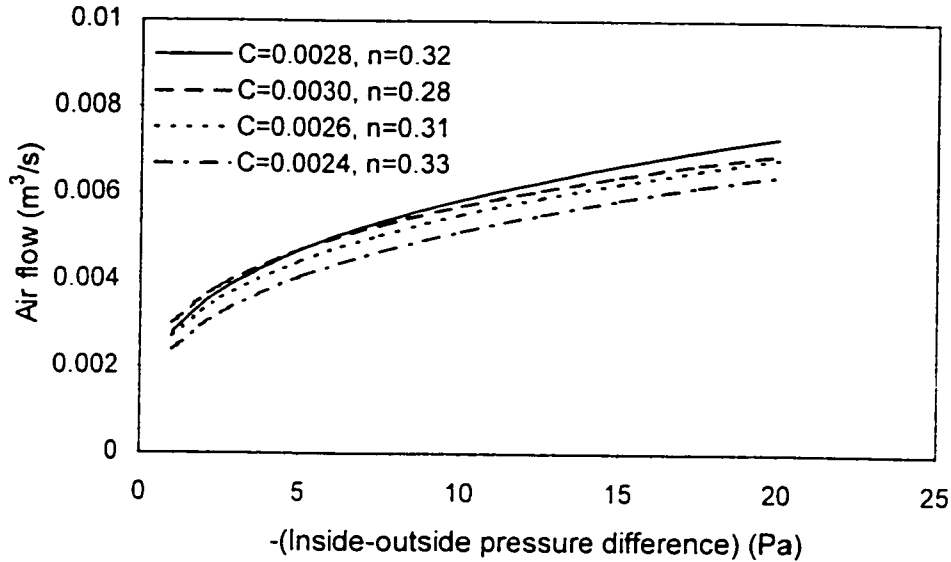


Fig. 4.8. Air flow through the pressure-controlled ventilator - repeatability of the results.

#### 4.3.2 Comparison with manufacturer's data and literature sources

According to manufacturer's specifications, the pressure-controlled ventilator is designed to give a constant air flow of about 6.25 L/sec at pressure differences between 20 and 100 Pa. Figure 4.9 shows typical experimental results of the air flow through the pressure-controlled ventilator and the straight line corresponds to air flow equal to 6.25 L/s. It is observed that the air flow through the pressure-controlled ventilator remains constant at about 6 L/s, even at lower values of pressure difference ( $\Delta P > 12$  Pa).

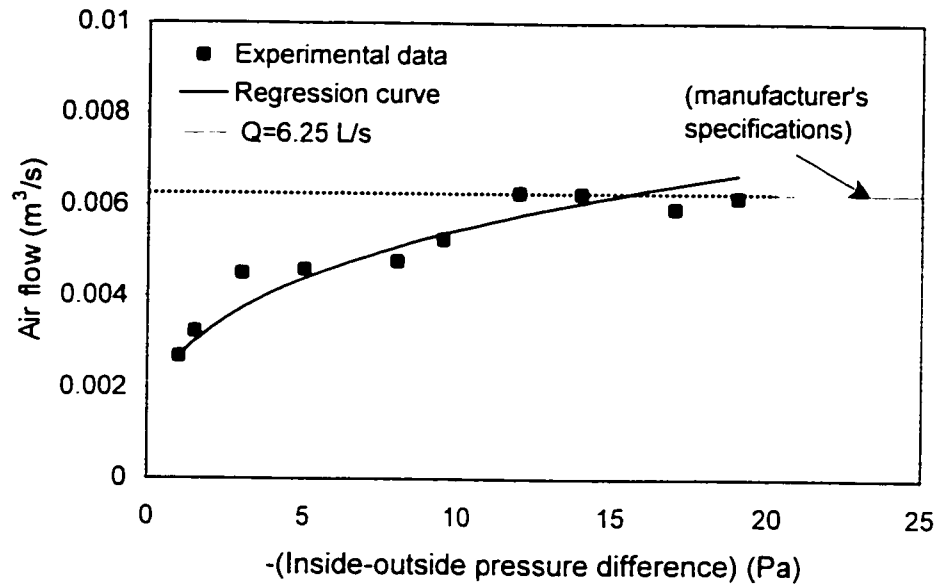


Fig. 4.9. Comparison of the air flow through the pressure-controlled ventilator by using field data and manufacturer's specifications.

As mentioned in the literature (see section 2.8), depressurization tests carried out by de Gids (1997) showed that for different pressure-controlled ventilator types, the pressure at which the air flow rate passing through becomes almost constant, varies from 1 to 20 Pa. This conclusion is consistent with the results of the present field study since the air flow through the pressure-controlled ventilator becomes constant at about 12 Pa.

#### **4.4 Sensitivity of the results to wind effect**

The experimental results are sensitive to weather conditions and especially to wind speed and direction variations. It also appears that the results are not affected by the inside-outside temperature difference since the experiment was carried out at different temperature differentials and no significant variation was observed (see Tables 4.1 and 4.2). Figure 4.10 illustrates experimental data for the air flow through the slot ventilator

under normal and windy conditions. In general, the measured inside-outside static pressure difference ( $\Delta P$ ) is overestimated for an opening located in the leeward wall (under suction) and underestimated for an opening located in the windward wall (positive pressure), due to pressure induced by the wind. As a result, the air flow through the slot ventilator is overestimated if the ventilator is located in the windward side of the test-room and underestimated if the ventilator is located in the leeward side due to wind-induced pressure that interfere with the fan pressure. Regarding the pressure-controlled ventilator, the wind speed and direction variations induce pressure differences that interfere with the test pressures caused by the fan, but due to the effect of the flap the observation of a potential overestimation or underestimation of the flow is more complex in comparison to the slot ventilator.

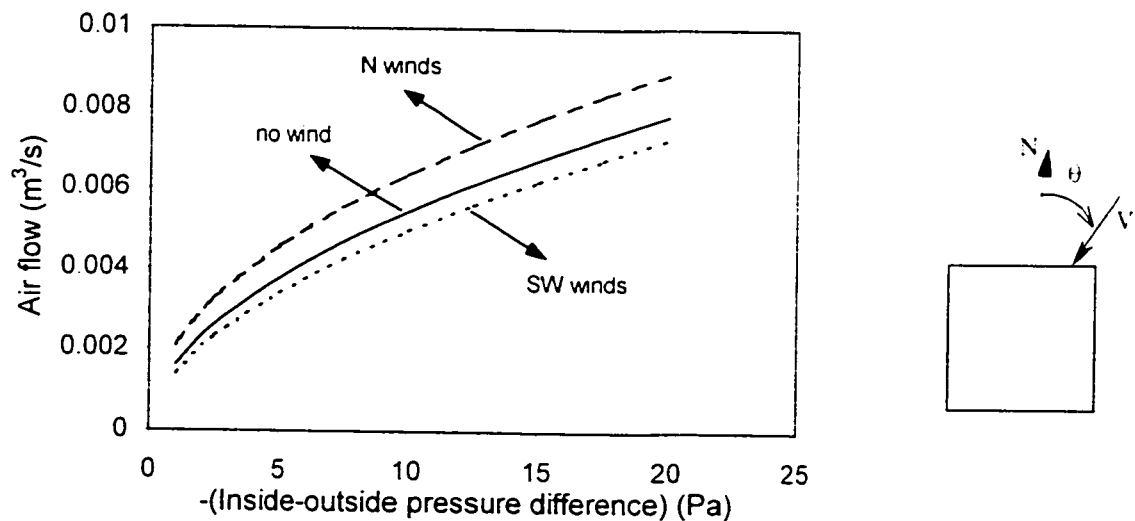


Fig. 4.10. Overestimation and underestimation of the air flow through the slot ventilator due to the wind.

Additional variations in the exhaust flow rate and in the resulting internal pressure can be caused due to the wind pressure on the fan outlet. In particular, the exhaust flow rate

decreases if the fan outlet is under positive pressure while the flow rate increases if the outlet is under negative pressure.

#### **4.5 Discussion of the fan depressurization results**

Figure 4.11 shows the air flow as a function of the inside-outside pressure difference for the two ventilator types. It is observed that more air flow is passing through the pressure-controlled ventilator in comparison to that through the slot ventilator at low  $\Delta P$  values (up to 10 Pa); for higher  $\Delta P$  values more air flow is passing through the slot ventilator. This happens due to the effect of the exterior flap, which moves, adjusting the actual opening area according to the pressure differential across it.

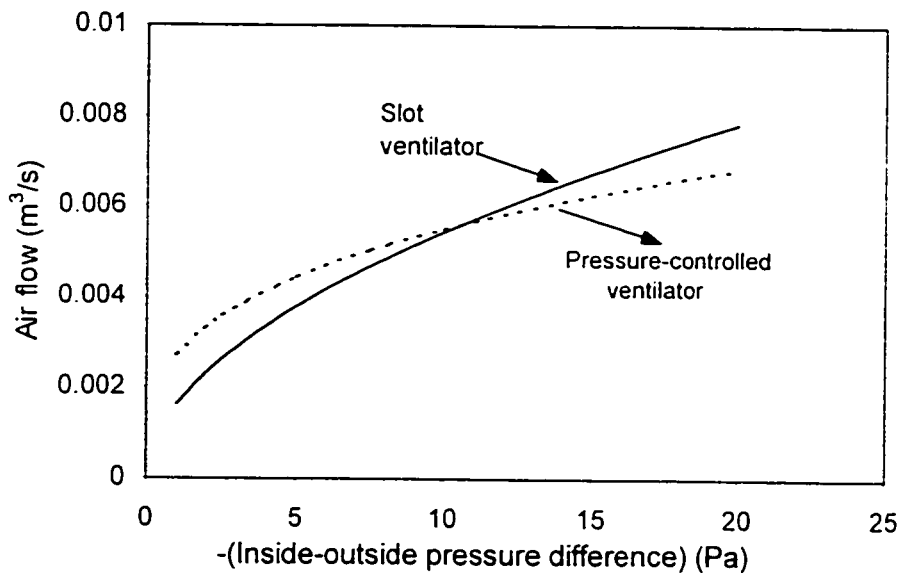


Fig. 4.11. Comparison between the airflow through the slot and the pressure-controlled ventilator.

#### **4.6 Wind effect on trickle ventilators performance**

In this section the performance of the trickle ventilators under the influence of the wind, which is the main driving force of the air flow through low-rise buildings, has been investigated. The wind speed and the internal pressure variation with time were measured for several cases and their correlation has been evaluated. For each case, the internal pressure coefficient is calculated using Bernoulli's equation:

$$C_{pi} = \frac{P_{in} - P_o}{(\frac{1}{2} \cdot \rho \cdot V^2)} \quad (4.6)$$

where  $P_{in}$  (Pa) is the internal pressure,  $P_o$  the outside static pressure (reference pressure),  $\rho$  ( $\text{kg/m}^3$ ) the air density, and  $V$  (m/s) the mean wind speed at the test-room height. Based on the internal pressure coefficient variation in a particular time duration, which is the same in all cases (8 min), and on the corresponding time-average  $C_{pi}$  values, a comparison related to the performance of the two ventilators is carried out. Considering the same input conditions (wind direction) for both ventilators, the mean internal pressure coefficient can provide information for their ventilation capacity while the standard deviation of the internal pressure coefficient provides information for their performance with respect to thermal comfort. The performance of the trickle ventilators is also compared with that of a simple rectangular opening that covers the same slot on the door. Finally, the results are compared with standards and related wind tunnel studies.

##### **4.6.1 Experimental results**

Experimental data regarding the 8 min average wind speed, internal pressure coefficient, and the prevailing wind direction are presented in Table 4.3. The standard deviation of the wind speed, direction and the internal pressure coefficient is also

illustrated. Each of the two ventilator types, as well as the simple rectangular opening, considered as windward openings or openings under suction. Experimental data with the ventilator closed (no opening) are also presented. More than 50 records were carried out during the period September 2001 to February 2002 and the results were repeatable: Table 4.3 shows representative results for each case. The time duration was selected to be 8 min because it is impossible to get larger duration data with almost the same wind direction due to the variability of the wind.

Table 4.3. Wind study experimental results

	V (m/s)	$\sigma_v$ (m/s)	$\theta$ (°)	$\sigma_\theta$ (°)	$\bar{C}_{pi}$	$\sigma_{C_{pi}}$
Closed ventilator	3.70	1.34	198	43	-0.22	0.32
Rectangular slot (windward)	3.96	1.11	49	26	0.21	0.40
Rectangular slot (leeward)	2.33	0.91	152	31	-0.50	0.20
Slot ventilator (windward)	3.60	1.49	39	15	0.10	0.30
Slot ventilator (leeward)	2.98	1.26	168	22	-0.26	0.20
Pressure-controlled ventilator (windward)	4.36	1.91	33	17	0.23	0.37
Pressure-controlled ventilator (side)	3.47	1.17	264	28	0	0.22

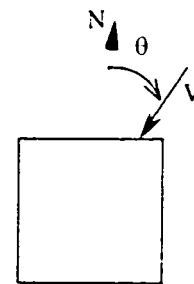


Figure 4.12 shows the variation of the internal pressure coefficient with time for the ventilator closed (no opening). The corresponding mean internal pressure coefficient is -0.22.

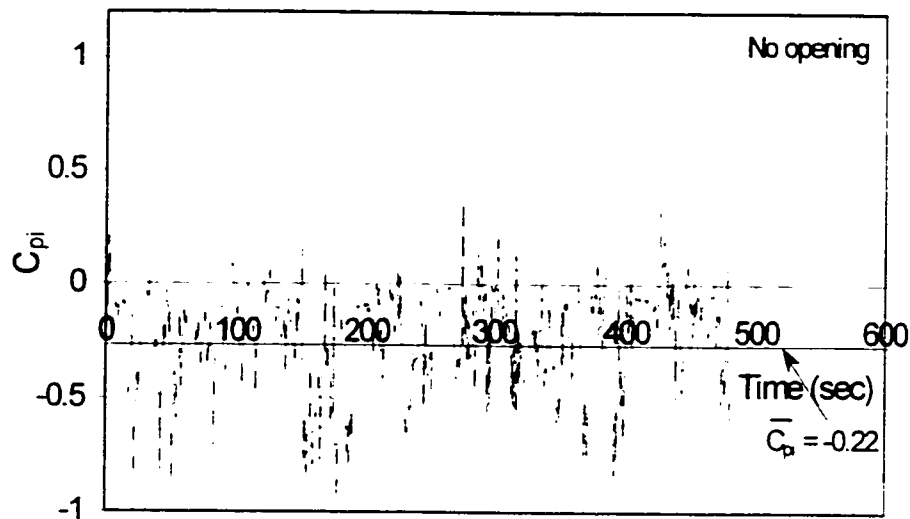


Fig. 4.12. Internal pressure coefficient variation with the ventilator closed (no opening).

Figure 4.13 shows the variation of the internal pressure coefficient with a simple rectangular opening, which covers the same slot with the trickle ventilators. When the opening is located in the windward façade of the test-room ( $\theta = 49^\circ$ ) the internal pressure coefficient is positive and the mean value is 0.21. When the opening is located in the leeward facade ( $\theta = 152^\circ$ ) the internal pressure coefficient is negative and the mean value is -0.50. It is also observed that the internal pressure coefficient varies between -1.0 and 1.0.

Figure 4.14 shows the effect of the slot ventilator in the internal pressure coefficient for  $\theta = 39^\circ$  (windward opening) and  $\theta = 168^\circ$  (leeward opening). For the windward case the internal pressure coefficient is primarily positive and the  $\bar{C}_{pi}$  is equal to 0.1; for the leeward case the internal pressure coefficient is negative and the  $\bar{C}_{pi}$  is equal to -0.26.



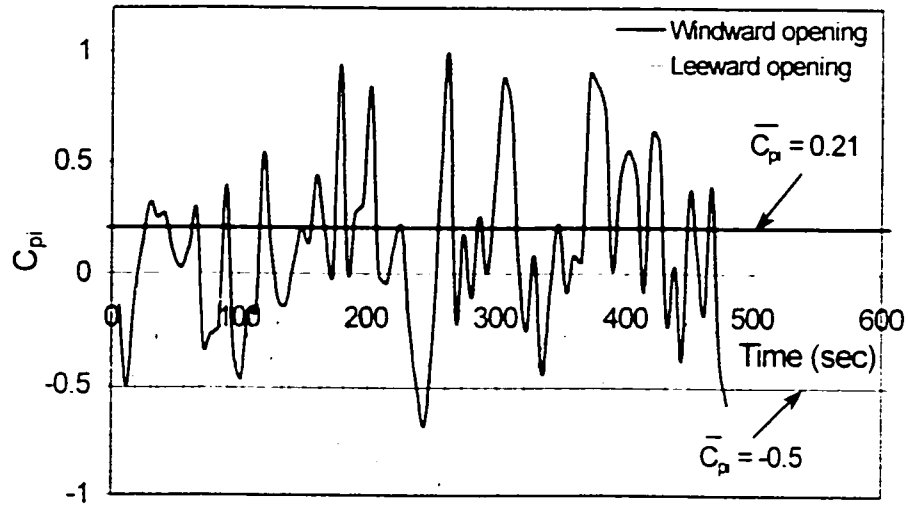


Fig. 4.13. Internal pressure coefficient variation with the rectangular slot open.

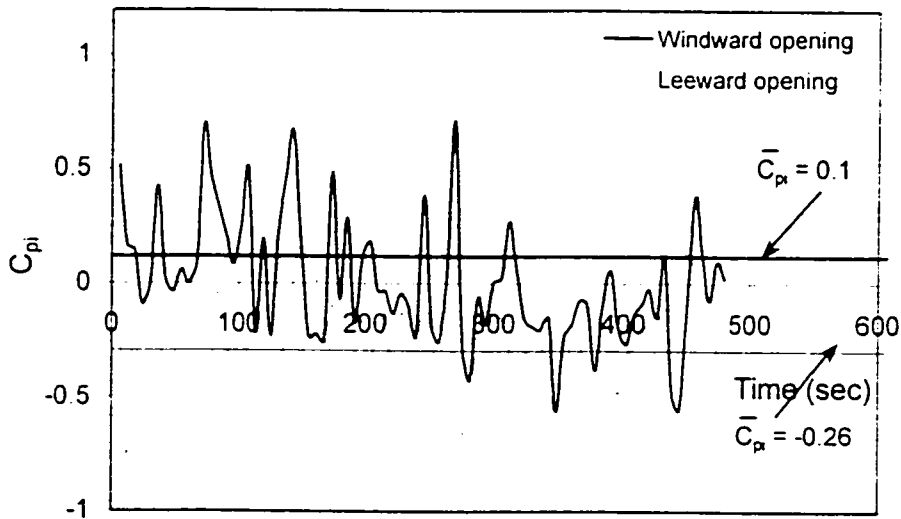


Fig. 4.14. Internal pressure coefficient variation with the slot ventilator open.

Figure 4.15 shows the effect of the pressure-controlled ventilator in the internal pressure coefficient for  $\theta = 33^\circ$  (windward opening) and  $\theta = 264^\circ$  (opening under

suction). When the ventilator is located in the windward façade of the test-room the internal pressure coefficient is positive and the  $\bar{C}_{pi}$  is equal to 0.23. When the ventilator is located on the side wall of the test-room the internal pressure coefficient varies between -0.7 and 0.6 and the mean value is equal to 0. In this case the internal pressure coefficient should be negative since the ventilator is under suction: it appears that due to the effect of the flap the air is restricted to flow from inside to the outside and the internal pressure coefficient has small negative and sometimes positive values.

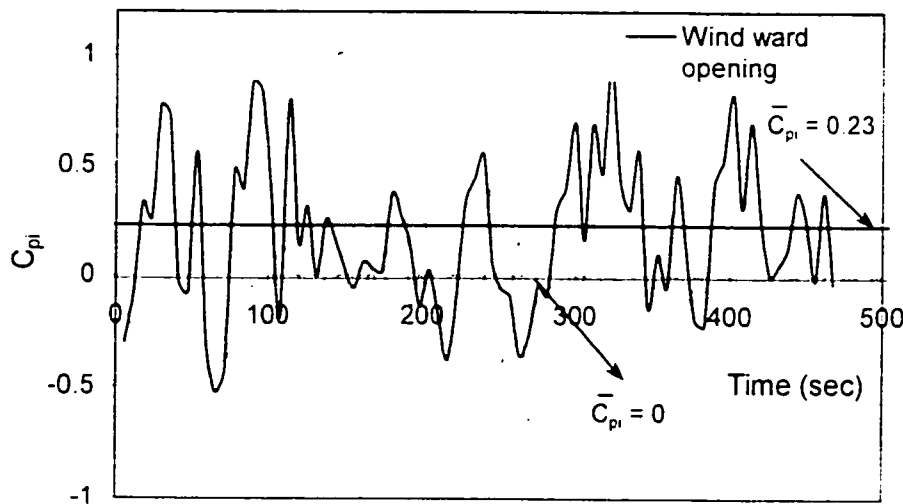


Fig. 4.15. Internal pressure coefficient variation with the pressure-controlled ventilator open.

#### 4.6.2 Discussion

Analysis of the previous data shows:

- Although the simple rectangular opening was expected to result in a higher mean internal pressure coefficient, due to its larger effective area, the highest  $\bar{C}_{pi}$  value for the

windward case, which is 0.23, corresponds to the pressure-controlled ventilator. This occurs because the incident wind angle is larger in the case of the rectangular opening ( $\theta = 49^\circ$  versus  $\theta = 39^\circ$ ), resulting in lower positive pressures in the windward wall, in comparison to that with the pressure-controlled ventilator; moreover, the standard deviation of the wind incident angle ( $\sigma_\theta$ ) is  $26^\circ$  with the rectangular opening, which is larger in comparison to  $17^\circ$  for the pressure-controlled ventilator.

It appears also that the mean internal pressure coefficient with the pressure-controlled ventilator is higher than that with the slot ventilator (0.23 and 0.1 respectively): this implies that the air flow through the pressure-controlled ventilator is higher at low values of pressure difference in comparison to the air flow through the slot ventilator, which was expected due to the effect of the flap, and it is in good agreement with the fan depressurization data (see Figure 4.11).

- Figure 4.16 illustrates the standard deviation of the internal pressure coefficient with the simple rectangular opening and the two ventilators for the windward and the leeward case. The  $\sigma_{C_{pi}}$  with the ventilator closed (no opening) is also shown. For the leeward case, the  $\sigma_{C_{pi}}$  is almost the same for the ventilators and the simple rectangular opening while for the windward case there is a clear trend, which shows higher variations with the rectangular opening; this is consistent with the results of a wind tunnel study carried out by Stathopoulos et al (1979). This study (Stathopoulos et al, 1979) found that for leeward openings the turbulence dominates and the internal pressure coefficient variations are less sensitive to opening area variations compared to windward openings. For the windward case, the  $\sigma_{C_{pi}}$  is higher with the rectangular opening in comparison to that with the ventilators because the ventilators are designed with air cavities in order to provide better

performance with respect to comfort (smaller  $C_{pi}$  variations). Comparing the two ventilators, higher  $\sigma_{C_{pi}}$  value corresponds to the pressure-controlled ventilator, which is due to the effect of the flap.

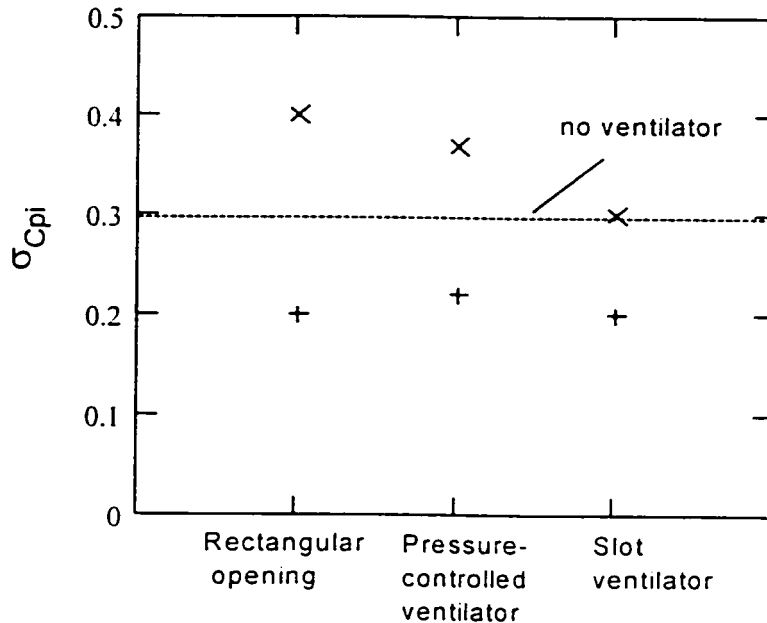


Fig. 4.16. Standard deviation of the internal pressure coefficient.

- Regarding the leeward case, the smaller  $\bar{C}_{pi}$  value corresponds to the simple rectangular opening (-0.5), which was expected due to its larger effective area. For almost the same wind direction the corresponding  $C_{pi}$  value with the slot ventilator is -0.26. Unfortunately, experimental data for the pressure controlled ventilator and South winds are not available; however, the internal pressure coefficient found about 0 for SW winds ( $\theta = 264^\circ$ ) due to the effect of the flap.

### 4.6.3 Comparison with literature sources

The value of the internal pressure coefficient recommended by ASHRAE (2001) for a low-rise building with uniform distribution of leakage ( $C_{DA}$  value equal for each wall) is -0.2. The internal pressure coefficient can be computed from a knowledge of the values  $C_D$ ,  $A$  and  $C_{pe}$  for each external surface by using of the mass balance equation (Aynsley et al, 1977). For a building with uniform distribution of leakage,  $C_{pe}$  equals 0.8 for the windward wall, -0.5 for the leeward wall and -0.6 for the side-walls, the mass balance equation has been solved by applying the trial and error method and the internal pressure coefficient found is -0.42. Table 4.3 shows that the internal pressure coefficient with the openings closed is about -0.22, which is in good agreement with the value of  $C_{pi}$  recommended by ASHRAE (-0.2), but it is not very close to the value suggested by Aynsley et al, (1977). This happens because the values of the exterior pressure coefficient used by the latter, especially for the side-walls, are high (-0.6 instead of -0.4 that recommended by ASHRAE).

According to ASHRAE (2001), and Simiu and Scanlan (1996), a building with only upwind openings is under positive internal pressure, while building internal pressures are negative when there are only leeward or side openings. These results are based on the assumption that the distribution of leakage is uniform. The results presented in Table 4.3 are consistent with these suggestions.

The effect of various opening configurations in the internal pressure was investigated in an experimental wind tunnel study that was carried out by Stathopoulos et al (1979). Figure 4.17 shows the variation of the internal pressure coefficient with the opening area of a windward opening, for different values of the background porosity. The opening area

is expressed as a percentage of the surface area of the windward wall. Regarding the present study, based on the fan depressurization test results, the background porosity of the test-room envelope was found about 0.5%. The opening area of the ventilators is about 1% of the windward wall surface area. The values of the internal pressure coefficient that were found for almost perpendicular winds are 0.1 for the slot and 0.23 for the pressure controlled ventilator (see Table 4.3). These two points were placed in the graph 4.17 and good agreement with the corresponding wind tunnel data is observed.

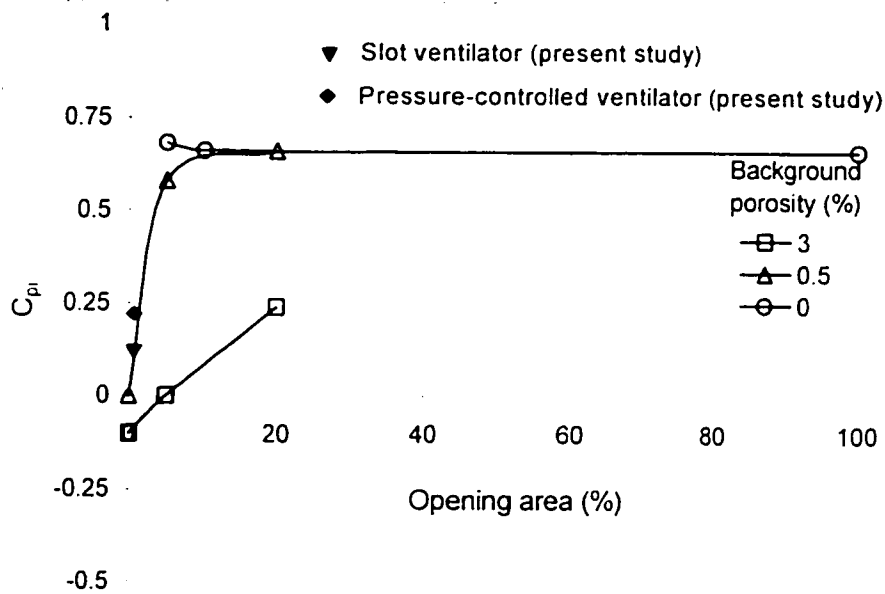


Fig. 4.17. Internal pressure coefficient - comparison between field and wind tunnel (Stathopoulos et al, 1979).

#### 4.6.4 Sensitivity of the results to the background leakage

At the first stage of the measurements some data were collected but the room was not well sealed. The analysis of these data showed that the internal pressure is very sensitive

to the leakage area of the test-room envelope and to the distribution of leaks in relation to the external pressure distribution (wind direction). The air flow through the leaks creates variations in the internal pressure, which interfere with the resulting pressure due to the air flow through the ventilator. For example, with the slot ventilator open and wind blowing from North, the 8 min  $\bar{C}_{pi}$  was about -0.1 instead of being positive. This is consistent with the results shown in Figure 4.17; for background porosity 3% and small opening area (less than 5%), the resulting internal pressure coefficient is expected to be negative due to the domination of the background porosity.

#### **4.7 Comparison between the fan depressurization and the wind study results**

This section refers to the comparison of the fan depressurization test results with the data obtained under the influence of the wind. This comparison is essential, since the depressurization technique is an artificial test (air flow due to the fan pressure), and it is possible to give different results from what happens in reality, when the wind flow dominates. It should be kept in mind that the opening may respond in a different manner under fan-induced pressures and under the influence of wind-induced pressures due to the variability of the wind. Numerous studies have been carried out to investigate the impact of the uncertainties on wind pressures on the prediction of the air flow rates in buildings, and thermal comfort, e.g. (Heijmans and Wouters, 2002, Etheridge and Sandberg, 1996, Haghghat et al, 1991, Rao et al, 1992).

Figure 4.11 shows that more air flow is passing through the pressure-controlled ventilator in comparison to that through the slot ventilator, for low values of pressure difference. As indicated in Table 4.3, the internal pressure coefficient is higher with the

pressure-controlled ventilator in comparison to that with the slot ventilator, for the windward case. Since the mean internal pressure in both cases is low (for the wind study about 1 Pa with the slot and 2.5 Pa with the pressure-controlled ventilator), it appears that the wind study results are consistent with the fan depressurization test results.

However, in order to carry out a more straightforward comparison regarding the results of the two different tests as well as the performance of the two ventilators, the concept of admittance function is used. An admittance function transforms a signal in a particular way in order to demonstrate some specific effects. Therefore, the admittance function can be used for comparison of input and output processes or any other variation occurring in two signals. In the present study, an admittance function can be defined as:

$$R = \frac{\text{air flow through the pressure - controlled ventilator}}{\text{air flow through the slot ventilator}} \quad (4.7)$$

assuming similar input conditions in both cases, and therefore, the same mean internal pressure and wind direction.

The air flow through the two ventilator types corresponding to wind data can be calculated using the empirical equations derived with the fan depressurization test, but instead of using measured values of  $\Delta P$ , values of pressure difference calculated with wind speed data (Bernoulli's equation) are used. For both ventilators the outside-inside pressure difference due to the wind may be written as follows:

$$\Delta P = \frac{1}{2} \cdot (C_{pe} - C_{pi}) \cdot \rho \cdot V^2 \quad (4.8)$$

For a low-rise building and angle of wind incidence about 30°, ASHRAE (2001) recommends a value for  $C_{pe}$  of about 0.4 and a value for  $C_{pi}$  of about -0.2. Considering 2 min duration wind speed signals of the same wind direction ( $\theta=30^\circ$ ), the mean wind



speed is computed; by using these input values ( $C_{pc}$ ,  $C_{pi}$ ,  $V$ ), the pressure differential due to the wind can be calculated. For the slot ventilator, the air flow due to the wind is calculated by substituting equation (4.8) in equation (4.2). For the pressure-controlled ventilator, instead of using equation (4.5), another regression curve for  $\Delta P$  up to 10 Pa was employed in order to achieve higher accuracy. The new empirical equation for the pressure controlled equation for  $\Delta P$  up to 10 Pa is:

$$Q_{pv,2} = 0.0028 \cdot (\Delta P)^{0.3} \quad (4.9)$$

Therefore, for the pressure-controlled ventilator, the air flow due to the wind is calculated by substituting equation (4.8) in equation (4.9).

The air flow through the ventilators corresponding to fan depressurization data is calculated by using the empirical equations (4.2) and (4.5) and typical values of the internal pressure from 1 to 20 Pa.

Figure 4.18 shows the variation of the air flow through the slot ventilator as a function of the internal pressure using fan depressurization data (see also Figure 4.3) and data obtained under the influence of the wind. Good correlation between the two sets of data is illustrated at least within the small range of availability of the wind data.

Figure 4.19 presents the variation of the air flow through the pressure-controlled ventilator as a function of the internal pressure using fan depressurization data (see Figure 4.7) and data obtained under the influence of the wind. In this case wind data up to 4.5 Pa are available because the pressure-controlled ventilator lets a larger amount of air passing through, resulting in higher internal pressures in comparison to the slot ventilator, for the same wind speed and direction. Observation of Figures 4.18 and 4.19 shows that better correlation between the two sets of data is obtained with the pressure-controlled

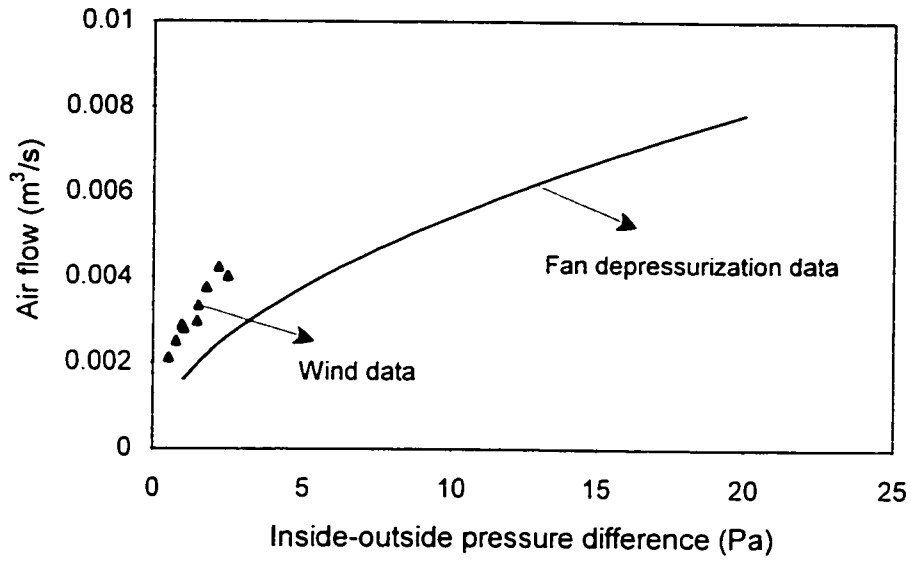


Fig. 4.18. Comparison between wind and fan depressurization data for the slot ventilator.

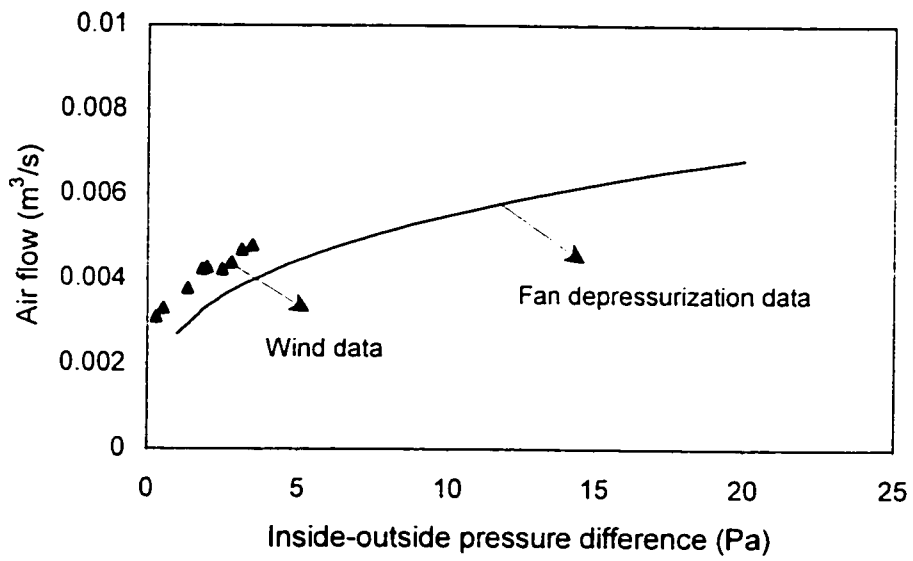


Fig. 4.19. Comparison between wind and fan depressurization data for the pressure-controlled ventilator.

ventilator. The small overestimation of the air flow corresponding to wind data is probably due to the variability (turbulence) of the wind and due to the values of  $C_{pe}$  and  $C_{pi}$  that were used.

As mentioned previously, the concept of admittance function is used in order to compare the results of the two tests as well as the performance of the two ventilators. The admittance function for wind data can be calculated as follows: for both ventilators values of the same 2 min average internal pressure are considered, for wind direction as close as possible to  $30^\circ$ . Because of the different leakage characteristics of the two ventilators this 2 min average measured internal pressure, corresponds to different wind speeds and to different air flow rates. The air flow rate through the slot and the pressure-controlled ventilator due to the wind is calculated by substituting equation (4.8) in equations (4.2) and (4.9) respectively. The admittance function for fan depressurization data is calculated by substituting equations (4.2) and (4.5) in equation (4.7). Figure 4.20 shows the variation of the admittance function with respect to internal pressure for fan depressurization data and data obtained under the influence of the wind. Unfortunately, for the second case only data up to 2.5 Pa are available due to the lack of very high wind speeds during the period that the experiments were carried out. Another reason for this lack of data is that both ventilators have small opening areas and due to the small amount of air passing through, low mean internal pressures are caused. However, good correlation between the two sets of data is illustrated at least within the small range of availability of the wind data. The underestimation of the admittance function corresponding to wind data is due to higher overestimation of the air flow with the slot

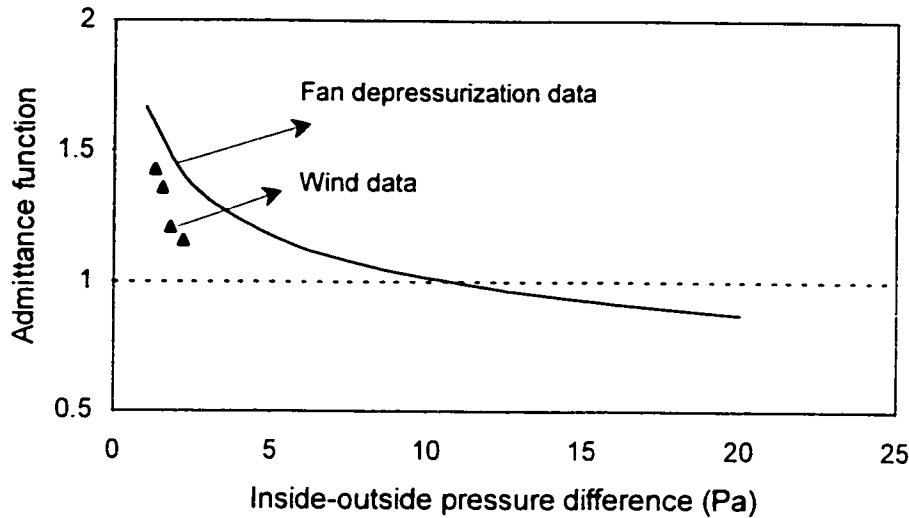


Fig. 4.20. Admittance function (air flow through the pressure-controlled ventilator/airflow through the slot ventilator) for wind and fan depressurization data.

ventilator compared to that with the pressure-controlled ventilator (see Figures 4.18 and 4.19). Regarding the comparison between the two ventilators, Figure 4.20 shows:

- (i) the admittance function is more than 1 for pressure differential ( $\Delta P$ ) less than 10 Pa, and therefore, more air flow is passing through the pressure-controlled ventilator in comparison to that through the slot ventilator, at this range of  $\Delta P$ .
- (ii) the admittance function is less than 1 for pressure differential higher than 10 Pa, and thus, more air flow is passing through the slot ventilator compared to the pressure-controlled ventilator, at this range of  $\Delta P$ .

#### **4.8 Selection criteria**

The fan depressurization test results and investigation of the performance of trickle ventilators under the influence of the wind show that more air flow is passing through the

pressure-controlled ventilator at low values of the inside-outside pressure difference ( $\Delta P < 10$ ), although the interior part of the pressure-controlled ventilator is smaller. At high values of  $\Delta P$  ( $\Delta P > 10$ ), the air flow through the pressure-controlled ventilator appears to be constant at about 6 L/s and lower than the air flow through the slot ventilator. Unfortunately, wind results for high values of  $\Delta P$  are not available, but since the comparison of the fan depressurization results with wind data shows good agreement at low values of  $\Delta P$ , the reliability of the fan pressurization results increases. Therefore, the pressure-controlled ventilator is preferable in comparison to the slot ventilator since the ideal opening in the building envelope should be as small as possible, it should provide adequate air flow even at low values of  $\Delta P$  (the pressure difference across the building envelope under normal conditions is between 2 and 5 Pa), and it should be controllable to prevent drafts, overflow and potential discomfort of occupants at higher values of  $\Delta P$  (see section 2.10).

Another advantage of the pressure-controlled ventilator is that it can be used at lower outside temperatures in comparison to the slot ventilator due to the controlled air flow passing through. In moderate climates, with an appropriate selection of the size and the location relative to the prevailing wind direction, the pressure-controlled ventilator can be used even during the heating period. In fact, according to BRE Digest 399 (1994), controllable trickle ventilators should be used in UK during the heating period also. It should be mentioned that during the period of measurements, neither rain nor snow penetration was observed through either ventilator type. With these characteristics, the pressure-controlled ventilator provides for better IAQ due to higher air flow at low values of  $\Delta P$ ; its performance appears to be more satisfactory with respect to comfort and energy

use to warm up the ventilated air during the heating season, because it provides constant air flow at high values of  $\Delta P$ . However, with better design, the pressure-controlled ventilator could provide constant air flow at lower values of  $\Delta P$  and its performance could be improved. Therefore, the improvement of its design is essential since most of the time the pressure difference across the building envelope is less than 12 Pa and constant air flow in this range is required for better comfort. As already mentioned in section 2.8, passively-controlled air inlets that provide constant air flow even at values of  $\Delta P$  as low as 1 Pa are available in the market, and it appears that their performance is satisfactory (de Gids, 1997).

Examination of the standard deviation of the internal pressure coefficient shows that higher variations are observed with the pressure-controlled ventilator in comparison to that with the slot ventilator at low value of  $\Delta P$ , which is due to the effect of the flap. This could be a potential source of discomfort and thus, a disadvantage of the pressure-controlled ventilator; unfortunately, standards for thermal comfort in terms of acceptable internal pressure coefficient variations are not available so far, and therefore it cannot be known whether the variation with the pressure-controlled ventilator is within acceptable limits. Furthermore, investigation of the performance of the pressure-controlled ventilator when it is under suction showed that the resulting internal pressure coefficient is 0; thus, the pressure-controlled ventilator cannot be used as an outlet (exhaust opening) in the case of cross ventilation.

## CHAPTER 5

### INVESTIGATION OF THE INTEGRATION OF TRICKLE VENTILATORS IN OFFICE BUILDINGS THROUGH FLOW NETWORK SIMULATIONS

#### **5.1 Introduction**

In this chapter the potential of trickle ventilator integration in ventilation design of office buildings is investigated through a simple flow network model. Design solutions for the required opening area of trickle ventilators to satisfy the fresh air requirements, as recommended by ASHRAE Standard 62 (1989), are presented and the results are compared with the BRE recommendations. The performance of slot ventilators is simulated since fan depressurization test results show that the air flow through slot ventilators is predictable for any pressure differential expected on the building envelope (see section 4.2). Simulation of the performance of pressure-controlled ventilators is more complex due to the effect of the exterior flap causing internal pressure variations (see section 4.5.2), which are difficult to simulate. Furthermore, the opening area of the interior part (actual opening) is not the same is not the same with that of the flap, and more experimental research is required to measure the air flow through the pressure-controlled ventilator as a function of the ratio of the interior part and the flap opening area.

The leakage characteristics of the slot ventilator are required for the development of the simulation flow network; these were experimentally determined and the results were presented in section 4.2. The total pressure (wind and stack-induced pressure) is calculated for different design parameters and a sensitivity analysis is carried out; the influence of

parameters such as wind speed, external pressure coefficient, outside temperature and opening height is analyzed.

## **5.2 Simulation study**

In the present study, a typical 4 m × 3 m × 4 m office space with a window is considered and the potential integration of trickle ventilators is investigated for different design parameters, i.e. exterior temperature, wind speed, pressure coefficient and opening height. Figure 5.1 shows a schematic of the simulated office. A slot ventilator, integrated in the upper part of the window frame at 3 m height from the floor, is considered as passive inlet to deliver fresh air inside the office. Exhaust grills, which are part of a low horsepower variable speed fan (exhaust part of the HVAC system) are considered as outlet. The fan may be considered when the natural driving mechanisms, wind and stack effect, are not adequate to drive the air flow (hybrid ventilation system).



Figure 5.1. Schematic of the simulated office.



An algorithm has been developed in Mathcad 2001 Professional to calculate the opening area of the trickle ventilators based on the occupancy (or air flow requirements) and a specified (desirable) internal pressure, for different design parameters. For the assumed occupancy, the ventilator should satisfy the fresh air requirements since it is the only inlet. The simulated office is assumed airtight and, therefore, the effect of the leakage is not considered. Based on the leakage characteristics of a 40 cm<sup>2</sup> slot ventilator, the flow coefficient per unit area is calculated and the wind and stack pressures are evaluated. By solving the mass balance equation, the required opening area of the trickle ventilators is calculated.

#### 5.2.1 Leakage characteristics

It was found that the flow coefficient of a 40 cm<sup>2</sup> opening area slot ventilator is 0.0016 m<sup>3</sup>/s/Pa<sup>0.53</sup> (see section 4.2). The flow coefficient of a ventilator with opening area  $A$  can be expressed as:

$$C = K \cdot A \quad (5.1)$$

where  $K$  is the flow coefficient per unit area which is equal to 0.4 (m/s/Pa<sup>0.53</sup>). BRE Digest 399 (1994) recommends 4 cm<sup>2</sup> opening area per m<sup>2</sup> of floor area to ensure an acceptable comfort level for the building occupants (maximum occupancy 8-10 m<sup>2</sup> per person). Thus, for the simulated office space, which has 12 m<sup>2</sup> floor area, 48 cm<sup>2</sup> of opening area is required. It is assumed that the flow exponent remains the same ( $n=0.53$ ) for such small variations in the opening area.

### 5.2.2 Stack pressure

During the heating period, outside air enters the building at the lower floors while the warmer inside air rises and flows out of the building from the upper floors. As already mentioned in section 2.4.2 the stack pressure,  $P_s$  (Pa) is given by the following equation:

$$P_s(T_o, h) = \rho \cdot g \cdot (H_{NPL} - h) \cdot \frac{T_i - T_o}{T_i} \quad (5.2)$$

where  $\rho$  is the air density,  $g$  the gravitational acceleration,  $T_i$  the inside temperature,  $T_o$  the outside temperature,  $H_{NPL}$  the Neutral Pressure Level (NPL) height, and  $h$  the opening height.

### 5.2.3 Wind pressure

For openings located on the windward side of the building, the air is forced into the building due to the existing positive wind pressure. For leeward openings the flow is directed from inside to the outside due to the existing negative pressures. The mean wind pressure,  $P_w$  (Pa) is given by the following equation:

$$P_w(V, C_{pe}) = \frac{1}{2} \cdot C_{pe} \cdot \rho \cdot V^2 \quad (5.3)$$

where  $C_{pe}$  is the mean external pressure coefficient and  $V$  (m/s) the mean wind speed at the opening height.

### 5.2.4 Opening area calculation

The driving mechanisms of the building pressurization are predictable for specified wind direction and location on the building envelope ( $C_{pe}$ ), outside temperature, wind

speed and opening height (design parameters). The total stack and wind- induced pressure is given by:

$$P_t(T_o, h, V, C_{pe}) = P_s(T_o, h) + P_w(V, C_{pe}) \quad (5.4)$$

The inside-outside pressure difference may be expressed as:

$$\Delta P(T_o, h, V, C_{pe}) = P_s(T_o, h) + P_w(V, C_{pe}) - P_{in} \quad (5.5)$$

where  $P_s$  and  $P_w$  are given by equations (5.2) and (5.3) and  $P_{in}$  (Pa) is the internal pressure relative to the outside static pressure at the same height (input value). It is assumed that the internal pressure is kept constant at a pre-specified value. The air flow required is based on the occupancy. According to ASHRAE Standard 62 (1989), about 10 L/s per person of outside air should be supplied to satisfy the fresh air requirements. Therefore, the supply flow rate ( $m^3/s$ ) may be expressed as:

$$Q = O Q_{req} \quad (5.6)$$

where  $O$  is the occupancy (number of persons) and  $Q_{req} = 0.01 m^3/s$ . According to mass balance, the exhaust flow rate is equal to the supply flow rate. Therefore, the air flow exhausted through the fan (exhaust grills) will be equal to the air flow coming in through the ventilator. Since the ventilator is the only inlet opening, the air flow passing through should satisfy the fresh air requirements:

$$Q = C \cdot (\Delta P(T_o, h, V, C_{pe}))^n \quad (5.7)$$

where  $C$  and  $n$  are the leakage characteristics of the ventilator,  $Q$  the supply air flow rate calculated from equation (5.6), and  $\Delta P$  (Pa) the inside-outside pressure differential. By substituting equations (5.1), (5.5) and (5.6) into (5.7) the required opening area ( $cm^2$ ) is calculated:

$$A(T_o, h, V, C_{pe}) = \frac{O \cdot Q_{req}}{K \cdot (P_s(T_o, h) + P_w(V, C_{pe}) - P_{in})^n} \cdot 10^4 \quad (5.8)$$

### **5.3 Case study**

#### **5.3.1 The building and its design environment**

A planned 17-storey, 68 m high building located in downtown Montreal is considered for the numerical simulations. Similar office spaces such as that described in the previous section are assumed on each floor in the windward façade of the building. Design conditions assume that natural ventilation can be used when the outside temperature is between 10° and 20°C and the relative humidity is less than 70%. When the outside conditions are not adequate to satisfy the design requirements, only mechanical ventilation is used. The building will not be exposed to extremely high wind speeds. The wind speed in Montreal typically varies between 0 and 10 m/s. The mean external pressure coefficient was assumed to vary between 0.2 and 0.8 (ASHRAE, Fundamentals, ch.16, 2001) since only windward openings are considered.

Figure 5.2 shows the hybrid ventilation strategy planned. The system is designed to satisfy the fresh air requirements according to ASHRAE Standard 62 (1989). Slot ventilators with appropriate sizing are considered as passive inlets to deliver fresh air inside the building. Since the stack effect is expected to be the main driving force for this high-rise building, a continuous path for air flow from bottom to top of the building is needed to achieve a satisfactory inside-outside pressure differential. Therefore, a 68 m high exhaust chimney is considered with a low horsepower, variable speed fan (exhaust part of the HVAC system) installed on the top. The fan may be operational to locate the NPL on the top of the building and to provide the total exhaust flow rate required only when the natural driving mechanisms

are not sufficient to drive the appropriate air flow (hybrid ventilation system). A chimney temperature  $T_i=26^\circ\text{C}$  is considered in equation (5.2) and the flow resistance between the room and the chimney as well as within the chimney is assumed to be negligible; these assumptions are not expected to lead to uncertainty in assessments for design purposes because the fan operates to minimize the effect of these resistances and to avoid possible cross-contamination of the stream of air in the chimney in the case of back drafts into rooms on the top floors if the vents are not properly sized. Proper design of the chimney is required to avoid possible cross-contamination and in insufficient exhaust flow for the case that the hybrid ventilation would be shut off suddenly.

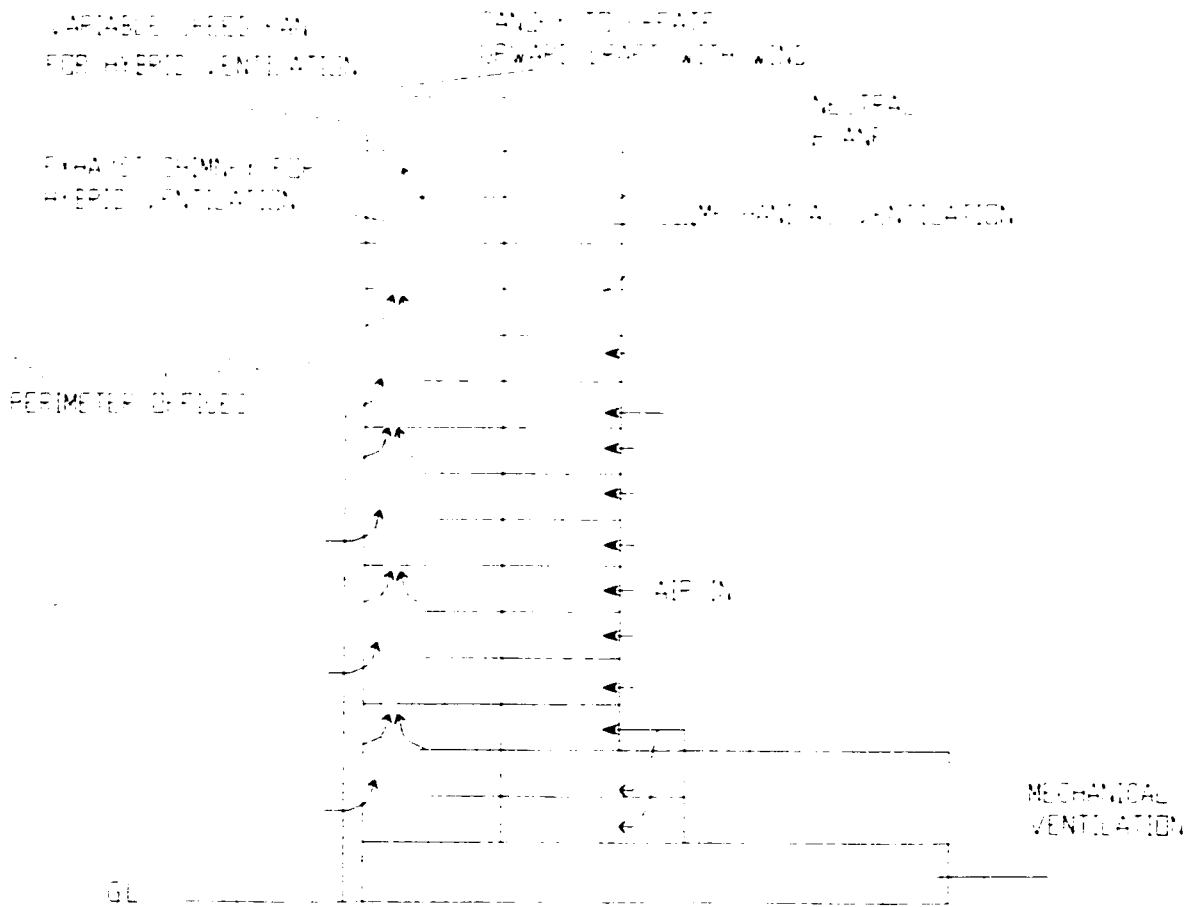


Figure 5.2. Hybrid ventilation strategy.

A variable air volume HVAC system (VAV) has been suggested for the conditioning of the indoor air. When the outside conditions are favourable, the trickle ventilators can be manually operated and the supply part of the HVAC system will be closed automatically by a damper. The exhaust part of the HVAC system (grills) is used continuously (as passive or active outlet) to exhaust the air coming in through the ventilator. When a sufficient amount of air can be delivered by the natural driving mechanisms, the grills are used as passive outlets; for insufficient flow of outside air inside the building, the fan exhausts air and thus the grills become active outlets. Dampers with pressure sensors may be installed in each office to ensure that the required flow is delivered and to keep the interior pressure at about  $-1$  Pa. The dampers can be located either at every trickle ventilator or in the exhaust grills. The ideal case with respect to comfort is a damper installed in the exterior part of the trickle ventilator and another one in the exhaust grills, but it would be expensive. Between the two possible locations of the damper, preferable is the damper installation in the exterior part of the trickle ventilator because it will provide better thermal comfort preventing from potential draft.

For a high-rise building the stack effect is expected to be the dominant driving force. Figure 5.3 shows the variation of the stack pressure with height evaluated by equation (5.2) for an outside temperature of  $15^{\circ}\text{C}$ . Wet labs will be located between the 13<sup>th</sup> and 17<sup>th</sup> floor and, therefore, mechanical ventilation is required to achieve the appropriate pressure drop and isolate contaminant sources. Natural ventilation is assumed for the 2<sup>nd</sup> to the 13<sup>th</sup> floor of the building (slot ventilator height from 7 to 51 m). The first floor, which is near pollutant sources (e.g. cars, dust, nearby building exhaust systems, etc), is mechanically ventilated to restrict the polluted outside air from coming into the building.

It is also assumed that this ventilation strategy is employed only in the perimeter zone of the building; the latter will be conditioned separately from the internal zones or spaces and, therefore, leakage between an office and the corridors is assumed to be minimal.

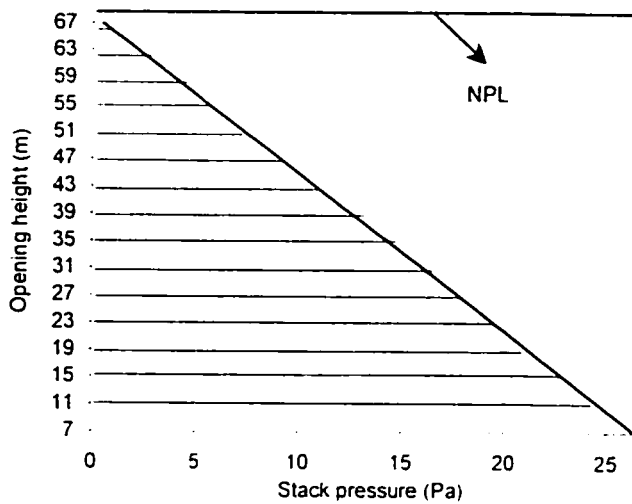


Figure 5.3. Stack pressure at the location of slot ventilators ( $T_o = 15^\circ\text{C}$ ).

### 5.3.2 Sensitivity analysis

A sensitivity analysis is carried out in order to validate the assumptions made in the previous section. Figure 5.4 shows the variation of the total pressure, which is calculated using equation (5.2), as a function of the wind speed at outside temperatures  $10^\circ$ ,  $15^\circ$ , and  $20^\circ\text{C}$  and results are given for four individual heights of the trickle ventilator (7, 23, 43 and 67 m). The external pressure coefficient was considered equal to 0.6. The total pressure is not sensitive to wind speed variation for wind speeds less than 4 m/s, which is the annual average wind speed for Montreal corresponding to open terrain data. Since the building considered is located in the

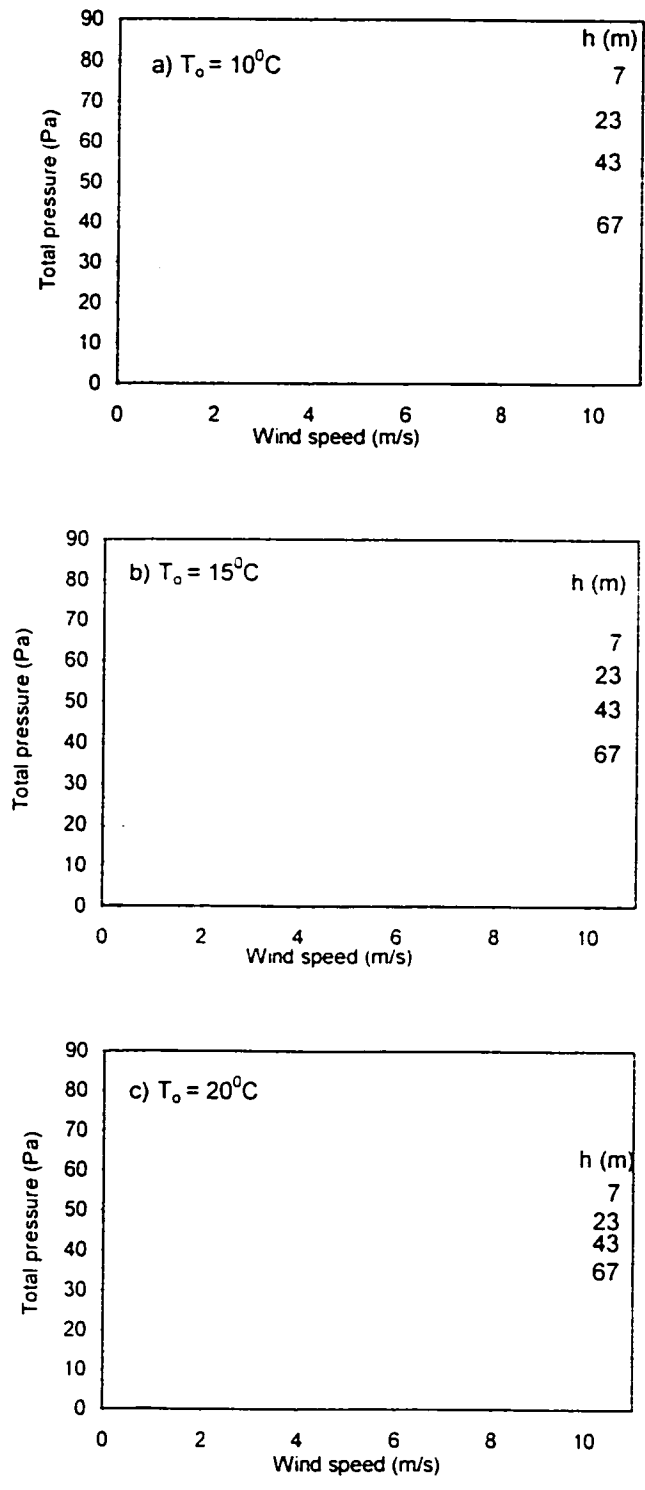


Figure 5.4. Effect of wind speed on total pressure for different outside temperatures ( $C_{pe}=0.6$ ).



downtown area, it is exposed to even lower wind speeds. Furthermore, natural ventilation will be used from March to November approximately (outside temperature between 10° and 20°C) and thus, the average wind speed for this period is about 2.5 m/s. Therefore, the results are relatively insensitive to the range of wind speeds expected but there are more sensitive to the outside temperature and the height location of the ventilator.

Figure 5.5 illustrates the total pressure as a function of the external pressure coefficient, outside temperature 10°, 15°, and 20°C respectively and results are given again for four individual heights of the trickle ventilator (7, 23, 43 and 67 m). The wind speed was considered equal to 2.5 m/s. The total pressure is not sensitive to pressure coefficient variations and thus, a pressure coefficient of 0.6 is assumed for the rest of the analysis.

Figure 5.6 shows the total pressure as a function of the opening height for three outside temperatures (10°, 15°, 20°C). The pressure coefficient and the wind speed were considered equal to 0.6 and 2.5 m/s respectively. It is observed that as the outside temperature decreases the results are more sensitive to height variations.

Figure 5.7 shows the total pressure as a function of the inside-outside temperature and the results are given for four individual heights of the trickle ventilator (7, 23, 43, 67 m). The pressure coefficient and the wind speed were considered equal to 0.6 and 2.5 m/s respectively. The total pressure is sensitive to opening height and temperature variations since the simulated building is high-rise and the stack effect dominates in the present case of low wind speeds. However, the stack effect is more dominant at the lower floors as they are far from the fan.

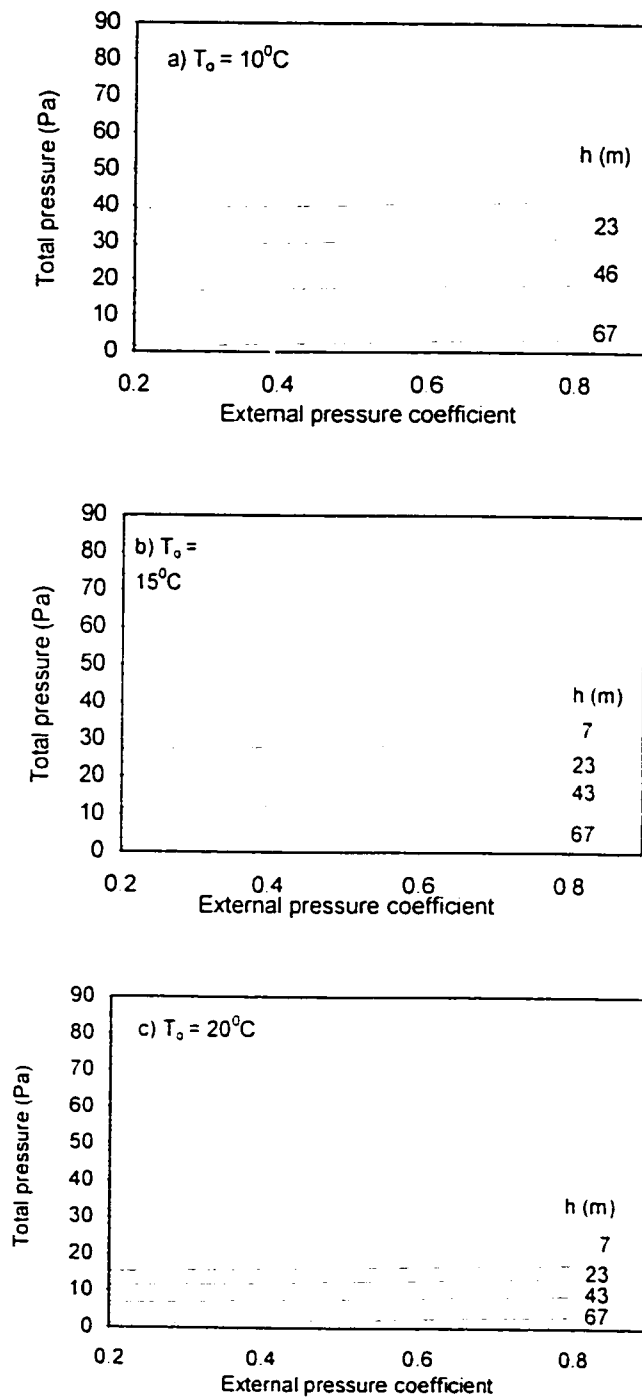


Figure 5.5. Effect of external pressure coefficient on total pressure for different outside temperatures ( $V=2.5$  m/s).

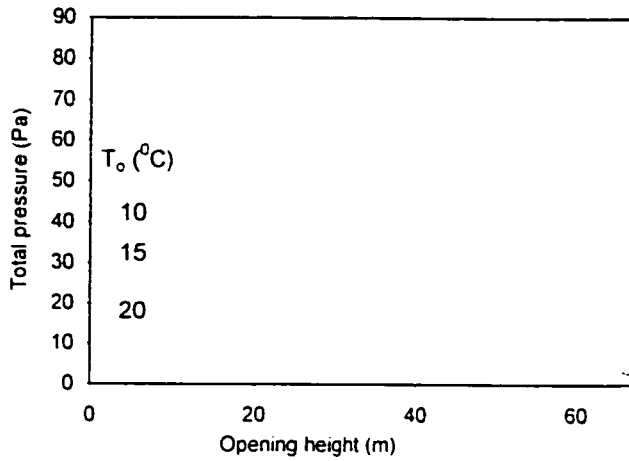


Figure 5.6. Effect of opening height on total pressure.

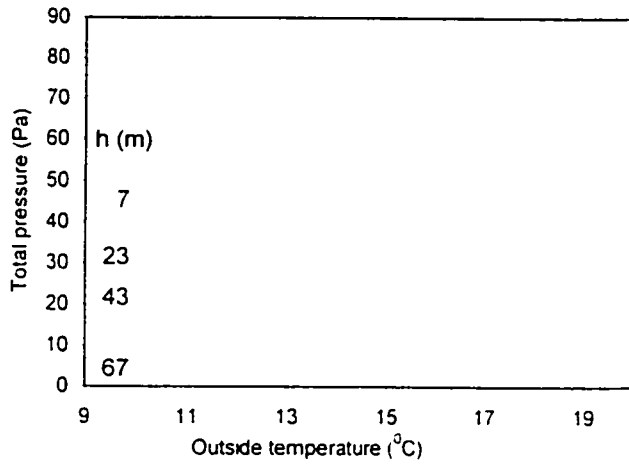


Figure 5.7. Effect of outside temperature on total pressure.

### 5.3.3 Simulation results

Based on the methodology described previously (section 5.2), the required opening area was calculated by using equation (5.8). Occupancy equal to one was assumed for the simulations. Only the variation of the opening height and the outside temperature was considered since the sensitivity analysis shows that these are the dominant parameters for

low wind speeds. Figure 5.8 illustrates the simulation results for the required opening area at different opening heights and outside temperatures for wind speed and external pressure coefficient equal to 2.5 m/s and 0.6 respectively. It is observed that:

- for high outside temperature (20°C), the required opening area varies from 55 to 85 cm<sup>2</sup> between the 2<sup>nd</sup> and the 13<sup>th</sup> floor respectively;
- for small outside temperature (10°C) the required opening area varies from 35 to 62 cm<sup>2</sup> between the 2<sup>nd</sup> and the 13<sup>th</sup> floor; and
- for outside temperature of 15°C, the required opening area varies from 40 to 70 cm<sup>2</sup> between the 2<sup>nd</sup> and the 13<sup>th</sup> floor respectively.

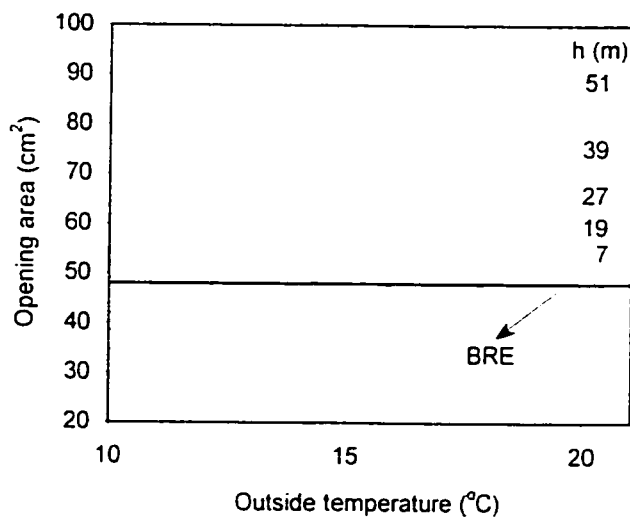


Figure 5.8. Opening area as a function of the outside temperature.

Hence, the required opening area of the trickle ventilators in order to supply 10 L/s per person (ASHRAE Standard 62, 1989) in the office space shown in Figure 5.8 is most of the time higher than the 48 cm<sup>2</sup> opening area recommended in the BRE Digest 399

(1994). This discrepancy is due to the lower fresh air requirement of 5 L/s per person recommended by BRE (1994).

In general, a larger opening area is required at the upper floors to reduce the resistance of the opening and to increase the air flow due to stack effect and thus, to reduce the operation of the fan. On the contrary, a smaller area is required at the lower floors to prevent possible overflow due to large stack effect and potential over-pressurization. There is no risk for draft if a large opening area is used at the upper floors (e.g. 85 cm<sup>2</sup>), because of the design of the slot ventilators with air cavities and due to the exterior mesh (small effective area). Furthermore, large opening areas are required for high outside temperatures, when the outside air is warm and cold drafts are not expected to occur. Detailed simulations are necessary to calculate the required opening area of trickle ventilators for their integration in a high-rise (stack - dominated) building, since this area should be selected as a function of fresh air requirements, height, design conditions and control system. For the case of Montreal, assuming that the design outside temperature is 15 °C, for an approximate selection of the opening area, 60 cm<sup>2</sup> is recommended to ensure an acceptable comfort level for occupants; this corresponds to 5 cm<sup>2</sup> per m<sup>2</sup> of floor area. With this size selection there is a risk for overflow at the lower floors for outside temperature around 10°C (large stack pressure) while insufficient air flow may be observed at the upper floors for outside temperature between 15 and 20 °C (small stack pressure). The best option, in order to prevent from these potential discomfort problems is to control the opening area with a damper installed on the exterior part of the trickle ventilator, although this may be expensive.

Therefore, for the particular case of Montreal and occupancy less than 12 m<sup>2</sup> per person, at least 5 cm<sup>2</sup> opening area per m<sup>2</sup> of floor area is recommended for spaces similar to the simulated space. For large office spaces with unknown occupancy, the use of dampers is desirable to ensure an acceptable comfort level. Furthermore, to avoid possible drafts when large opening area is required, two or more ventilators (instead of one) located on the same wall are recommended.

### **5.5 Limitations of the proposed methodology - Further study**

A simple simulation model was presented in this chapter to investigate the potential of trickle ventilator integration in ventilation design of office buildings. Detailed analysis would require a multi-zone approach and more inputs as follows:

- Wind speed variation with height considering the local terrain and the immediate shielding of the building
- Consideration of leeward openings also (in this study only windward openings are considered)
- Consideration of the potential leakage to the outside as well as leakage through the floors separations.
- Consideration of heat gains (solar and internal), thermal mass, solar control etc in order to study the trickle ventilator's effectiveness to provide potential cooling.

All the previous aspects, together with the detailed simulation (multi-zone approach) of hybrid ventilation systems, including variable air volume HVAC systems and passively-controlled trickle ventilators, are recommended for further study.

## CHAPTER 6

### CONCLUSIONS AND RECOMMENDATIONS

#### **6.1 Conclusions**

A full-scale experimental study to determine the air leakage characteristics of two trickle ventilator types, namely slot and pressure-controlled, in an outdoor test-room was carried out. The performance of trickle ventilators under the influence of the wind, which is the main driving force of the air flow through low-rise buildings, and the validity of the orifice equation to represent their behaviour have been assessed. The potential of trickle ventilator integration in ventilation design of office buildings was also investigated through flow network simulations. Design solutions for the opening area of trickle ventilators to satisfy the fresh air requirements, as recommended by ASHRAE, were presented and the results were compared with the BRE recommendations.

A fan depressurization test was performed to determine the leakage characteristics of the trickle ventilators. The empirical equations developed from the regression analysis of the experimental data can predict the trickle ventilators' capacity and can be utilized in the design of natural/hybrid ventilation systems. Comparison of the field data with theoretical estimation of the air flow through the slot ventilator by using the orifice equation with discharge coefficient equal to 0.6 shows that the orifice equation overestimates the air flow. This discrepancy can be explained by the value of the discharge coefficient used. Based on the evaluation of the orifice equation with field data,

it was found that a value of discharge coefficient approximately equal to 0.34 should be used for application of the orifice equation in the case of slot ventilators.

Regarding the wind study, each of the two ventilators as well as a simple rectangular opening that covers the same slot were considered as windward and leeward openings. For each case, the wind speed and the internal pressure variation with time were measured and the internal pressure coefficient was calculated. Based on the investigation of the standard deviation of the internal pressure coefficient, it was found that higher variations are caused with the rectangular opening and thus, the performance of the two ventilators appears to be better with respect to comfort. The concept of the admittance function was used to compare the results of the two different tests (fan depressurization and wind study) as well as the ventilation capacity of the two ventilators. Good correlation between the two sets of data was illustrated at least within the small range of availability of the wind data. Regarding the comparison between the two ventilators, the study found:

- (i) more air flow is passing through the pressure-controlled ventilator compared to the slot ventilator, for pressure differential ( $\Delta P$ ) less than 10 Pa.
- (ii) more air flow is passing through the slot ventilator compared to the pressure-controlled ventilator, for  $\Delta P$  more than 10 Pa.

With these characteristics, the pressure-controlled ventilator provides for better IAQ due to higher air flow at low values of  $\Delta P$ ; its performance appears to be more satisfactory with respect to comfort and energy use to warm up the ventilated air during the heating season, because it provides constant air flow at high values of  $\Delta P$  ( $\Delta P > 12$  Pa). However, with better design, the pressure-controlled ventilator could provide constant air



flow at lower values of  $\Delta P$  and its performance could be improved. Therefore, the improvement of its design is essential since most of the time the pressure differential across the building envelope is less than 12 Pa and constant air flow at this range is required for better comfort.

An algorithm has been developed to calculate the opening area of the trickle ventilators based on the occupancy (or air flow requirements) and a specified (desirable) internal pressure for different design parameters. Based on the leakage characteristics of a 40 cm<sup>2</sup> slot ventilator that were determined with the fan depressurization technique, the flow coefficient per unit area is calculated and the wind and stack pressures are evaluated. By solving the mass balance equation, the required opening area of the trickle ventilators is calculated for different design parameters. A planned 17-storey, 68 m high building located in downtown Montreal was considered as a case study for the numerical simulation of the performance of trickle (slot) ventilators. The sensitivity analysis shows that the opening height and the inside-outside temperature difference are the dominant parameters in the ventilation design of high-rise buildings for wind speeds lower than about 4 m/s. On the basis of the results of the case study, the main conclusions regarding the integration of trickle ventilators in hybrid ventilation are as follows:

- (i) The opening area of trickle ventilators should be selected as a function of fresh air requirements, height, design conditions and control system. For the particular case of Montreal and occupancy less than 12 m<sup>2</sup> per person, at least 5 cm<sup>2</sup> opening area per m<sup>2</sup> of floor area is recommended for office spaces similar to the simulated space.
- (ii) For proper control of fresh air intake through the trickle ventilators, inlet or exhaust dampers in conjunction with fan speed control may be utilized.

## **6.2 Recommendations and possible extensions of current work**

As already mentioned, the present study found that the air flow passing through the pressure-controlled ventilator remains constant for pressure differential more than 12 Pa. However, passively-controlled trickle ventilators that provide constant air flow even at values of  $\Delta P$  as low as 1 Pa are available in the market. Therefore, it would be very interesting to investigate their performance experimentally, including:

- Fan depressurization tests to determine the ventilation capacity of passively-controlled ventilators at several pressure differentials
- Smoke tests and velocity measurements to observe flow patterns and differences between different ventilation strategies (single-sided or cross ventilation) and to estimate thermal comfort in the occupied zone under different conditions and with different opening strategies.
- Temperature and CO<sub>2</sub> monitoring to investigate the ventilation effectiveness of the openings.
- Measurements under the influence of the wind are also recommended, including internal pressure monitoring for different inlet areas, wind speeds and directions.
- Investigation of the performance of the trickle ventilators under buoyancy forces for zero (very small) wind speed would be interesting, since this is the main driving force in high-rise buildings for low wind speeds.

With the establishment of the flow characteristics of these openings, multi-zone air flow network models can be developed to simulate their integration in ventilation design of buildings (hybrid ventilation systems). As a result, the performance of hybrid ventilation

systems can be improved and control strategies including several aspects as heating, cooling, lighting and ventilation can be developed.

## **REFERENCES**

Ad van der Aa, May, 2002, "Hybrid ventilation Waterland school building The Netherlands – First results of a monitoring case", Proceedings of 4<sup>th</sup> Annual Hybvent Conference, Concordia University, Montreal, Canada.

Ajiboye P. J. 28-30, September 1998, "A simple interactive design tool for sizing, locating and determining pollution attenuation features, of Urban Air Inlets suitable for office buildings". 19<sup>th</sup> Annual AIVC Conference, Oslo, Norway.

Ajiboye, P.J., 1998, "An air inlet device suitable for noisy and polluted urban environments", VATVENT Project, CD Rom.

Albrecht T., Gritzki R., Grundman R., Perschk A., Richter W., Rosler M., Seifert J., May 2002 "Evaluation of a coupled calculation of a hybrid ventilated building from a practical and scientific point of view", Proceedings of 4<sup>th</sup> Annual Hybvent Conference, Concordia University, Montreal, Canada.

ASHRAE Fundamentals Handbook, 1997, ch.25: "Ventilation and infiltration", American Society of Heating Refrigeration and Air-conditioning Engineers, Atlanta, GA.

ASHRAE Fundamentals Handbook, 2001, ch.16: "Airflow around buildings".  
American Society of Heating Refrigeration and Air-conditioning Engineers. Atlanta,  
GA.

ASHRAE Fundamentals Handbook, 2001, ch.26: "Ventilation and infiltration".  
American Society of Heating Refrigeration and Air-conditioning Engineers. Atlanta,  
GA.

ASHRAE Fundamentals Handbook, 1985, ch.22: "Ventilation and infiltration".  
American Society of Heating Refrigeration and Air-conditioning Engineers. Atlanta,  
GA.

ASHRAE Standard 62, 1999, "Ventilation for acceptable indoor air quality".  
American Society of Heating Refrigeration and Air-conditioning Engineers. Atlanta,  
GA.

ASTM E783, 1993 "Test Method for field measurement of air leakage through  
installed exterior windows and doors", American Society for Testing and Materials.  
Philadelphia.

ASTM E283, 1991, "Test method for determining air leakage through exterior  
windows, curtain walls, and doors under specified pressure difference across the  
specimen", American Society for Testing and Materials, Philadelphia.

Athienitis A. K., Santamouris M., 1999, "Thermal analysis and design of passive solar buildings", James & James Pub, London, UK.

Awbi H. B., 1991, "Ventilation of Buildings", E. & F. N. Spon. London, Great Britain.

Awbi H. B., Allwinkle S. J., 1986, "Domestic ventilation with heat recovery to improve indoor air quality", Energy and Buildings, Vol. 9, p. 305.

Axley J., 1999, "Passive ventilation for residential air quality control", ASHRAE Transactions, pp.864.

Aynsley R. M., Melbourne W., Vickery B. J., 1977, "Architectural Aerodynamics". Applied Science Publishers LTD, London.

Baker A. J., Kelso R. M., Gordon E. B., Subrata R., Schaub E. G., August 1997 "Computational Fluid Dynamics: A Two-Edged Sword", ASHRAE Journal.

Battle G. S., Zanchetta M., Heath P., 2000, "Wind towers and wind driven ventilation", World Renewable Energy Congress VI, Elsevier Science Ltd.

Bradshaw V., 1993 "Building Control Systems", 2<sup>nd</sup> Edition, John Wiley & Sons, Inc., New York.

Building Research Establishment, 1994 "Natural ventilation in no-domestic buildings". BRE Digest 399, UK.

Building Research Establishment, 1992, "Manual of BREEZE", Garston. Watford, UK.

CIBSE, 1998, "Natural ventilation in non-domestic buildings: A guide for designers, developers, and owners", DETR Good Practice Guide 237, ETSU, UK.

CIBSE, 1997, "Natural ventilation in non-domestic buildings". Applications Manual, AM10, UK.

CIBSE, 2000, "Natural ventilation in non-domestic buildings". Applications Manual, AM10, UK.

Clarke J., 1993 "Manual of ESP", Univ. of Strathclyde, Glasgow, UK.

Clements-Croome D., 1997, "Naturally ventilated buildings", F & FN Spon, London.

Dascalaki E., Santamouris M., Argiriou A., Helmis C., Asimakopoulos D. N., Papadopoulos K., Soilemes A., 1995, "Predicting single sided natural ventilation rates in buildings", Solar Energy, Vol. 55, p. 327.

Dascalaki E., Santamouris M., Argiriou A., Helmis C., Asimakopoulos D. N., Papadopoulos K., Soilemes A., 1996, "On the combination of air velocity and flow measurements in single sided natural ventilation configurations". *Energy and Buildings*, Vol. 24, p. 155.

Dascalaki E., Santamouris M., Asimakopoulos D. N., 1999 "On the use of deterministic and intelligence techniques to predict the air velocity distribution on external openings in single sided natural ventilation configurations". *Solar Energy*. Vol. 66, p. 223.

Dascalaki E., Santamouris M., 1995, "PASSPORT-AIR", draft final report. PASCOOL Research Program European Commission.

Daugherty R. L., Franzini J.B., Finnemore J. E., 1985 "Fluid mechanics with engineering applications", 8<sup>th</sup> Edition, McGraw-Hill Book Company, New York.

De Gids W. F., 1997 "Controlled air flow inlets", NATVENT project, CD Rom.

DOE-2, 1993, Supplement version 2.1E, Lawrence Berkeley Laboratory.

Dorgan C. B., Dorgan C. E., Kenarek M. S., Willman A.J., 1999 "Health and productivity benefits of improved Indoor Air Quality", *ASHRAE Transactions*, p. 658.



Etheridge D., Sandberg M “Building Ventilation: Theory and Measurement”. John Willey & Sons. London, 1996.

Feustel H., Raynor-Hoosen A., 1990 “Fundamental of the Multizone Air Flow Model COMIS”, Air Infiltration and Ventilation Centre, Coventry, UK.

Gan G., 2000 “Effective depth of fresh air distribution in rooms with single-sided natural ventilation”, Energy and Buildings, Vol. 31, p. 65.

Haghighat F., Rao J. Fazio P., 1991, “The influence of turbulent wind on air change rates – a modelling approach”, Building and Environment, Vol. 26, pp. 95-109.

Haghighat F., Megri A. C., 1996, “ A comprehensive validation of two air flow models- COMIS and CONTAM” Indoor Air, Vol. 6, pp. 278-288.

Heijmans N., Wouters P., May 2002, “Impact of the uncertainties on wind pressures on buildings on the prediction of thermal comfort performances” Proceedings of 4<sup>th</sup> Annual Hybvent Conference, Concordia University, Montreal, Canada.

Haines R. W., 1983, “Control Systems for Heating Ventilating and Air Conditioning”, 3<sup>rd</sup> Edition, Van Nostrand Reinhold Company, New York.

Heiselberg A., Dam H., Sorensen L. C., Nielsen P. V., 1999, "Characteristics of air flow through windows", First International One day Forum on Natural and Hybrid Ventilation. Sydney, Australia.

Heiselberg P., Tjelflaat P. O., 1999, "Design procedure for hybrid ventilation". IEA-ECBCS Annex 35 Hybvent.

Heiselberg P., Bjorn E., Jensen True J. P., May 2002 "Window openings – air flow and thermal comfort" Proceedings of 4<sup>th</sup> Annual Hybvent Conference, Concordia University, Montreal, Canada.

Herrlin M. K., 1999, "Multi-zone and contaminant modelling: Performance of two common ventilation systems in Swedish apartment buildings", ASHRAE transactions, p. 931.

Hutcheon N., Handegord G., 1995. "Building Science for a Cold Climate", 3<sup>rd</sup> Edition. SI Metric, National Research Council of Canada.

Jones J., West A. W., November 2001, "Natural ventilation and collaborative design". ASHRAE Journal, Vol. 43, No 11.

Jones W. P., 1994, "Air conditioning Engineering", 4<sup>th</sup> Edition, WP Jones, London.

Knoll B., Phaff J.C., December 1998, "Controlled natural ventilation for commercial and industrial buildings", Proceedings of 5<sup>th</sup> conference "System Simulation in Buildings", Liege, Belgium.

Kolokotroni M., Marshall S. G., Perera S., September 1995 "Trickle ventilators: effective natural background ventilation for offices", Proceedings of 16<sup>th</sup> Annual AIVC Conference, California.

Kosik W. J. October 2001 "Design strategies for natural ventilation", ASHRAE Journal, Vol. 43, No 10.

Kronvall J., Svensson C., Adalberth K., 1998 "Practical guidelines for integral natural ventilation design", NATVENT project, CD Rom.

Musser A., Yuill G. K., 1999, "Comparison of residential air infiltration rates predicted by Single-zone and multi-zone models", ASHRAE Transactions, p. 951.

Rao J. Haghghat F., Bienfait D., 1992, "Fluctuating air flow in buildings", Proceedings of Indoor Air Quality, Ventilation and Energy Conservation Conference, Concordia University, Montreal, Canada, pp. 484-489.

Riain C. N., Kolokotroni M., July 2000, "The effectiveness of ventilation stacks in enhancing natural ventilation in non-domestic buildings". Proceedings of PLEA, Cambridge, UK.

Santamouris M., Asimakopoulos D., 1996, "Passive cooling of buildings". James and James Ltd, London.

Santamouris M., 1994. "NORMA: A simplified model for passive cooling". Manual written by P. Kelly, Zephyr Architectural Competition, Univ. College Dublin.

Simiu E., Scanlan R.H., 1977, "Wind effects on Buildings". John Willey & Sons Inc.

Stathopoulos T., Surry D., Davenport A.G., July 1979 "Internal pressure characteristics of low-rise buildings due to wind action", Proceedings of the 5<sup>th</sup> International Wind Engineering Conference, vol. 1, Forth Collins, Colorado USA.

Svensson C. Aggerholm S., July 1998, "The NatVent programme 1.0. Fundamentals", CD Rom.

Ternoveanu A., December 1998, "Simplified model for natural ventilation as cooling potential in multifamily buildings", Proceedings of 5<sup>th</sup> conference "System Simulation in Buildings", Liege, Belgium.

Titon Inc., 2002, "Experimental data". personal communication. Peartree road Stanway Colchester Essex CO35JX.

The American Architectural Manufactures Association. 2000. "Airflow through integral ventilating systems/devices". Schaumburg. AAMA TIR A12.

Tsangrassoulis A., 1997, "Contribution in the mass flow and visible radiation flow phenomena through partly opened openings". PhD Thesis. Department of Applied Physics, University of Athens.

Tsangrassoulis A., Samtamouris M., Asimakopoulos D., N., 1997. "On the air flow and radiation transfer through partly covered external building openings". Solar Energy Vol. 61, p. 355.

Walton G. N., 1993, "CONTAM93 User Manual", Building and Fire Research Laboratory.

Walton G., 1988, "AIRNET: A computer program for building air flow modelling". NIST, 89-4072, National Institute of Standards and Technology (NIST), USA.

Wangly A. Y., 2001, "The impact of airtightness on system design". ASHRAE Journal, Vol. 43, No. 12, December.

Wouters P., Heijmans N., Delmotte C., Vandaele L., 1999, "Classification of hybrid ventilation concepts". IEA-ECBCS Annex 35 Hybvent.

Yakubu and Sharples, 1991, "Airflow through modulated louvre systems". Building Serv. Res. Technol., Vol. 12 (4), p.151.

## APPENDIX: CALIBRATION CURVES

This appendix includes the calibration curves of the meters (pressure-transducer, anemometer and vane) that were used for the measurements. A schematic of the vane orientation is also included.

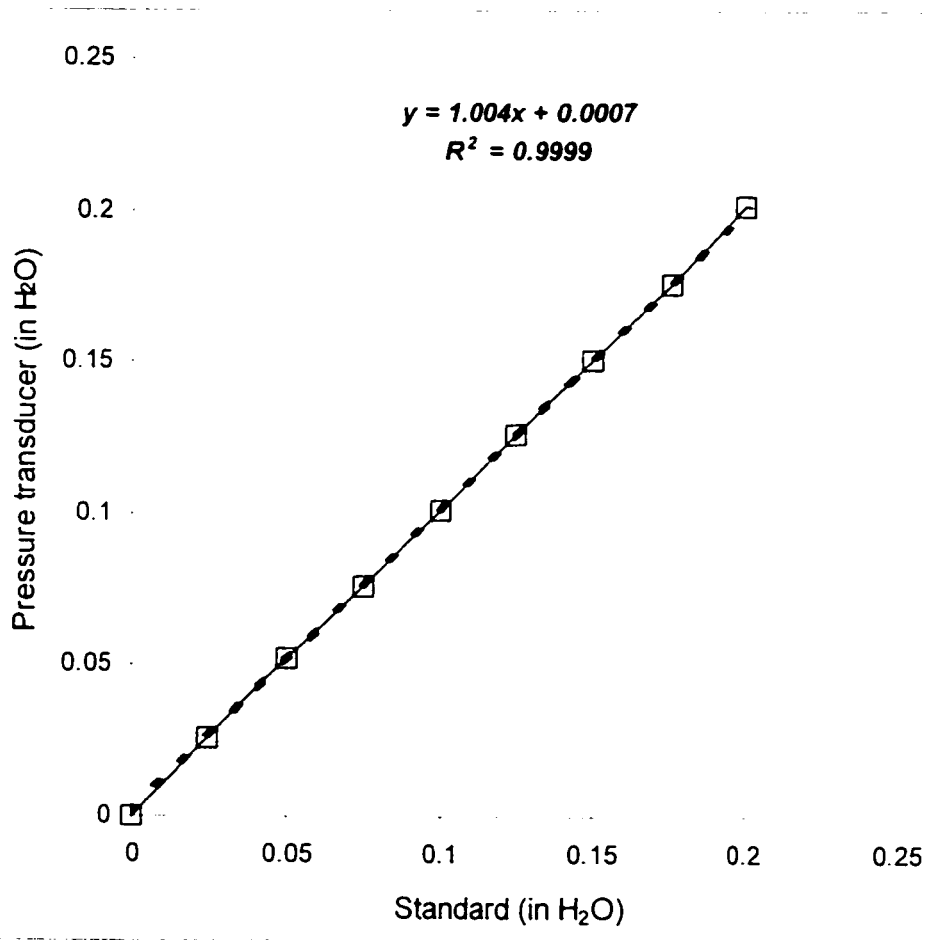


Fig. 1. Calibration curve of the pressure transducer (Air Neotronics MP6KP).

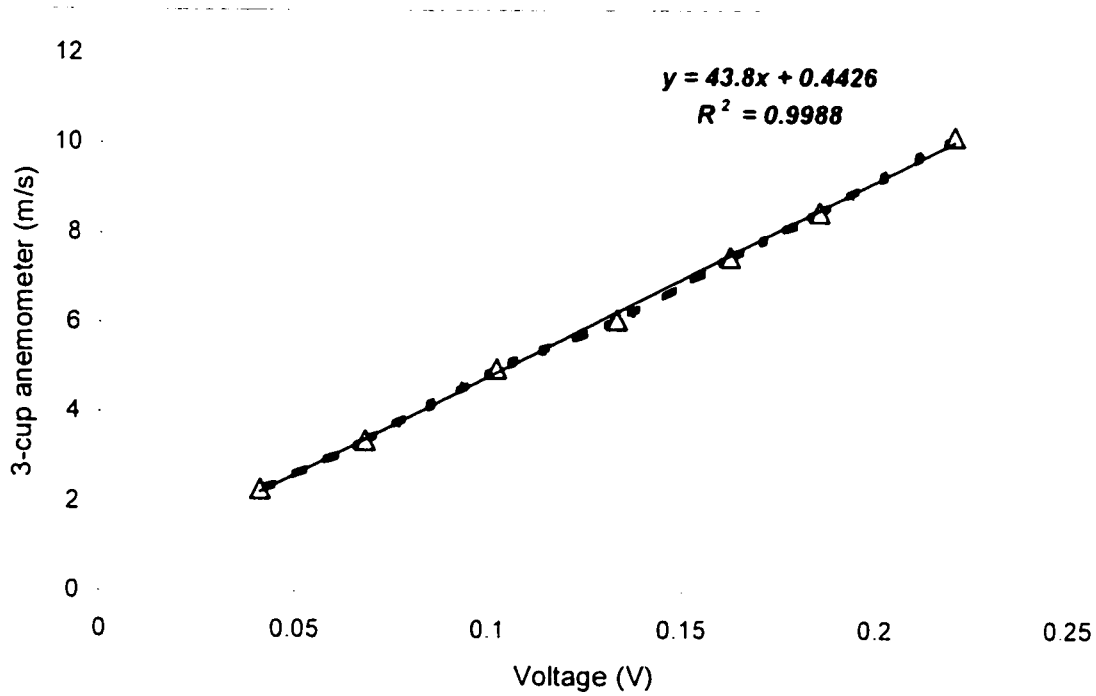


Fig. 2. Calibration curve of the 3-cup anemometer



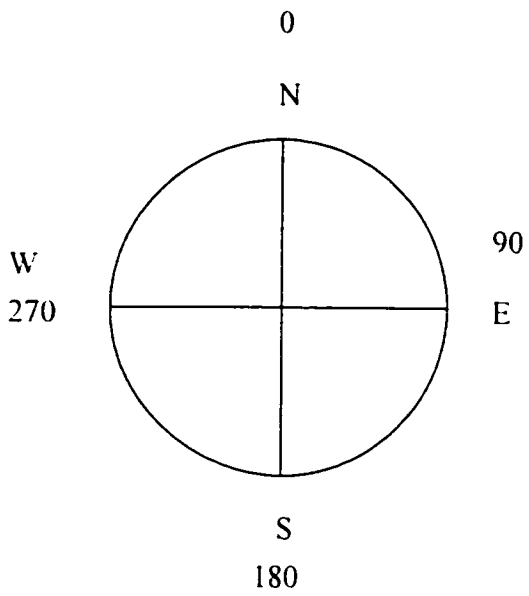


Fig. 3. Schematic of the vane orientation

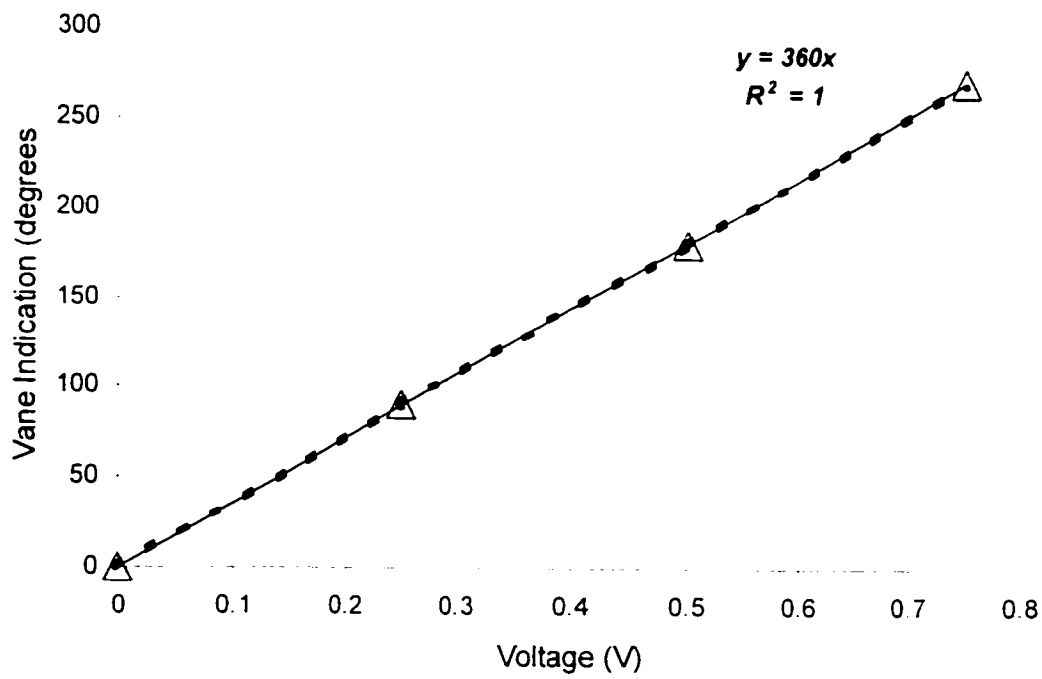


Fig. 4. Calibration curve of the vane